LOAD CARRYING CAPACITY OF BATTENED COMPOSITE COLUMNS UNDER MINOR AXIS BENDING

BY

OMAR AWAD AL-HALLIE

Submitted in partial fulfillment of the requirements for the degree of
Master of Science in Civil Engineering

Department of Civil Engineering
Faculty of Graduate Studies
University of Jordan

Amman
March , 1990

To the soul of my father,
to my mother, and
to my family.

The Examining Committee considers this thesis satisfactory and acceptable for the award of the Degree of Master of Science in Civil Engineering

Dr. Y. Hunaiti (Supervisor)
University of Jordan

Prof. S. Qaqish (Member)
University of Jordan

Dr. A. Tayem (Member)
University of Jordan

TABLE OF CONTENTS

ABSTRACT.....I
ACKNOWLEDGEMENT II
LIST OF TABLES.....III
NOTATION.....IV

CHAPTER I : INTRODUCTION TO COMPOSITE COLUMNS.....1
1.1 General.....1
1.2 The battened composite column 2
1.3 Previous research.....4

CHAPTER II : THEORY & ANALYSIS.....11
2.1 General.....11
2.2 Assumptions.....12
2.3 Stress-strain curves.....12
2.4 Cross-sectional geometry.....14
2.5 Computation of the failure loads for ashort column..15
2.6 Computation of the moment-curvatures-thrust values..18
2.7 Determination of the true equilibrium shape.....20
2.8 Computation of the failure loads for
a slender column.....24

CHAPTER III : COMPUTER PROGRAM.....27
3.1 LZERO routine.....30
3.2 MOMCURV routine.....33
3.3 NEWMARK routine.....36

CHAPTER IV : NUMERICAL RESULTS AND DISCUSSION.....38
4.1 Column section properties.....39
4.2 Cases of loadingips.....41
4.3 M-Φ-P relationships.....42
4.4 Failure load, length and eccentricity relationships..46

4.5 Parametric study.....57
4.5.1 Effect of the ultimate concrete strain (∈cu) on the column capacity.....57
4.5.2 Effect of concrete strength (Fcu) on the column capacity.....58
4.5.3 Effect of steel strength on the column capacity.....59
4.5.4 Effect of the concrete contribution on the column capacity.....59
4.6 Ductility of the battened composite column section..61
4.7 Accuracy of the presented computational method.....65
4.8 Comparison with available test results.....66

CHAPTER V :SUMMARY & CONCLUSION.....68

APPENDIX A : IDEALIZATION OF THE CHANNEL SECTIONS.....71

APPENDIX B : SAMPLES FROM THE COMPUTER OUTPUT.....76
B.1 Load carrying capacity results for the section due to a uniaxial bending moment about major axis.....77
B.2 Number of iterations for computing the equilibrium deflected shape.....90
B.3 Run time on the VAX-8700 for computing the M-Φ relations and the failure loads.....99

APPENDIX C : MOMENT - CURVATURE CURVES & INTERACTION DIAGRAMS.....100

REFERENCES :.....123

ABSTRACT

A computer algorithm is presented for calculating the failure loads of pin-ended battened composite columns of rectangular x-sections, under minor axis bending.

This type of composite column consists of battened steel channels with in-filled concrete. Five different column sections of this type are analyzed under applied load of equal and unequal end eccentricities, and having different slenderness ratios.

The method is based on classical inelastic column theory for obtaining the true equilibrium shape of deflected column.

Results are obtained from a computer program, which enable solutions to be obtained for a wide range of columns, and which can be used for preperation of design rules.

The validity of the presented solution is demonstrated by comparison with available test results for battened composite columns tested elsewhere , and good agreement is found.

An introduction to composite columns includes a review of literature is presented in chapter I. Detailed presentation of the theory and anlysis which are adopted in this study is given in chapter II. The use of the computer program, including a simplified flow charts oriented towards FORTRAN-77, is presented in chapter III. Discussion of the numerical results is given in chapter IV, and finally the conclusions are given in chapter V.

ACKNOWLEDGEMENT

This work was carried out at the Computer Center in the Faculty of Engineering & Technology at the University of Jordan under the supervision of Dr. Hunaiti, Y, to whom I wish to express my gratitude for his inspiring motivation, brilliant guidance, unceasing patience, encouragement and precious advice throughout the course of this study.

I would like to express my appreciation to Miss. Raida Shouhada, Mr. Yousef Majdalawi and Mr. Mahmoud Abu Shalanfah, for their invaluable assistance and helpful notes.

Special mention should be given to Engineers Maher Hamdan , Sami Ryalat, Mahmoud Al-Khoshman and other fellow engineers and friends for their help and suggestions.

I would like to express my sincere appreciation to my mother for her patience and moral support.

LIST OF TABLES

Table (4.1) : Properties of column sections
Table (4.2) : Increase in column strength (M/Mu) due to reduction of β from 1.0 to 0.0, L/D = 30.
Table (4.3) : Increase in column strength (M/Mu) due to reduction of β from 1.0 to 0.0, L/D = 40.
Table (4.4) : Increase in column strength (M/Mu) due to reduction of β from 0.0 to -1., L/D = 30.
Table (4.5) : Increase in column strength (M/Mu) due to reduction of β from 0.0 to -1., L/D = 40.
Table (4.6) : Effect of the ultimate concrete strain on the column capacity.
Table (4.7) : Effect of the concrete strength on the column capacity.
Table (4.8) : Effect of the steel strength on the column capacity.
Table (4.9) : Effect of the concrete contribution factor on the column capacity.
Table (4.10) : Properties of column sections tested by Hunaiti.
Table (4.11) : Comparison of theoretical results with experimental results by Hunaiti.
Table (A.1) : Idealized properties of channel sections.
Table (B.1) : CPU time (in seconds) for computing M-Φ values and failure loads (β = 1.0).

NOTATION

A_c	Area of concrete
A_s	Total cross sectional area of structural steel
A_{ss}	Cross sectional area of each channel
B	Width of column section
B_{CH}	Width of channel section
D	Depth of the column section
dA	Area of the strip element.
Dc	Distance from the tape edge of the cross-section to the centroid of dA.
D_{CH}	Depth of the channel section.
Dn	Depth of the nuetral axis.
d_r	Distance from the centroid of dA to mid depth of the cross section.
Dy	Depth of yielding.
E_c	Modulus of elasticty of concrete.
E_s	Modulus of elasticity of structural steel
e	Eccentricity of the load
F	Applied stress on the strip element dA.
F_c	Applied stress on concrete.
$\bar{F_c}$	Maximum stress reached in concrete (i.e $\bar{F_c}=0.67F_{cu}$)
F_{cu}	28-day concrete cube strength.

I_{xxi}	Idealized second moment of area about the major axis (for the channel)
I_{yyi}	Idealized second moment of area about the minor axix (for the channel)
K	Numerical factor equal to $\sqrt{\frac{EI_{(pinc)}}{P_{inc}}}$
L	Length of the column
L_c	Critical length.
M	Bending moment
M_i	Bending moment for block number i
M_{Ri}	Moment of resistance due to initial deflection at node i
M_u	Ultimate bending moment (axial load = 0.0)
n	Number of nodes along the column length
Nb	Total number of blocks (i.e concrete plus steel blocks)
Ns	Number of strip element in the block.
P	Axial load
P_i	Axial load for block number i.
P_{inc}	Load increment equal to Pu/20.
P_u	Squash load of the column
S_i	Uncorrected slope at node position i
T	Average flange thickness of channel.
T_1,T_2	Flange thickness to calculate idealized properties of the channel section
t	Thickness of the channel web
U_i	Uncorrected deflection at node position i
Y	Depth of plastic nuetral axis

Y_i	Deflection at node position i due to load
Yi	Deflection at node position i after each iteration
Y_1	Deflection at node position 1
Y_2	Deflection at node position 2
α_c	Concrete contribution factor
β	Eccentricity ratio; (small end bending moment divided by the larger one), $-1 \leq B \leq 1.0$
ϵ	Strain across the strip element dA
ϵ_c	Strain in concrete.
ϵ_{co}	Strain in concrete at the begining of horizontal plateau.
ϵ_{cu}	Ultimate concrete strain.
ϵ_s	Strain in structural steel
ϵ_y	Yield strain in structural steel
θ	Rotation at the end of the column
λ	Length of the column divided by number of nodes;L/n
μ	Numerical factor depends on β (i.e $\mu = 1$ for sigle curvature, 1.5 & 2. for $\beta = -0.5$ & -1 respectively).
Φ	Curvature 1/mm
Φ_i	Curvature at node number i
Φ_m	Curvature at the ultimate concrete strain ϵ_{cu}.
Φ_y	Curvature at first yield of the tension steel

CHAPTER I

INTRODUCTION TO COMPOSITE COLUMNS

1.1 GENERAL

A composite column is a compression member that is constructed with load-bearing concrete plus steel in any form different from reinforcing bars. Several examples of cross sections of composite columns are shown in Figure (1.1).

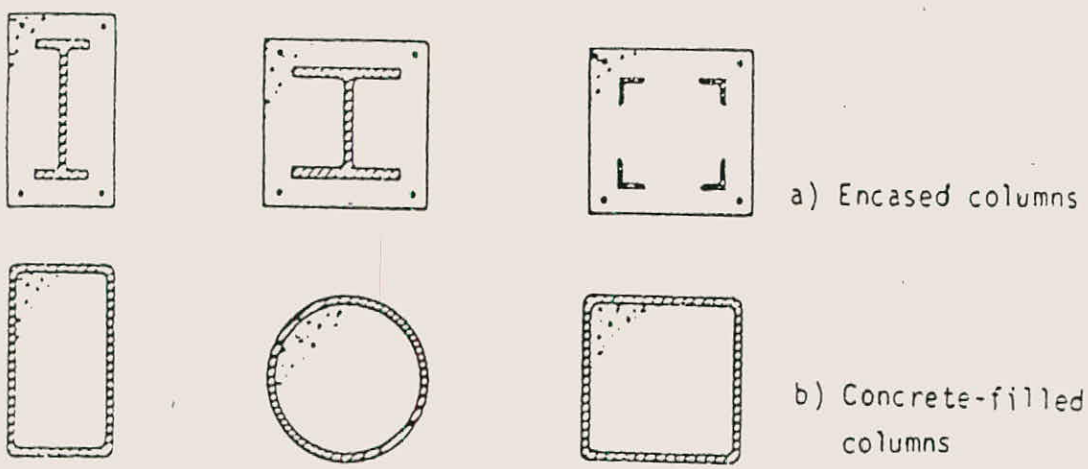

FIG. (1.1) Composite-column cross sections

Cnocrete encasement of columns in a steel frame building was first used as a convenient method of providing fire protection, and until the 1950's it was the normal practice to neglect its contribution to the strength of the column.

Tests then showed that this encasement, using a strong concrete mix, accomplishes a double benefit of providing the steel core with insulation from heat while supporting enough load to permit a reduction in the required size of the core, which at the end implies a reduction in cost.

Afterwards, more research has been carried out so that the behavior of an isolated pin-ended composite column subjected to axial compression and also to combinations of end moments about one, or both, axes is now well understood.

Most of the research has dealt with both the concrete-encased and concrete-filled columns. However, some research related to the behavior of built-up composite columns was also carried out.

1.2 BATTENED COMPOSITE COLUMN

A new type of composite column section has recently been suggested for use in multi-story framed structures by Yee and Shaker khalil in 1982 [16] . This column consists of two steel channels joined together using welded batten plates to form a rectangular shaped section. The interior of the column is subsequently filled with in situ concrete (see Figure 1.2).

1. Steel channels
2. End and intermediate batten plates
3. In-Situ concrete

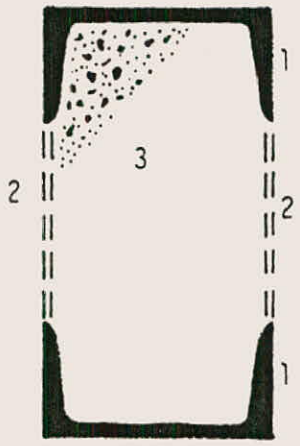

FIG. (1.2) Battened composite column section

This composite column is considered to be a special usefull type of composite construction in multi-storey buildings. It can, under certain circumstances, provide a favourable alternative to the traditionally used composite column.The use of this column appears to be both a matter of economy, and structural performance.

In common with the concrete-filled steel tubes; the battened composite column misses one advantage of the concrete encasement, which is the fire protection. However, compared to the traditional composite columns; the battened composite column offers the following advantages :

1. The shuttering required, is of a simple and inexpensive form.
2. The flexibility, in the arrangement of the steel channels, provides a range of the load-carrying capacity simply by changing the depth of the column.
3. Although no reinforcement cage is required, reinforcement could be used to increase the load-carrying capacity when the dimensions of the column section are restricted.
4. The steel is placed on the outside where it is most needed, making the column very efficient in resisting the applied loads.
5. The spacing between the channels provides easy access to the inside core, and hence makes for easy beam-column connection. This space, also, allows for pipes (mechanical and electrical works) to go through the column in cases where such details are necessary.

1.4 PREVIOUS RESEARCH

Most of the previous research, both experimental and theoretical, has dealt with concrete-encased and concrete-filled columns. However, some investigation were carried out to study the behaviour of built-up composite columns.

Early in the 1950's Faber [6], stevens [11], and others carried out tests on encased steel stanchions of I-sections to investigate the strengthening effect of the concrete encasement, and this led to the cased-strut method

of design which was incorporated in the 1959 eddition of BS499.

Research on improved methods of design has been continued since the early 1960's. Jones and Rizk [8] carreid out a series of tests on encased stanchions both in field and laboratory to investigate the general behavior of composite columns. It was concluded that the calculated ultimate loads, of encased columns from BS499 recommendations, were very conservative when compared to the test results.

Further research was carried out by Steven [12]; to investigate the general behaviour, modes of failure, and the ultimate loads of encased stanchions. The following conclusions were reported :

1. The strength of a short encased stanchion in axial compression (i.e squash load **Pu**) is given by the sum of the products of steel area and its yield strength, and the concrete area and **0.67Fcu** (i.e **Pu = AsFy+Ac 0.67Fcu**).
2. As the slendeness increases, the strength of axially loaded encased stanchions decreases, which is similar to that of reinforced concrete.
3. A simple emperical formula can be used to relate the strength of encased stanchions under axial load and under eccentric loads.

In 1967, a method for computing the failure loads for eccentrically loaded composite column of rectangular section was proposed by Basu [2]. The method was based on the assumption that the initial deformation (if any) and the deflection due to load form part of a cosine curve. The

main conclusion was that the error in the failure load computed by this theory, based on the assumption of a part cosine curve for the deflected shape of the column, was proved to be small, and so the computed failure loads would be sufficiently accurate for practical purposes.

Moreover, in 1968, a computer method for calculating the failure loads of pin-ended composite columns of rectangular section and having equal or unequal end eccentricities was carried out by Basu and Hill [3]. The above method was based on classical inelastic column theory, and on obtaining the true equilibrium shape of the deflected column, unlike the previous treatment [2] in which the deflected shape was assumed to be part of a cosine curve. Solutions have been obtained by this method and by the approximate method of the previous research (based on part cosine-curve assumption) for major and minor axes bending of two steel I-sections with or without concrete encasement, for eccentricity ratios of 0 and 1. Results demonstrate that the approximate method is sufficiently accurate for practical purposes, although it takes a fraction of the computation time required by the exact method.

In 1969, an extensive theoretical study on design methods was conducted by Basu and Sommerville [4]. Pin-ended composite columns with both equal and unequal eccentricties was treated in this study which has become the basis of current methods of design (The British Bridge Code Method [BSS400] and the ECCS method [EC4]). The method, which adopted in this study, was also considered applicable to the case of concrete-filled circular tubes as well as for the rectangular reinforced concrete columns.

The most important conclusion was related to the

calculation of the moment carrying capacity of the section. A constant compressive stress of 0.45Fcu acting over the area of concrete above the plastic neutral axis was shown to be justified. In addition to that, for the case of biaxial bending, the load can be estimated from failure loads under uniaxial bending about the major and minor axis with the help of an interaction formula proposed in the paper.

A series of tests on built-up composite columns was carried out by Bridge and Roderick [5]. This type of composite columns consists of two battened steel channels facing each other and encased in concrete. Two types of columns were tested, with and without intermediate batten plates, the latter was to investigate the effect of the batten plates on the shear resistance between the two channels. Numerical Integration procedure was also adopted in the above study for determining the deflected shapes and failure loads. Comparison of the test results with the theory showed good agreement. The results also demonstrated that the function of transmitting shear between the steel channels can be performed by the concrete encasement even if there is no reinforcement, while the main function of the batten plates was to enable the steel channels to carry construction loads. In addition to that it was demonstrated that there is arange of slender columns of the type considered, failed by instability before full flexural strength was reached.

Evidence indicate that there has been little research carried out to investigate the behaviour of the filled battened composite columns. Taylor, Shakir-Khalil and Yee [13], investigated the behavior of battened steel columns in-filled with concrete under eccentric loading. Nine large-scale columns of this type were tested at the

University of Manchester, in order to achieve a good understanding of the behavior of the newly suggested composite column. The load-carrying capacities of the battened columns were compared with the ultimate loads predicted by some simple design expressions suggested in the study. However, the following conclusions were reported :

1. The proposed new type of battened composite column behaved well under load, and is a possible form of construction worthy of further research.
2. The ultimate loads of the columns were always well in excess of the values estimated using the proposed design expressions. Also, the Bridge Code Method proved to be very conservative.
3. Strain measurements showed that the composite action between the steel and concrete, was achieved, indicating that two materials acted together in resisting the load.
4. The first sign of damage to the concrete occurred only at loads well in excess of loads corrosponding to the service load.

Moreover, another research was carried out by Hunaiti [7] to study the behaviour of the battened composite columns under large eccentricities, and the following conclusions were drawn :

1. The steel channels and the concrete area acted compositely in resisting the applied load.
2. Type of failure, the columns exhibited, indicated no sign of either overall or local instability.

3. There exists a simple relationship between "Pu/Mu" and the section properties.

Recently a method for performing inelastic stability analysis of composite beam-columns under different load and end conditions was conducted by Metwally Abo-Hamd [1]. Nondimensional analytical expressions describing the true moment-thrust-curvature curves were derived. The method has been used to develop typical axial load-bending moment interaction curves for composite beam-columns under different end and load conditions. The accuracy of the method was demonstrated by comparison with the available results obtained by Basu and Sommerville [4], for a steel I-section, for end eccentricity ratios of 1 and 0, and good agreement was found.

As a part of a general investigation on the analysis and behaviour of battened composite column at the University of jordan,a computer method was developed by Ryalat [10]. The method based on inelastic column theory for calculating the failure loads of pin-ended battened composite columns under uniaxial bending about major axis. The following conclusion was reported :

1. The capacity of the battened composite column decreases as the eccentricity ratio ,β, increases.
2. Significant loss of strength was observed for slender columns. Also it has been demonstrated that there is a range of slender columns for which instability will occur prior to developing the full flexural strength.
3. Inclusion of reiforcement bars was found to

have a great influence on the capacity.

4. Initial curvature reduces the strength of the column. The reduction in strength is more pronounced for slender columns.

CHAPTER II

THEORY AND ANALYSIS

2.1 GENERAL.

The fundamental problem involved in any method of computing the failure loads of columns is to determine their load-deflection relationship. For a given length and eccentricity , if the deflected shape is obtained for successively increasing values of axial load, the failure load , according to the inelastic column theory, may be defined as the peak of the load-deflection curve.

Alternatively, if for a given length of column, the axial load is kept constant; the failure criterion becomes one of the maximum eccentricities. The latter criterion is utilized for the present solution. The end eccenttricities are increased proportionally, and the deflections are obtained in the plane of the eccentricities as the failure is assumed to occur due to excessive bending in this plane.

It is known that the computation of the failure loads proceeds from the knowledge of the moment-curvature characterstics of the column; which are a family of curves defining the curvature values (Φ) for various combination of axial load (P) and bending moment (M). The M-Φ-P curves are derived from the cross-sectional geometry of the column and the material properties of the section. Onces these curves are established, the true equilibrium shape of the deflected column in the plane of the end eccentricities can be obtained by an itarative numerical procedure, provided that the column is subjected to loads less than critical. At failure, the iterattions do not converge, indicating that the equilibrium

is no longer possible to obtain.

A detailed description of the above method which used in this study is presented in this chapter.

2.2 ASSUMPTIONS:

The principal assumptions upon which the method is based on, are as follows:

i- Plane section before bending remains plane after bending. Therefore no relative movement takes place between steel and concrete (i.e they act compositely).

ii- Tensile strength of concrete and residual stresses in steel are not taken into account.

iii- Strain hardening in steel is ignored.

2.3 STRESS-STRAIN CURVES:

Idealized stress-strain curves for concrete and steel, as recomended by CEB and CP110, are used in the analysis as shown in Figure (2.1).

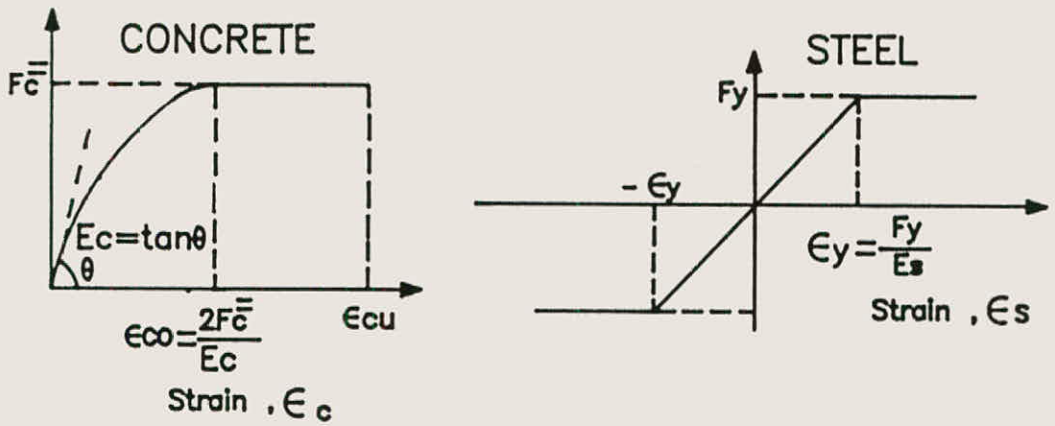

FIG.(2.1) Idealized stress – strain curves for concrete and steel .

Referring to Figure (2.1), it can be seen that the stress-strain curve for concrete consists of two parts; the first one is parapolic , and the second is taken to be constant for any value of concrete strain (∈c), from (∈co) up to (∈cu); because of steel confinement [9]. Thus, for computing the concrete stress (Fc) for any given strain distibution across the column section, the following equations can be used:

$$F_c = F_c^{=}\left[\frac{\epsilon_c}{\epsilon_{co}} - \left(\frac{\epsilon_c}{\epsilon_{co}}\right)^2\right] \quad \text{for } 0 \le \epsilon_c \le \epsilon_{co} \qquad (2.1)$$

$$F_c = F_c^{=} \quad \text{for } \epsilon_{co} \le \epsilon_c \le \epsilon_{cu} \qquad (2.2)$$

Where:

$\bar{Fc}$: The maximum stress reached in concrete, according to CEB and the British code of practice [15].

$$\bar{Fc} = 0.67Fcu \qquad (2.3)$$

Fcu: The 28-day cube strength of concrete.

ϵco: The concrete strain at $\bar{Fc}$, which can be taken equal to $2\bar{Fc}/Ec$.

Ec : The modulus of elasticity for concrete, according to CP110.

$$Ec = 5500\sqrt{F_{cu}} \qquad (2.4)$$

Regarding the suggested steel curve; it can be seen that a bilinear stress-strain curve is used. So the steel stress (Fs), can be computed using the following equations.

$$Fs = \left(\frac{\epsilon s}{\epsilon y}\right) Fy \qquad \text{for } -\epsilon y \le \epsilon s \le \epsilon y \qquad (2.5)$$

$$Fs = Fy \qquad \text{for } \epsilon s > \epsilon y \qquad (2.6)$$

$$Fs = -Fy \qquad \text{for } \epsilon s < \epsilon y \qquad (2.7)$$

Where:

Fy : Yeild stress of steel.

ϵy : Yeild strain of steel and is equal to Fy/Es

Es : The modulus of elasticity for steel.

2.4 CROSS-SECTIONAL GEOMETRY:

The composite section, under consideration, consists of two steel channels. In an attempt to make the

calculations of M-Φ easier; idealization of the channel sections is employed in the analysis as given in Appendix [A].

2.5 COMPUTATION OF THE FAILURE LOADS FOR A SHORT COLUMN:

The computation of the failure loads for a short column (i.e L/D≅0.) involves the axial load (P), the bending moment (M), and the depth of yielding (Dy) across the section. The last one can be defined as the distance from the top edge of the cross-section to the point, at which the applied stress in concrete (Fc) is equal to 0.67Fcu, and the stress in steel (Fs) is equal to Fy (in compression or in tension), as shown in Figure (2.2).

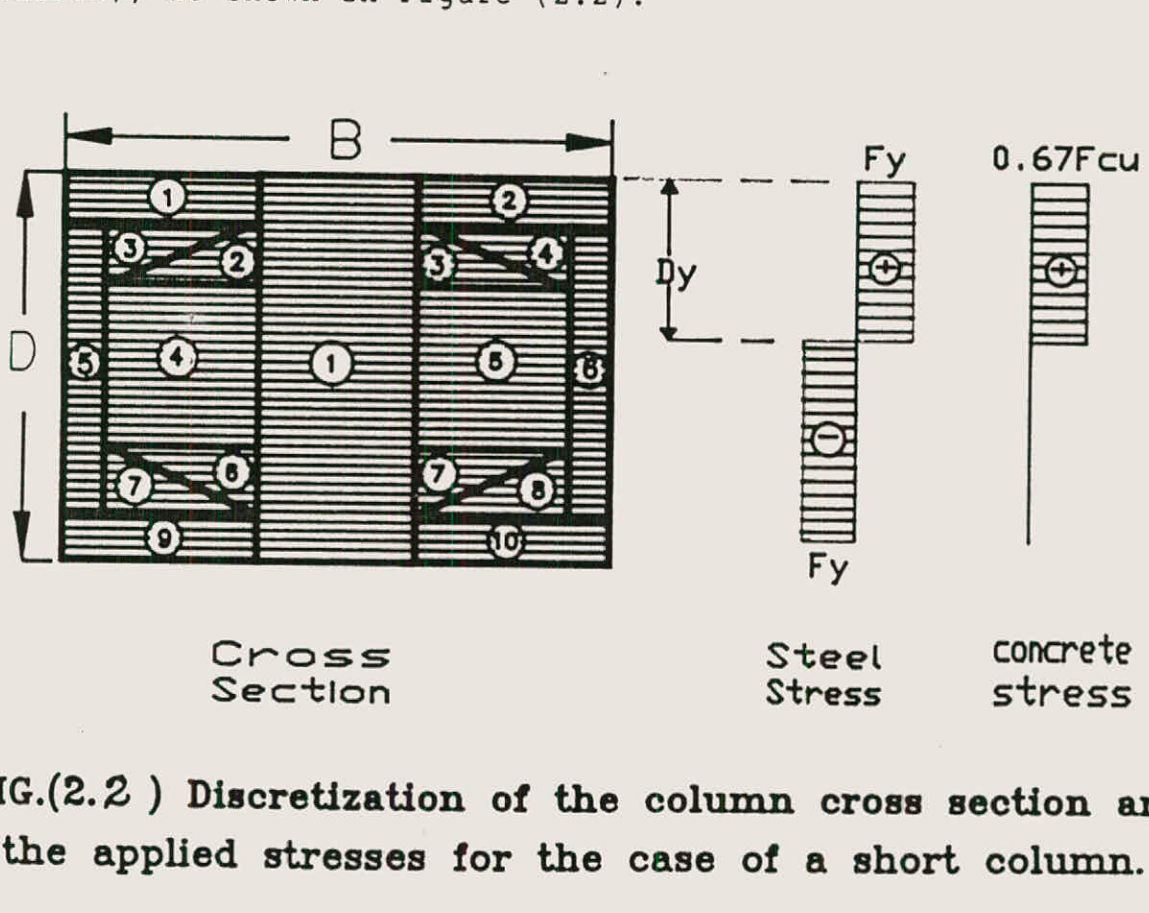

FIG.(2.2) Discretization of the column cross section and the applied stresses for the case of a short column.

Now, for computing the axial load (P) and bending moment (M), for a specified value of depth of yielding (Dy); the column cross-section is subdivided into ten blocks of structural steel, and seven blocks of concrete. Then each of these blocks is subdivided into a small size strip elements as shown in Figure (2.2).

In each strip element, depending on the depth of yielding (Dy), and the material composed in it, the axial load and bending moment can be calculated, and then, by summation, the value of P and M in each block is computed. The resultant P and M will be evaluated for the specified value of Dy, by adding the axial loads and bending moments for all blocks which can be given as follows:

$$P = \sum_{i=1}^{17} P_i \qquad (2.8)$$

$$M = \sum_{i=1}^{17} M_i \qquad (2.9)$$

Where:

Pi : The axial load for block number i.

Mi : The bending moment for block number i.

Pi and Mi can be also given by the following two equations.

$$P_i = \sum_{j=1}^{Ns} F \, dA \qquad (2.10)$$

$$M_i = \sum_{j=1}^{Ns} F \, dA \, dr \qquad (2.11)$$

Where:

Ns : Number of strip elements in the ith block.

dA : The strip element area.

F : The applied stresses on dA.

dr : Distance from the centroid of dA to the mid depth of the cross-section.

It should be mentioned that the applied stress (F) has different values, depending on the material composed in the strip element (dA), the distance from the top edge of the cross-section to the centriod of dA (Dc), and the value of the depth of yielding (Dy). Hence, F can be expressed as follows:

$$\left.\begin{array}{ll} F = 0.67\ Fcu & \text{for } Dc \le Dy \\ F = 0.0 & \text{for } Dc > Dy \end{array}\right\} \text{concrete} \qquad (2.12)$$

$$\left.\begin{array}{ll} F = Fy & \text{for } Dc \le Dy \\ F = -Fy & \text{for } Dc > Dy \end{array}\right\} \text{steel} \qquad (2.13)$$

By subsituating equations (2.10) and (2.11) into (2.8) and (2.9) for Pi and Mi respectively, we can set the following generlized equations for computing the resultant P and M.

$$P = \sum_{i=1}^{Nb} \sum_{j=1}^{Ns} F\ dA \qquad (2.14)$$

$$M = \sum_{i=1}^{Nb} \sum_{j=1}^{Ns} F\ dA\ dr \qquad (2.15)$$

Where:

Nb : The total number of blocks that form the column cross-section (i.e Nb=17, for the battened composite column section).

F,dA,dr : As defined previously.

As a result, the scheme for computing the failure loads (P/Pu Vs. M/Mu) can be summarized through the following steps:

Step 1. Calculate the squash load (Pu), which can be estimated by adding the products of the steel area (As) and steel yield strength (Fy) to the product of concrete area (Ac) and two thirds of the concrete strength.

Step 2. Calculate, for succesively increasing values of Dy, the resultant axial load (P), and bending moment (M) as given by equations (2.14) and (2.15) respectively.

Step 3. Using linear interpolation; calculate the ultimate moment (plastic moment) Mu for a resultant axial load (P) equal to zero.

Step 4. Divide each value of P and M by Pu and Mu respectively.

Step 5. Finally, calculate the non-dimensional values P/Pu and M/Mu for the load increments of Pu/50.

2.6 COMPUTATION OF THE MOMENT-CURVATURE-THRUST CURVES:

The scheme which is developed as a part of the present theoretical investigation for computing M-Φ-P curves is very simple, and is applicable not only for battened composite sections, but also for any composite sections of rectangular shape, with or without reinforcement, and for plain concrete sections as well; provided that the column section can be presented to computer as being composed of small size strip elements as explained previously in section

(2.4). This flexibility has been retained in the computer program, which can be used not only for preparing design curves or tables involving a large number of standard column sections, but also for numerical studies of the influence of various parameters on column strength and to examine the validity of design formulae.

The method of computing M-Φ-P curves is presented here with particular reference to the battened composite column section, and its application to other types of column section requires no additional difficulty. The same procedure described previously in section (2.4) for computing the failure loads for the case of a short column section, is also used here with a difference related to the applied stresses (i.e Fc or Fs), which are now computed, making use of the stress-strain curves for the material composed in the strip element dA. In order to compute these stresses, the strain (∈) across dA, must be evaluated. Thus for a given values of Φ and neutral axis (Dn), the strain (∈) can be estimated as follows:

$$\epsilon = (Dn - Dc) \Phi \qquad (2.16)$$

Where:

Dc : As previously mentioned in section (2.4)

The following steps summarize the present method of computation.

Step 1. Select suitable values for curvatures (the smallest values, the largest values, and the increments) and the intervals of the neutral axis position.

Step 2. Choose the set of values of the axial load increment (Pinc) for which M-Φ relationships are required. These may be conveniently choosen as a multipiles of Pu/20.

Step 3. Take the smallest value of Φ.

Step 4. Calculate for successively increasing values of Dn, the strain distribution (∈), and hence the values of P and M, making use of the assumed stress-strain curves as given by equations (2.14) and (2.15) respectively.

Step 5. Divide each value of P and M, calculated in Step 4, by ,Pu, and Mu respectively.

Step 6. Repeate Step 3 to Step 5 for other values of Φ, until the maximum moment for the load increment (Pinc), is reached. Five additional values of the moment (M) beyond the maximum were calculated for the purpose of presentation.

Step 7. Repeate all previous steps for other values of load increment (Pinc).

2.7 DETERMINATION OF THE TRUE EQUILIBRIUM SHAPE:

The theory presented below is in a general form,so it can be applied to any eccentrically loaded pin-ended column, assuming that the (M-Φ) characteristics of the section have already been established.

Consider a column of length L loaded with an axial load ,P, having different end eccentricities e and βe respectively, where β is a constant called the eccentricity ratio, such that, ($-1 \leq \beta \leq 1$). The column shown in Figure (2.3) has been divided into n equal intervals of length $\lambda = L/n$.

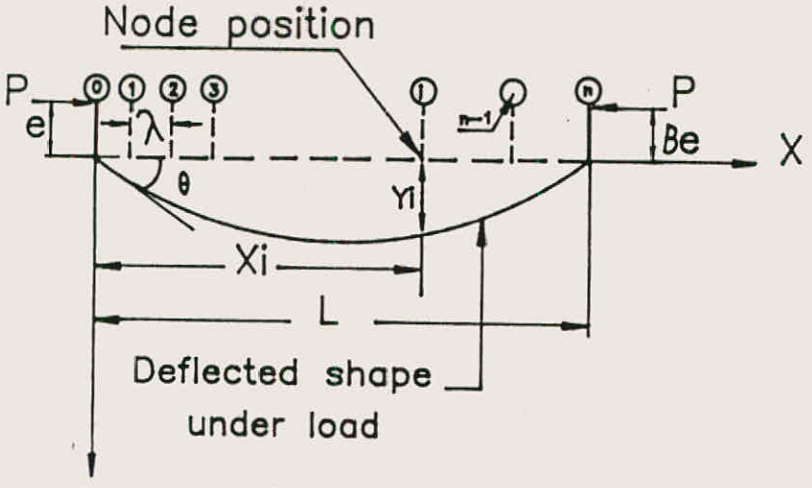

FIG.(2.3) Applied loading system .

The numerical integration process for determining the equilibrium shape of the deflected column is based on assuming values for the initial deflections Yi due to the loading. For convenience, the deflections obtained from an elastic solution [14] for the column, are used as initial approximation and are given by:

$$Y_i = e\left[\frac{\beta \text{ Sin } KL(i/n) + \text{Sin } KL\,(1-i/n)}{\text{Sin } KL} - 1 + (1-\beta)\, i/n\right]$$

$$i = 0,1,2,.....,n \qquad (2.17)$$

Where $K = \sqrt{(P/EI)}$, and EI is the elastic flexural rigidity of the column section.

For plain steel sections, the EI value corresponds to the slope of the initial straight portion of M-Φ-P curves. For composite sections, the M-Φ-P curves do not have an initial elastic region and the initial slopes of curves for the various axial loads may differ quite considerabley, and therefore the EI value is taken as the slope at the origin of the M-Φ-P curve corresponding to the axial load under consideration. This means that the assumed deflections as calculated by equation (2.17) will always be smaller than the true deflections.This will avoid the possibility of computing

moments that exceed the maximum value of the column for the axial load concerned and indicating, incorrectly, that the iteration process did not converge.

For a given load increment (Pinc), the failure length (Lc) can be calculated as follows:

$$L_c = \mu \pi \sqrt{\frac{EI_{(pinc)}}{P_{inc}}} \qquad (2.18)$$

Where μ is a constant depends on the eccentricity ratio (β). Values of μ can be given as follows:

$\mu = 1.$ for $\beta = 0., 0.5$ and $1.$ (single curvature)
$\mu = 1.5$ for $\beta = -0.5$ (double curvature)
$\mu = 2.0$ for $\beta = -1.0$ (double curvature)

Having obtained values for the assumed deflections as given by equation (2.16) for the given loading (see Figure 2.3) and section parameters involved, Newmark's integration procedure [9] is used to successively correct these values until the true deflected shape of the column is obtained to the desired accuracy. The steps involved in this process are as follows:

Step 1. Compute the moment of resistance at the node points due to the deflections Yi, as follows:

$$M_{Ri} = P\, e\left[\, 1 - (1-\beta)\, \frac{i}{n} \,\right] + PY_i$$

$$i = 0,1,2,\ldots,n \qquad (2.19)$$

Step 2. Refer to the M-Φ curve for the axial load concerned and obtain, by interpolation, the curvature at node points Φi (i=0,1,...,n) corresponding to the node moment computed above.

Step 3. Compute the equivalent concentrated angle changes (i.e curvatures) at node points, as follows:

$$(\phi\lambda)_i = (\phi\lambda)_{i-1} \qquad i=1,2,\ldots,n \tag{2.20}$$

Step 4. Compute the values for the uncorrected slopes between node positions, as follows:

$$S_o = 0.$$

$$S_i = \sum_{k=1}^{i} (\phi\lambda)_k \qquad i=1,2,\ldots,n \tag{2.21}$$

Step 5. Compute the uncorrected deflections at the node position as follows:

$$U_o = 0.$$

$$U_i = \sum_{k=1}^{i} S_k \lambda \qquad i=1,2,\ldots,n \tag{2.22}$$

Step 6. Apply a linear correction to the previous deflections (ui) to obtain zero deflection at both ends of the column and therefore a new set of values for the deflections are given by:

$$\overline{Y}_i = U_i - i\, U_n/n \qquad i=0,1,2,\ldots,n \tag{2.23}$$

Step 7. Replace the assumed values for Yi used in step 1 by the new values $\bar{Y}i$ calculated in step 6 and repeat step 1 to step 6 until convegence is obtained to the desired accuracy. For the purpose of this study, this condition is assumed satisfactory if for all nodes

$$| Y_i - \bar{Y}_i | \leq 0.0001 \quad i=1,2,\ldots,n \tag{2.24}$$

If the required convergence can not be obtained within a reasonable number of cycles (depending on the accuracy desired), or if the moment at any node during the iterations exceeds the maximum moment of the section corresponding to the applied end load, it is concluded that the eccentricity is too high for equilibrium to be possible.

If the moment-rotation characteristics for the column section are required, the deflections can be used to calculate the end rotation of the column. Assuming that the deflected shape within two end segments can be represented by a parbola, the end rotation in terms of the known deflections (see Figure 2.3) is given by:

$$\theta = (4 Y_1 - Y_2) / 2\lambda \tag{2.25}$$

2.8 COMPUTATION OF THE FAILURE LOADS FOR A SLENDER COLUMN:

Using the maximum eccentricity criterion, the method described in the previous section, can be used to determine the maximum value of the larger end eccentricity ,e (see Figure 2.3) that a given column can sustain for specified values of eccentricity ratio. The failure combination, of

the end moment and axial load, can be determined systematically for various lengths of a column. Then the interaction curves relating these quantities are constructed.

In the present investigation, all the calculation steps involved in evaluating the failure load-end moment combinations have been programmed using Fortran-77. For a given geometry of the column cross-section and the stress-strain properties of the materials, the computer produces, for specified lengths, the interaction curves corresponding to the given eccenticity ratio. Details of the computer program will be described in the next chapter, only an outline of the scheme of computation is given below.

Assuming that the M-Φ-P characteristics have already been calculated and stored, and that the specified eccentricity ratio and column lengths have also been stored , the steps embodied in the computer program are as follows:

Step 1. Take the first specified eccentricity ratio β.

Step 2. Take the first value of load increment (Pinc).

Step 3. Calculate EI, which is the slope of M-Φ curve at the origin for this load increment (Pinc).

Step 4. Calculate the critical length (Lc) for the specified load increment, and eccentricity ratio β as given by equation (2.16) in the previous section.

Step 5. Take the first value of the length L.

Step 6. Compare the given length L with the critical length (Lc) computed in step 4. If L is less than Lc, then go to step 7, otherwise

repeat both steps 2 and 3 for another load increment (Pinc).

Step 7. Assume an initial value of the larger of the two eccentricities (e) to be 0.005 Mu/Pinc

Step 8. Apply the method of previous section, to ascertain whether or not the equilibrium is possible for the assumed end eccentricity of loading, this can be demonstrated as follows:

When the condition as given by equation (2.22) in the previous section is achieved, the equilibrium is possible, then calculate the rotation as given by equation (2.23). Then increase the applied eccentricity by 0.005 Mu/Pinc, until the resistant moment as given by equation (2.17) exceeds the maximum moment for this load increment (Pinc), at this stage print out the non-dimensional values Pinc/Pu and e Pinc/Mu.

Step 9. Repeat steps 3 to 8 for other values of load increment.

CHAPTER III

COMPUTER PROGRAM

The computational procedure described previously in chapter II was programmed by FORTRAN-77 language, using the VAX-8700 computer of the Faculty of Engineering and Technology at the University of Jordan. A simplified flow chart of the main program is shown in Figure (3.1). A listing of the program is presented in a seperate report submitted to the Department of Civil Engineering.

The program starts by calling subroutine DATA, which reads and prints the input data, related to the geometrical properties of the column, the material properties and the eccentricity ratio (β).

Subroutine LZERO is then called by the main program to compute the failure loads for the battened composite column section bending about the minor axis. These failure loads are computed as a non-dimensional values of the axial load (P/Pu) and bending moment (M/Mu) for the case of zero-length column (i.e L/D=0).

The squash load (Pu) and the concrete contribution factor ,αc, are also computed using this subroutine. Also using the same subroutine, the ultimate bending moment ,Mu, is computed by linear interpolation, of the data previously computed (P/Pu & M/Mu) for an axial load ,P, equal to zero.

Subroutine MOMCURV is then called by the main program to compute the moment-curvature ($M-\Phi$) values for the battened composite column section for a given increment of axial load.

After that, Subroutine NEWMARK is called by the main program to compute the failure loads, for a given eccentricity ratio (β), and for slenderness ratio of L/D=10,20,30 & 40.

Subroutine DRAWMC is then called by the main program to plot the moment-curvature (M-Φ) values for the given load increments computed previously by subroutine MOMCURV. Those values, when plotted against each other, are called the Moment-Curvature-Thrust (M-Φ-P) curves*.

Finally, subroutine DRAWIA, is called by the main program, to plot the failure loads (P/Pu Vs. M/Mu), which were computed previously by subroutine LZERO for L/D=0, and subroutine NEWMARK for L/D=10,20,30 & 40 respectivly.

For each slenderness ratio (L/D), the above computed failure loads are expressed by an interaction curve showing the reduction in the axial load with increase in the moment. Usually these curves are called The Ultimate Strength Interaction curves*.

---

* These curves are plotted using the HGRAPH backage which is installed on the VAX -8700 computer.

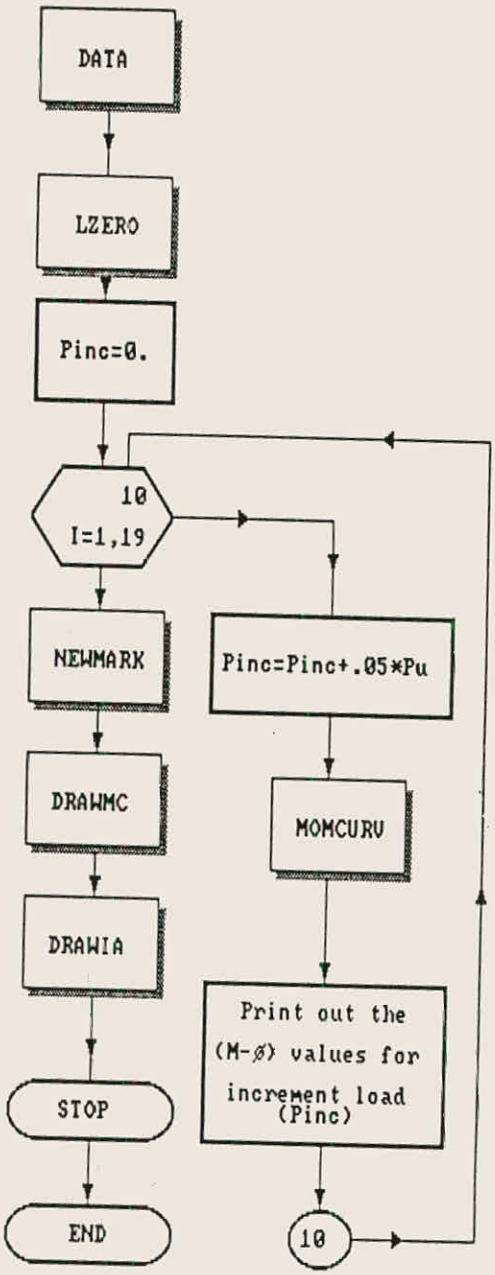

FIG. (3.1) Flow chart of the main program

3.1 LZERO ROUTINE.

The computational procedure described in section (2.5)of chapter II is used in this routine to compute the failure loads for a slenderness ratio (L/D) equal to zero. A simplified flow chart of this routine can be seen in Figure (3.2).

The computation of the failure load values involves the moment (M), the axial load (P), and the depth of yielding (Dy) across the column section. These calculations are based upon a compressive stress for concrete equal to 0.67*Fcu and a stress of Fy for steel.

The battend composite column section is subdivided into ten blocks of structural steel and seven blocks of concrete. Each of these blocks is then subdivided into a large number of small size strip elements (see Fig. 2.2 of chapter II).

In each strip element, for a given value of depth of yeilding (Dy), the stress is computed depending on the material composed in this strip element. Then the values of P and M can be calculated for each strip, and by summation, the axial force and bending moment in each block is computed. The resultant P and M will be evaluated for the specified values of Dy, by adding the axial loads and bending moments for all blocks, as given by equations (2.14), (2.15) of chapter II. Then each value of P and M is divided by Pu and Mu to give the non-dimensional values P/Pu and M/Mu respectively. A simplified flow chart of the computation of the axial loads and bending moments in a block is shown in Figure (3.3).

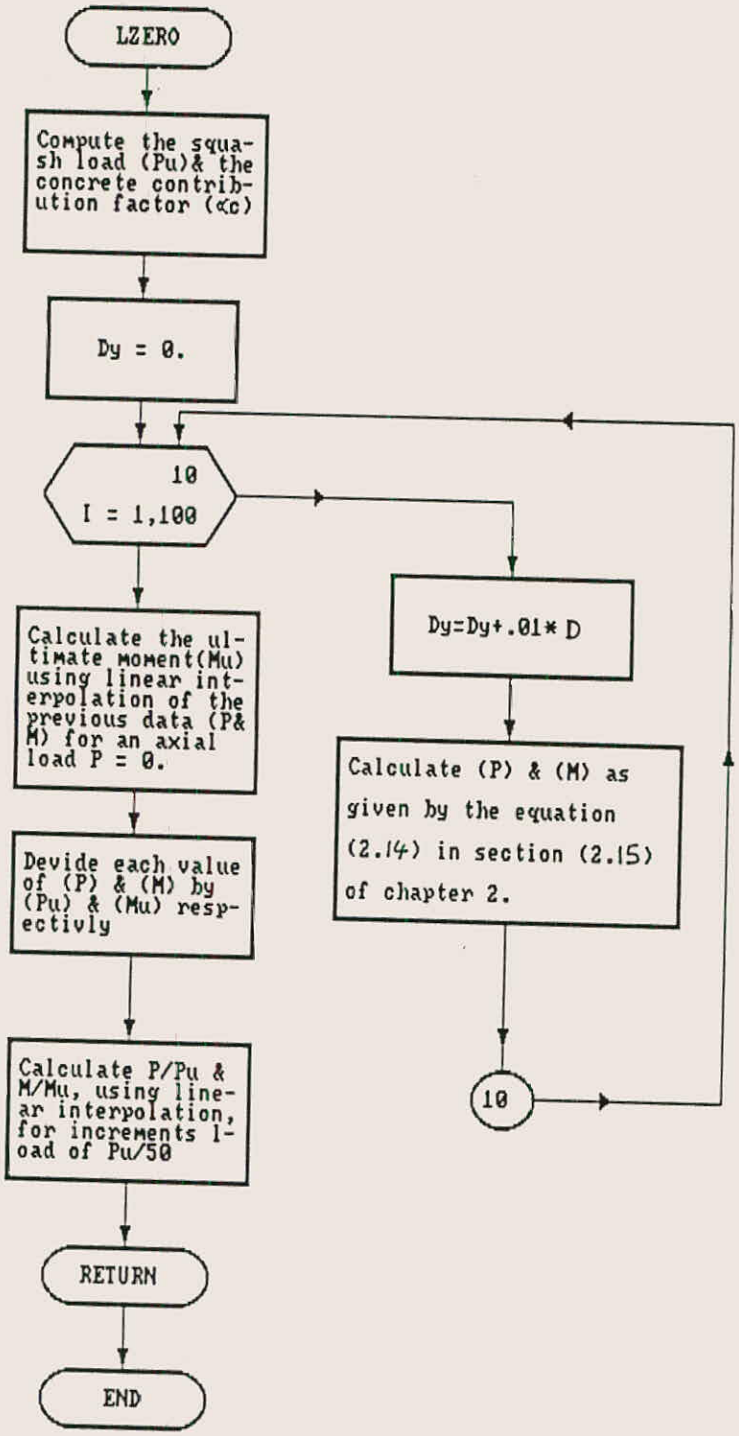

FIG. (3.2) Flow chart of LZERO Subroutine.

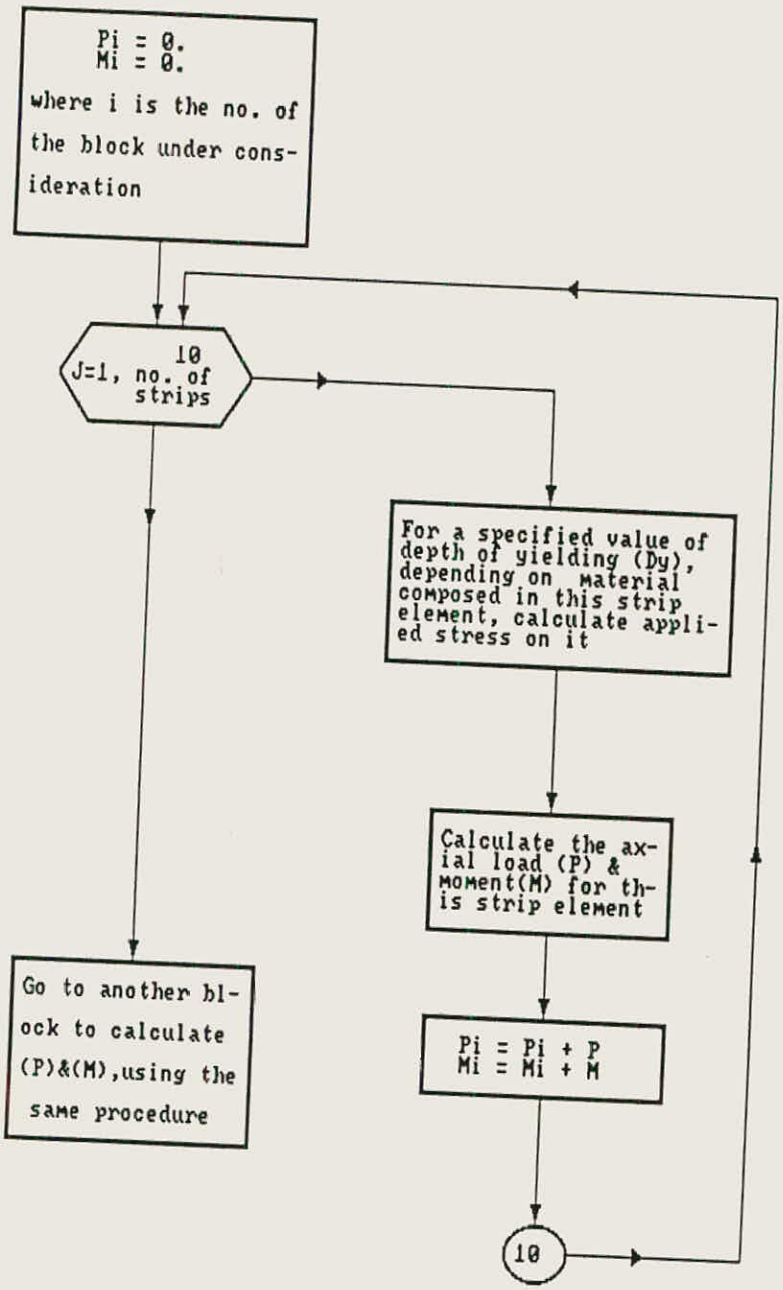

FIG. (3-3) Flow chart for calculating the axial loads and bending moments in a block.

3.2 MOMCURV ROUTINE.

This routine includes the computational procedure described previously in section (2.6) of chapter II. The moment-curvature (M-Φ) values are computed by calling this routine for a desired increment of axial load. A simplified flow chart of this routine can be seen in Figure (3.4).

The computation of M-Φ values involves the moment (M), the axial load (P); the curvature (Φ) and the neutral axis (Dn). The last two specify the strain distribution across the column section.

The same procedure described previously in subroutine LZERO for calculating the resultant axial load (P) and bending moment (M) is also used in subroutine MOMCURV with minor modifications related to the induced sresses for both concrete and steel.

Then for the desired increment of axial load (P), using linear interpolation, the moment-curvature (M-Φ) values are calculated.

The computation of moment-curvature values for each increment of axial load is terminated when the value of the bending moment starts to decrease for increasing values of curvature (Φ). For the purpose of plotting the (M-Φ) relations, the computation is extended for five curvature increments beyond the maximum value. A simplified flow chart for calculating the axial loads and bending moments in a block is shown in Figure (3.5).

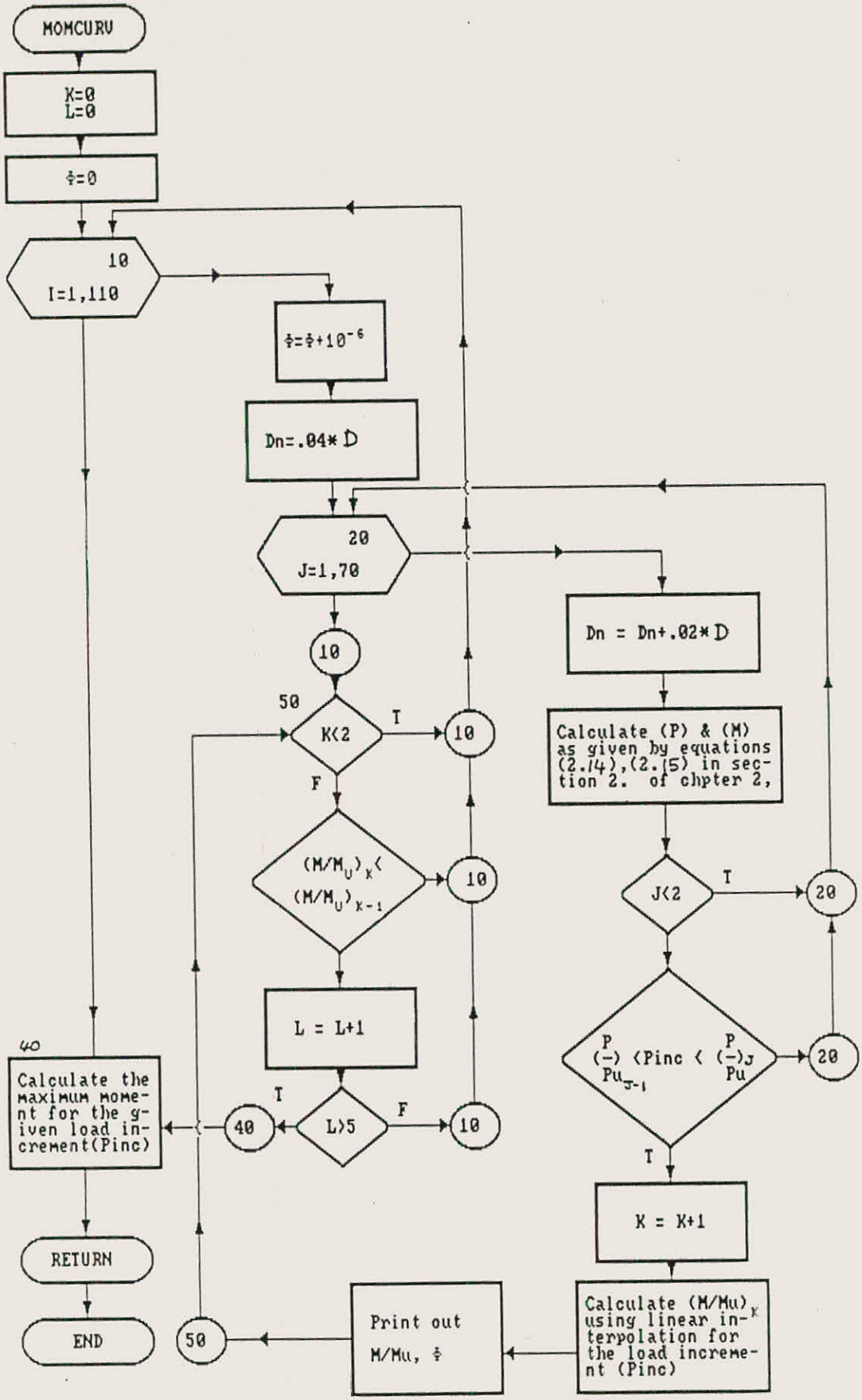

FIG. (3.4) Flow chart of the MOMCURV Subroutine.

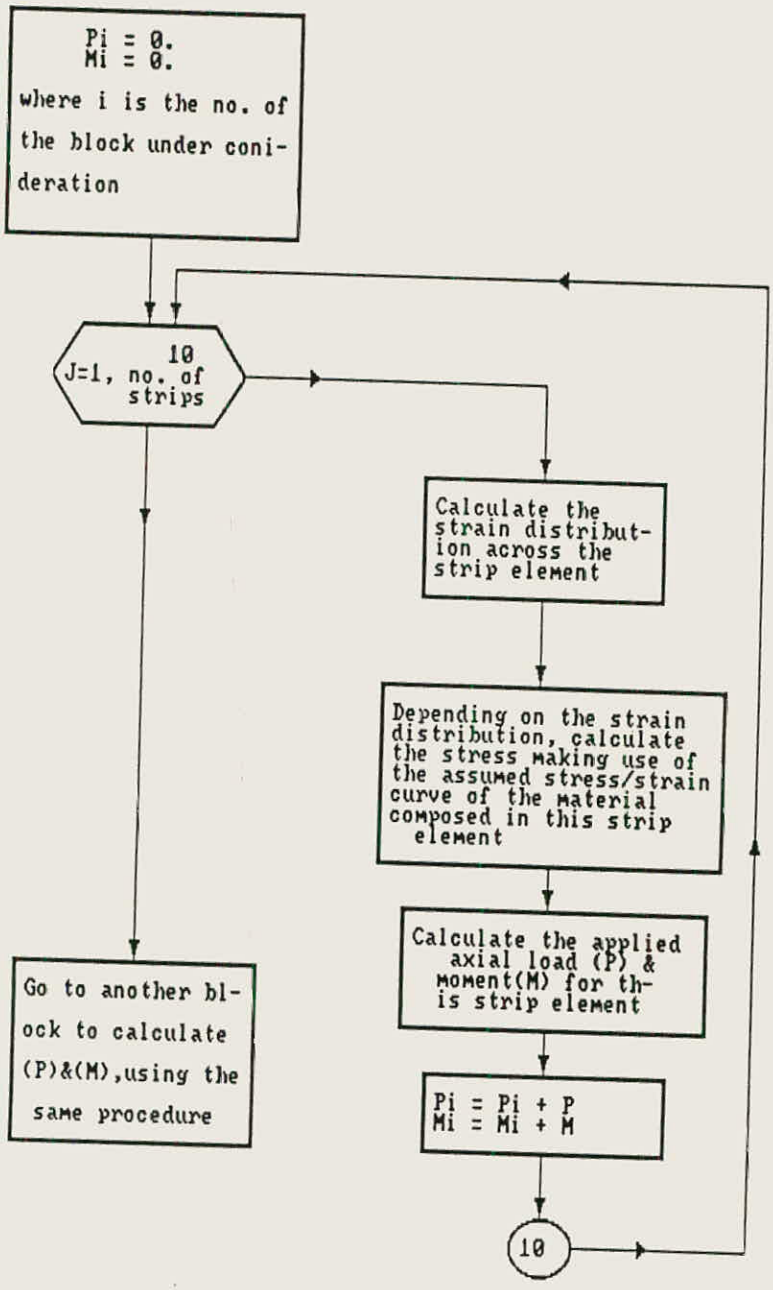

FIG. (3.5) Flow chart for calculating the axial loads and bending moments in a block.

3.3 NEWMARK ROUTINE.

Subroutine NEWMARK is called by the main program, to compute the failure load using the maximum eccentricity criterion described previously in section (2.8) of chapter II. A simplified flow chart of this routine is shown in Figure (3.6).

In computing the failure end moments; increments of 0.005Mu were incorporated until the maximum moment, corresponding to the applied end load at any node during the iteration, is exceeded, or the required convergence can not be obtained within "the fifty cycles" used in this research as a limit to the convergence process. This means that the eccentricity is too high for equilibrium to be possible(i.e critical end bending moment).

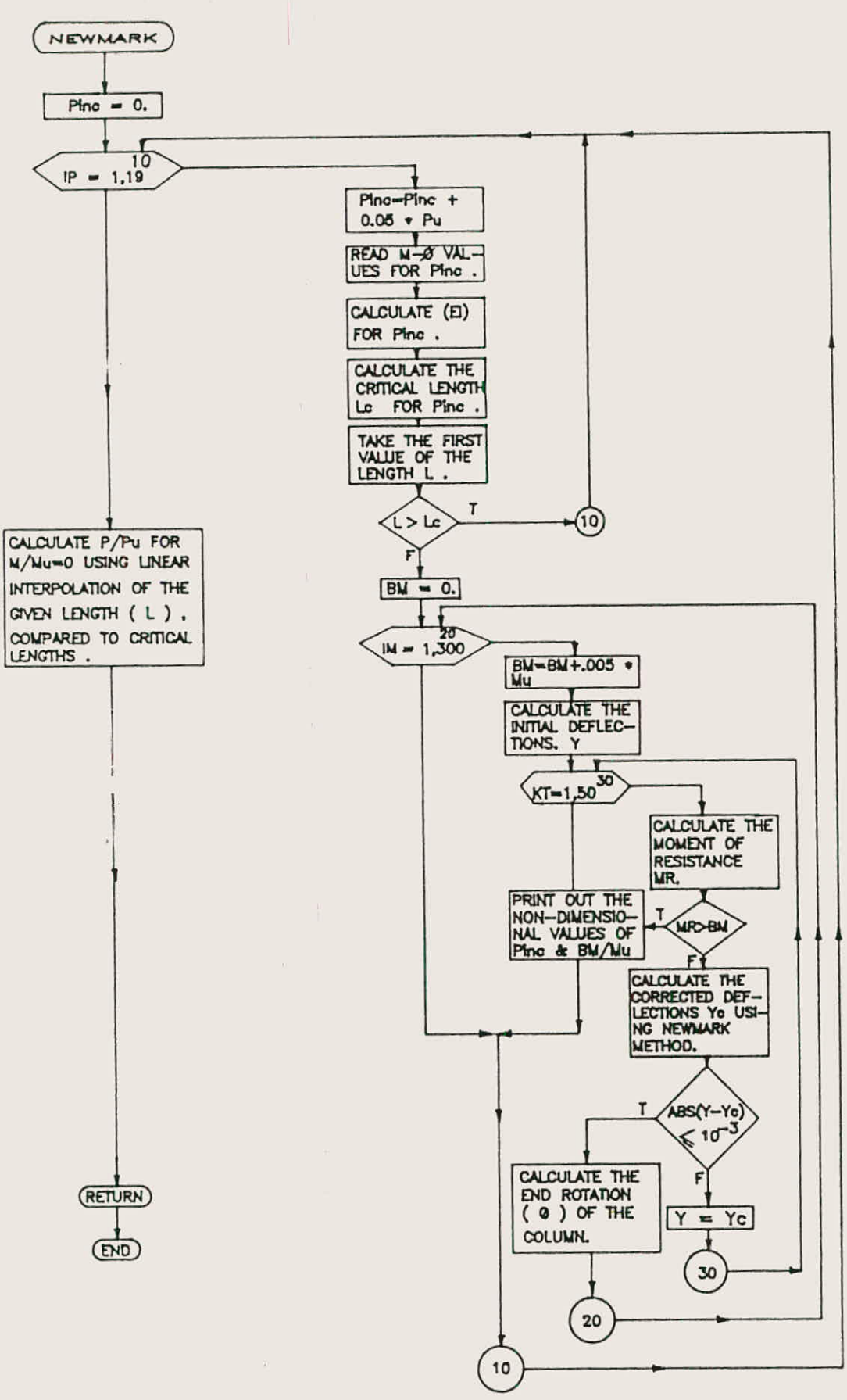

FIG.(3.6) FLOW CHART OF THE NEWMARK ROUTINE

CHAPTER IV

NUMERICAL RESULTS AND DISCUSSION

It is known that a compression member subjected to axial load rarely, if ever, exists. Thus all columns are considered to be subjected to some moment, which may be due to end restraint from the monolithic placement of floor beams and columns, or due to accidental eccentricity from imperfect alignment and variable material. According to BS499 , such columns in a building-frame may be considered in isolation and treated as being pin-ended and eccentrically loaded.

The above fact is taken into acount in calculating the failure loads for five different battened composite column sections, under applied load of equal and unequal end eccentricities, and having different slenderness ratios.

The failure loads of a column can be expressed by an interaction curve showing the reduction in the axial load associated with an increase in the moment. Equilibrium conditions and the moment-curvature-thrust relationships, for the column, are the two basic requirements for computing its strength.

Most of the moment-curvature curves and interaction diagrams are presented in Appendix [C] . Also, samples of the computer output results, related to these curves, are presented in appendix [B].

The effect, of several parameters on the strength and ductility of the battened composite column section, is taken

into acount through the discussion.

The validity of the present method is demonstrated by comparison with the available test results for the battened composite columns, tested elswhere [7], and a good agreement is found as will be seen in this chapter.

4.1 COLUMN SECTION PROPERTIES:

Five different battened composite column sections are selected for the anlysis. The properties of these sections are presented in Table (4.1).

In selecting these sections, the following limitations were applied:

1. The most commonly used channels in steel construction, were selected in forming these sections.
2. The smallest and largest channels included, were C152x76x6.4 and C381x102x10.4.
3. Several sectional widths were used, which give different concrete contribution factors (αc)* ; to see the effect of the concrete area on the column strength.
4. The sectional dimensions of the column were selected such that:

   Depth < Width < 3*Depth

---

* αc can be defined as the ratio of the resultant product of the maximum concrete stress and concrete area to the squash load (i.e $\alpha c = 0.67*Fcu*Ac/Pu$).

Col. No.	Size of channel mmxmm	Wedth of colum B mm	Steel channels			Concrete core				Squash load Pu KN	Ultimate moment Mu KN.m	Concrete contribution factor ∝c
			Area As/2 cm^2	Yield strengt Fy N/mm^2	Elastic modulus Es Kn/mm^2	Area Ac mm^2	Cube strength Fcu N/mm^2	Elastic modulus Ec KN/mm^2	Ultimate concrete strain εcu			
1	152x76	275.	22.77	275.	200.	373.56	30	30.13	0.006	2003.21	79.76	0.375
2	203x89	375.	37.94	275.	200.	686.12	30	30.13	0.006	3465.8	177.07	0.398
3	254x89	450.	45.52	275.	200.	1051.96	30	30.13	0.006	4618.04	263.56	0.458
4	305x10	525.	58.83	275.	200.	1482.54	30	30.13	0.006	6215.56	409.43	0.479
5	381x10	600.	70.19	275.	200.	2145.62	30	30.13	0.006	8173.15	614.10	0.528

Table (4.1) Properties of column sections.

4.2 CASES OF LOADING:

For each column section, described previously in sectio (4.1), five cases of loading were investigated for lengths within the range ($0 \leq L/D \leq 40$), which includes both short and long columns as defined by CP114. These cases shown in Figure (4.1), are as follows:

Case 1 : End moment applied at one end of the column, (single curvature : $\beta = 0.0$).

Case 2 : End moment applied at one end, and half of it is applied at the other end, (single curvature : $\beta = 0.5$).

Case 3 : Equal moment at both ends of the column, (single curvature : $\beta = 1.0$).

Case 4 : End moment applied at one end, and half of it, but in oppsite direction, is applied at the other end, (double curvature $\beta = -0.5$).

Case 5 : Equal end moment at both ends of the column with opposite sense, (double curvature : $\beta = -1.0$).

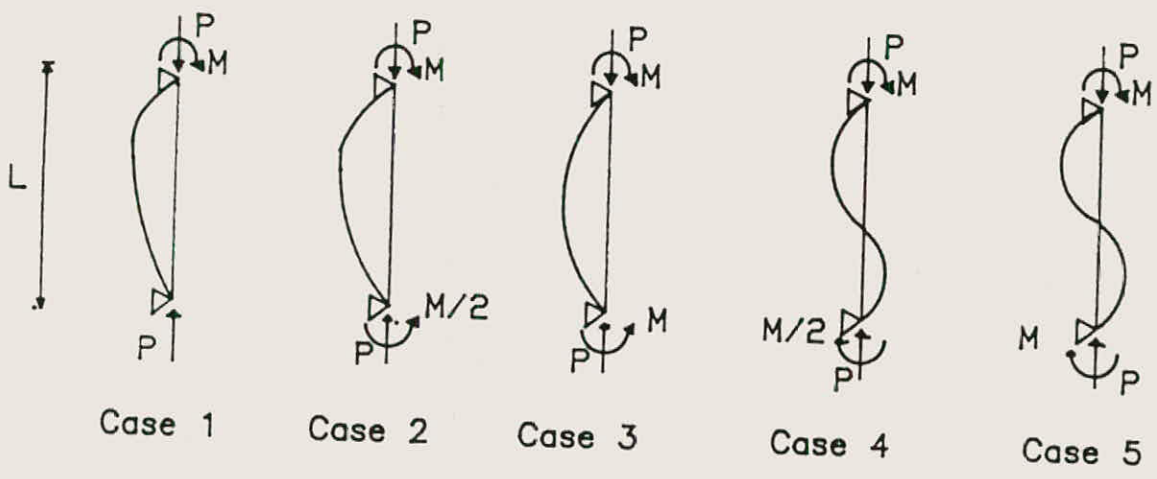

FIG.(4.1) Cases of loading

4.3 M-Φ-P RELATIONSHIPS:

In calculating the M-Φ values, it was assumed that the column cross section composed of a small size strip elements. It has been found out that the steel elements have a great influence on the accuracy of the results, than those for concrete. Therefore larger number of steel elements were used in the analysis.

Figures 4.2 and 4.3 show the M-Φ curves for sections number 1 and 3 of the battened composite column. These curves present the combinations of non-dimensional values of the moment (M/Mu), axial load (P/Pu), and the curvature (Φ).

For the purpose of plotting, load increments of 0.1Pu were used while increments of 0.05 Pu were adopted in the analysis. It should be mentioned that the part of the M-Φ curves beyond the peak is considered of no interest in this investigation, and hence, in plotting the results, only five points were considered beyond the peak.

As can be seen from Figures 4.2 and 4.3, there is a sharp drop in the M-Φ curves for each load increment when the maximum moment is reached. This is because the concrete is modelled by a stress-strain relationship in which the stress drops suddenly to zero at ultimate strain ($\in_{cu}$).

Also it can be seen from these Figures, that when the load increment (beyond 0.2 Pu) increases, the maximum moment and curvature decrease.

Unlike the bare steel column, in which the moment capacity never exceeds the ultimate moment, the battened composite column (as well as other composite columns) shows

an increase in the moment capacity (beyond the ultimate moment) at relatively low values of axial load. This increase in the moment capacity proved to be dependent on the concrete contribution to the total area of the section and its strength.

More about moment curvature curves is presented next in section 4.5, through studying the effect of many parameters, such as the concrete strength, ultimate concrete strain, yield strength of steel.....etc, on the column strength.

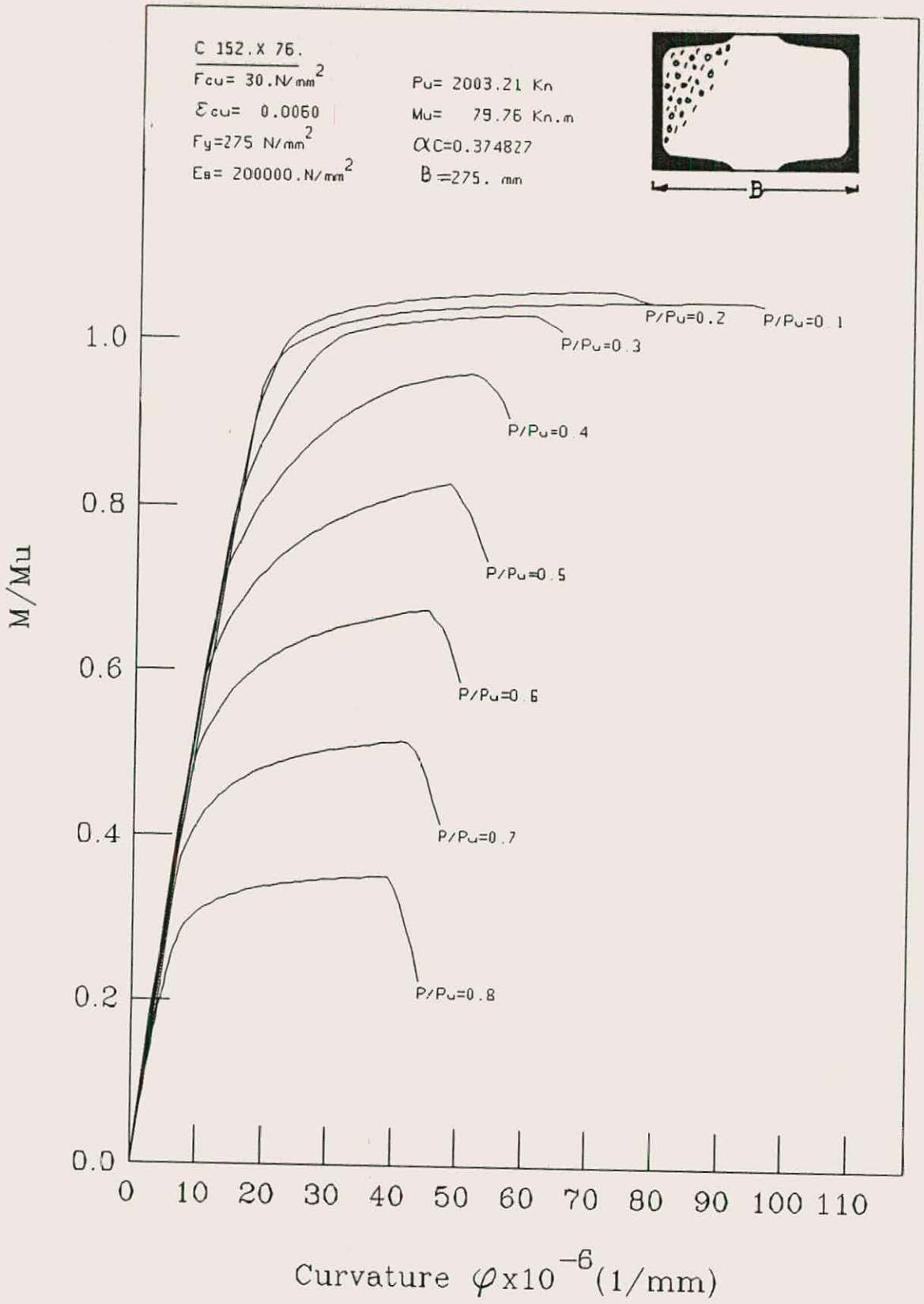

FIG.(4.2):MOMENT-CURVATURE-THRUST CURVES FOR BATTENED COMPOSITE COLUMN UNDER UNIAXIAL BENDING MOMENT ABOUT MINOR AXIS .

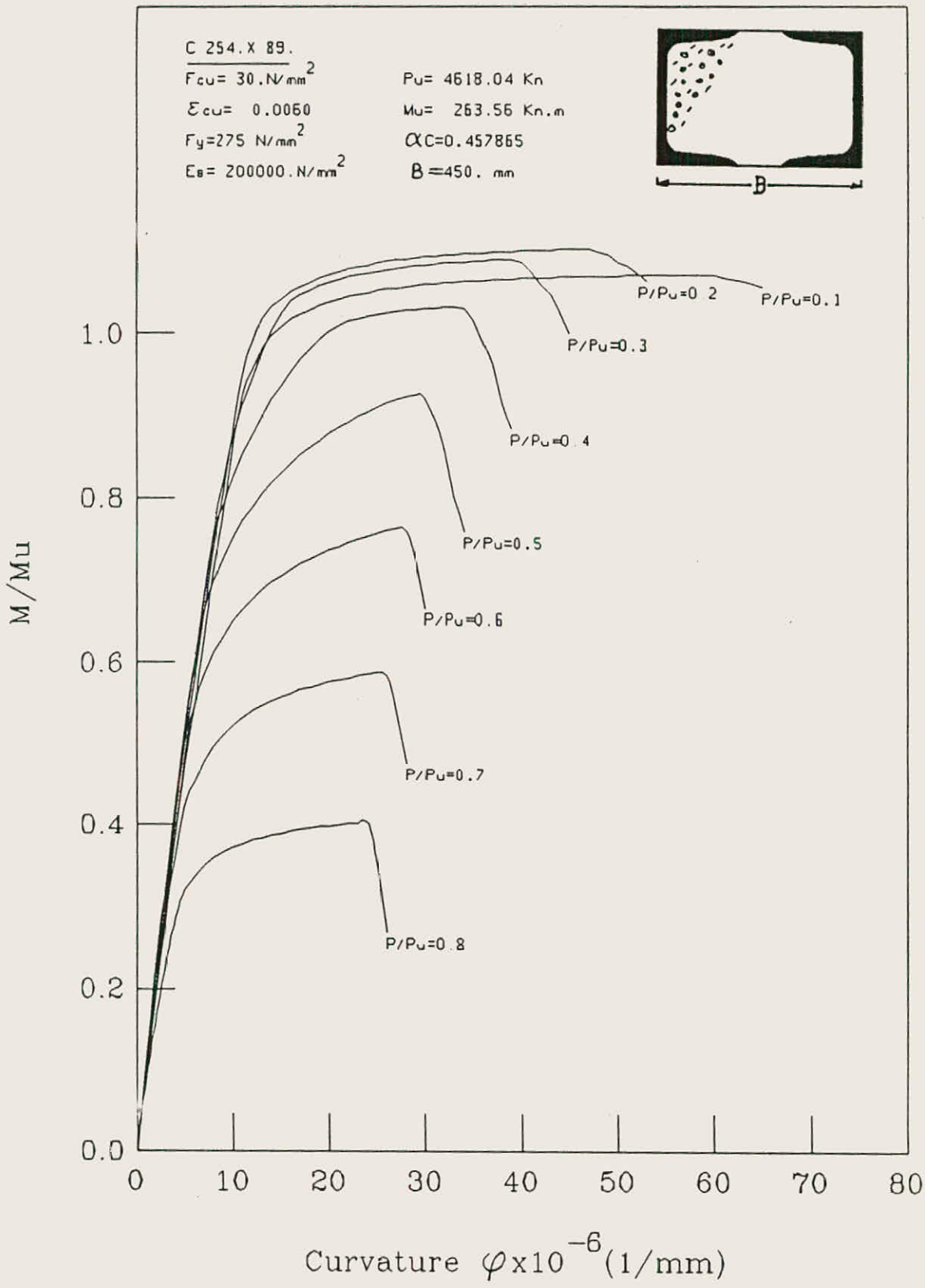

FIG.(4-3):MOMENT-CURVATURE-THRUST CURVES FOR BATTENED COMPOSITE COLUMN UNDER UNIAXIAL BENDING MOMENT ABOUT MINOR AXIS .

4.4 FAILURE LOAD, LENGTH AND ECCENTRICITY RELATIONSHIPS:

In computing the failure loads, it is essential to determine the true equilibrium shape of the column. For this purpose Newmark numerical integration process was used in this investigation. This process is based on assuming values of the initial deflections (Y) due to loading. For convenience, the initial deflections are obtained from an elastic solution [14].

The tangent flexural rigidity (EI) is the most important variable which controls the deflections (Y). As mentioned before, EI value is taken as the slope at the origin of the M-Φ-P curves corresponding to the axial load under consideration. This means that the assumed deflections (Y) will always be smaller than the true deflections and this will avoid the possibility of calculating moments that exceed the maximum moment value of the column for the particular axial load concerned.

Interaction curves for column sections 1 and 3 for β values of 0.0,1.0 and -1.0 are presented in Figures 4.4 to 4.9.

It can be seen from the Figures, that columns of slenderness ratios (L/D) of 20, develop the full flexural strength of the section, and beyond this range failure occurs due to some form of instability before reaching the full flexural strength. Therefore, it can be emphasized that there is a range of slender columns for which design can not be based upon the assumption of reaching full flexural strength.

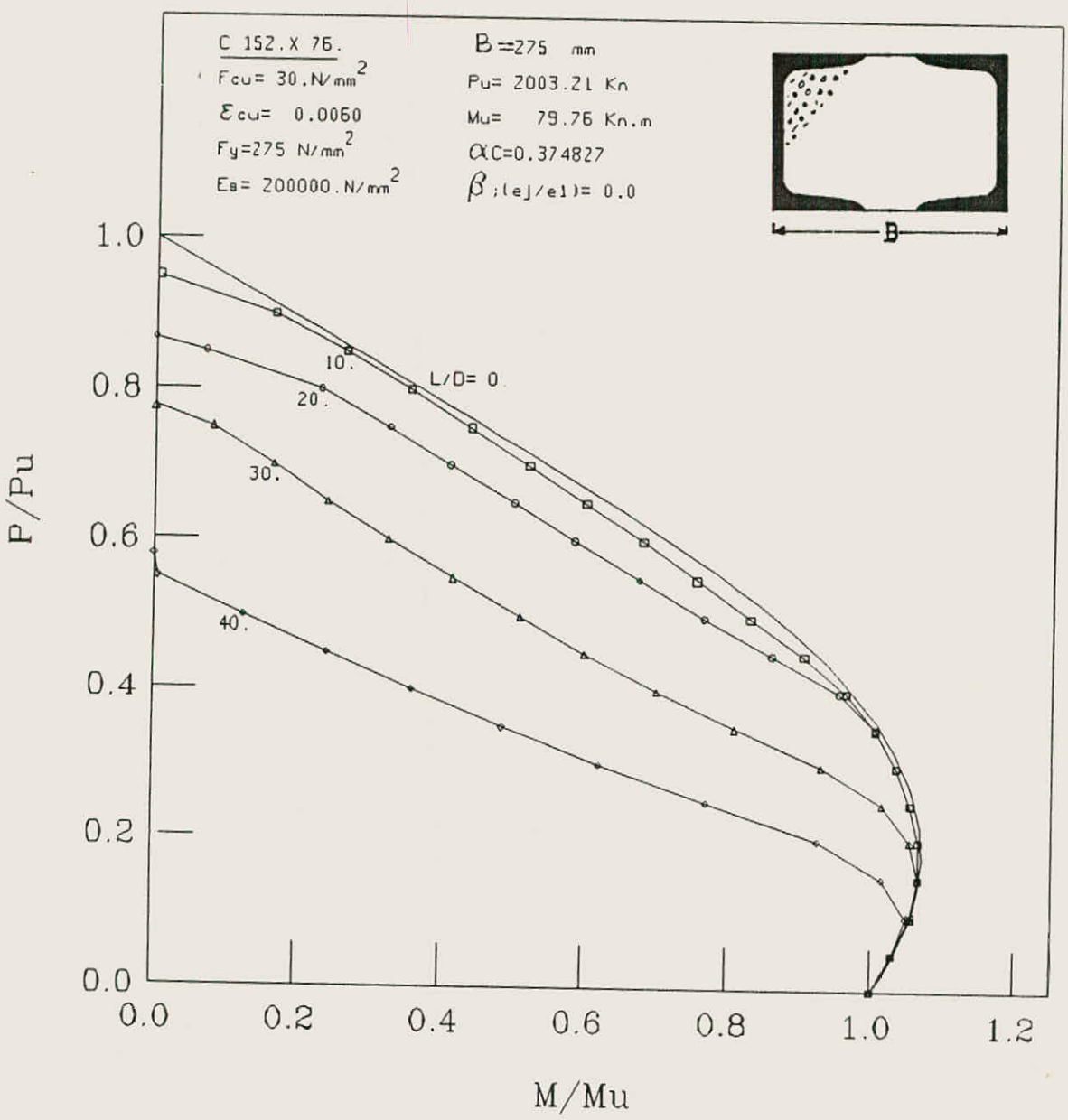

FIG. (4-4): ULTIMATE STRENGTH INTERACTION CURVES FOR SLENDER BATTENED COMPOSITE COLUMN UNDER UNIAXIAL BENDING MOMENT ABOUT MINOR AXIS

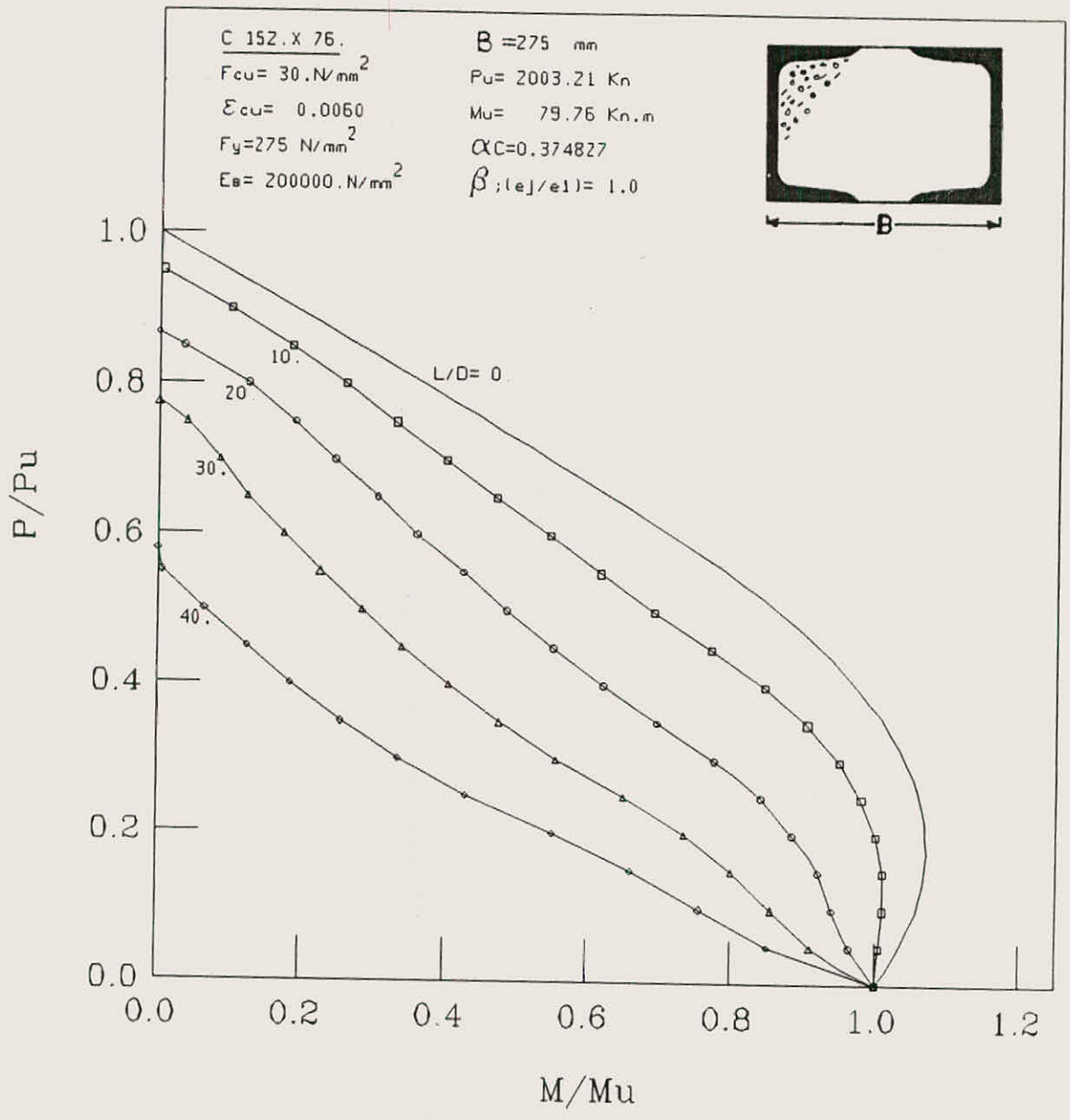

FIG. (4-5): ULTIMATE STRENGTH INTERACTION CURVES FOR SLENDER BATTENED COMPOSITE COLUMN UNDER UNIAXIAL BENDING MOMENT ABOUT MINOR AXIS

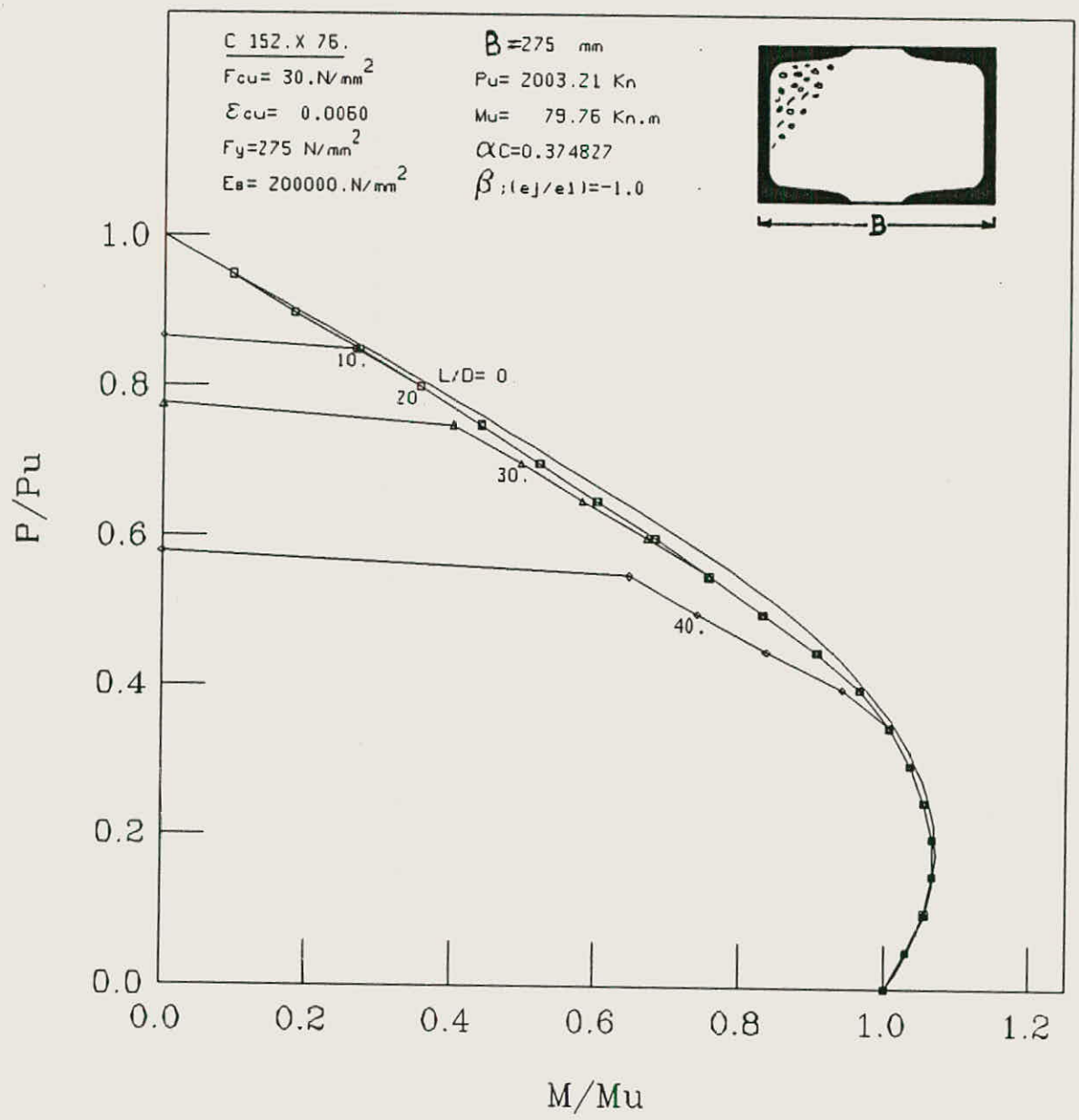

FIG.(4.6):ULTIMATE STRENGTH INTERACTION CURVES FOR SLENDER BATTENED COMPOSITE COLUMN UNDER UNIAXIAL BENDING MOMENT ABOUT MINOR AXIS

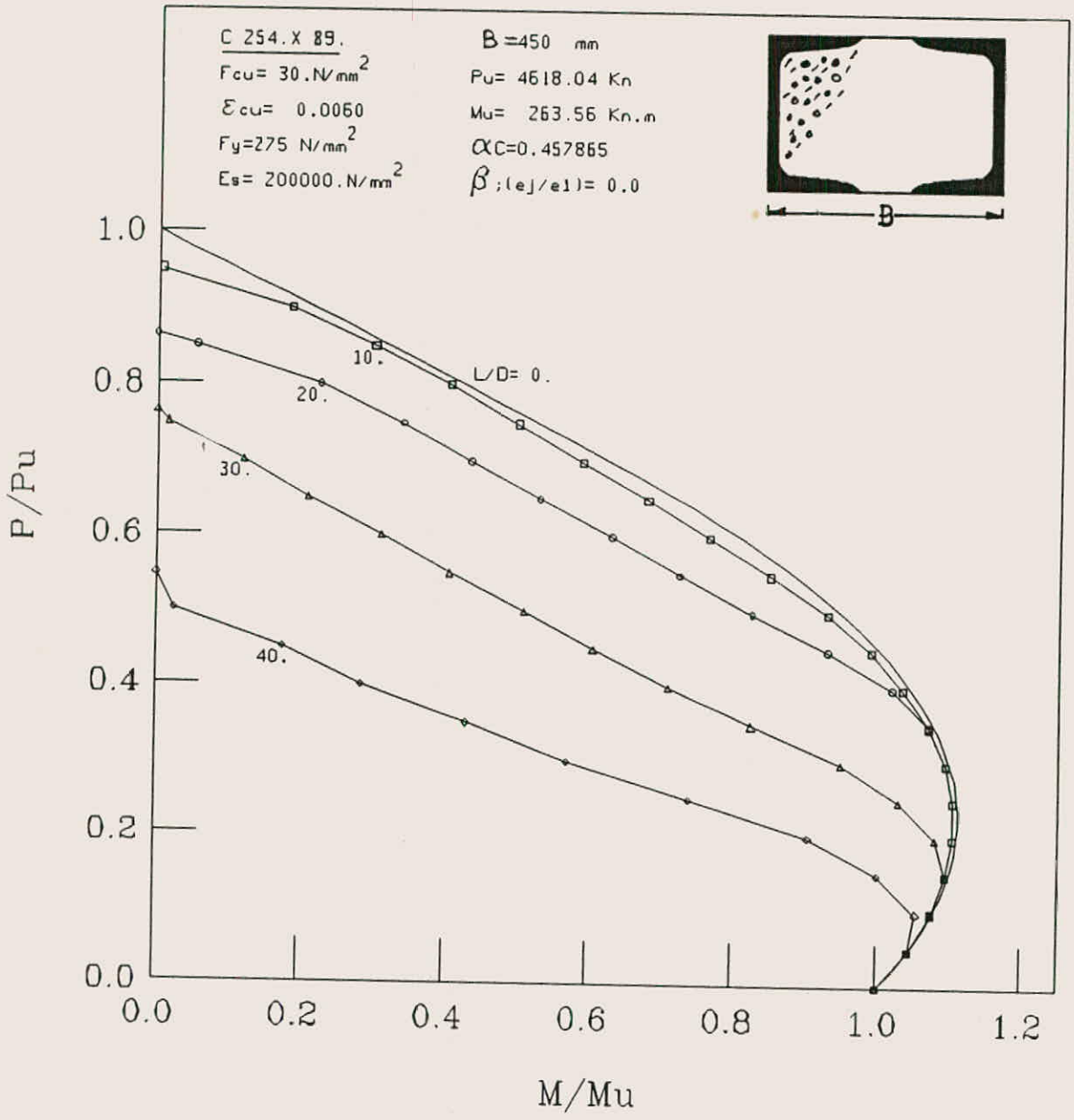

FIG. (4.7): ULTIMATE STRENGTH INTERACTION CURVES FOR SLENDER BATTENED COMPOSITE COLUMN UNDER UNIAXIAL BENDING MOMENT ABOUT MINOR AXIS

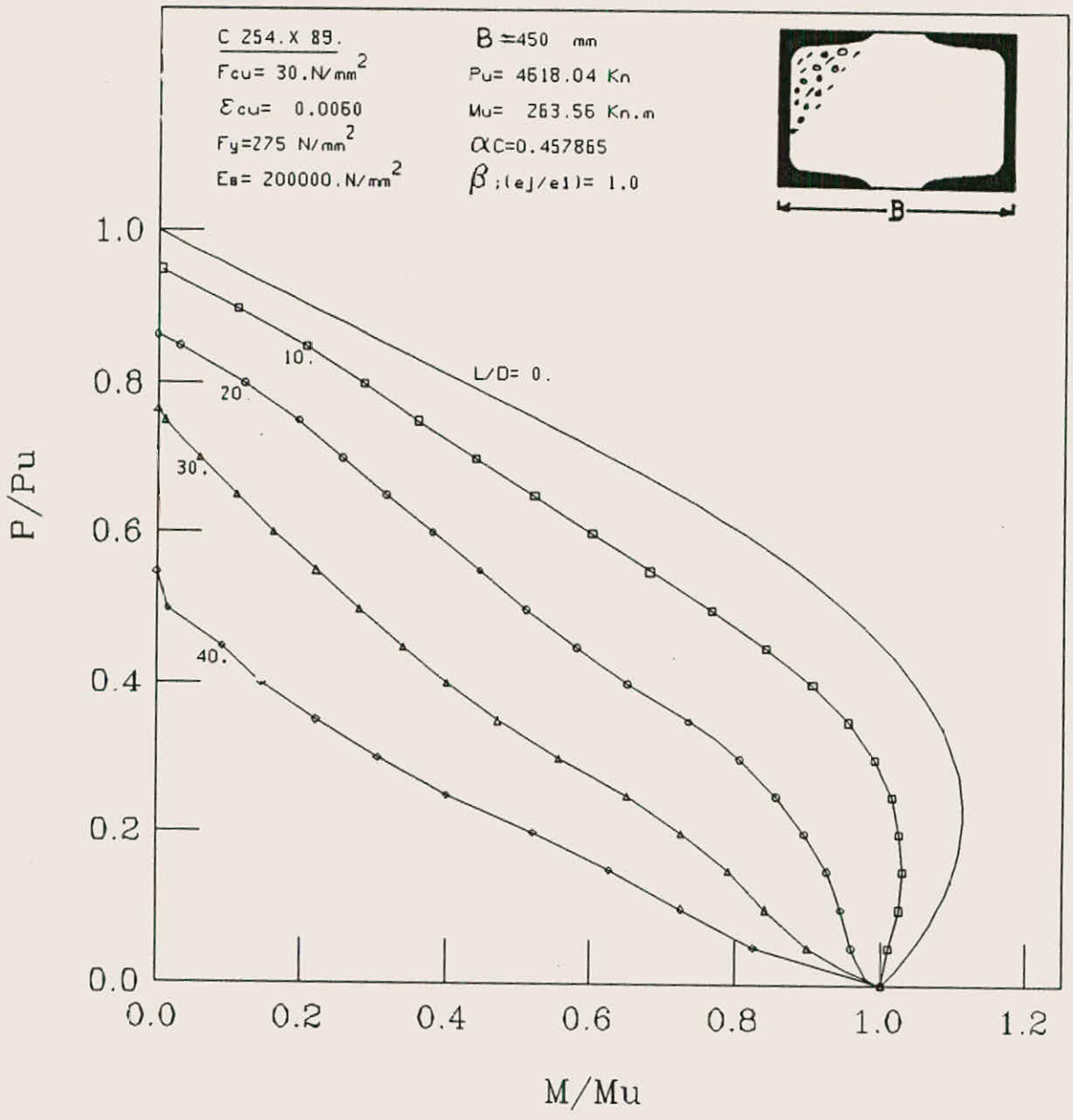

FIG.(4-8): ULTIMATE STRENGTH INTERACTION CURVES FOR SLENDER BATTENED COMPOSITE COLUMN UNDER UNIAXIAL BENDING MOMENT ABOUT MINOR AXIS

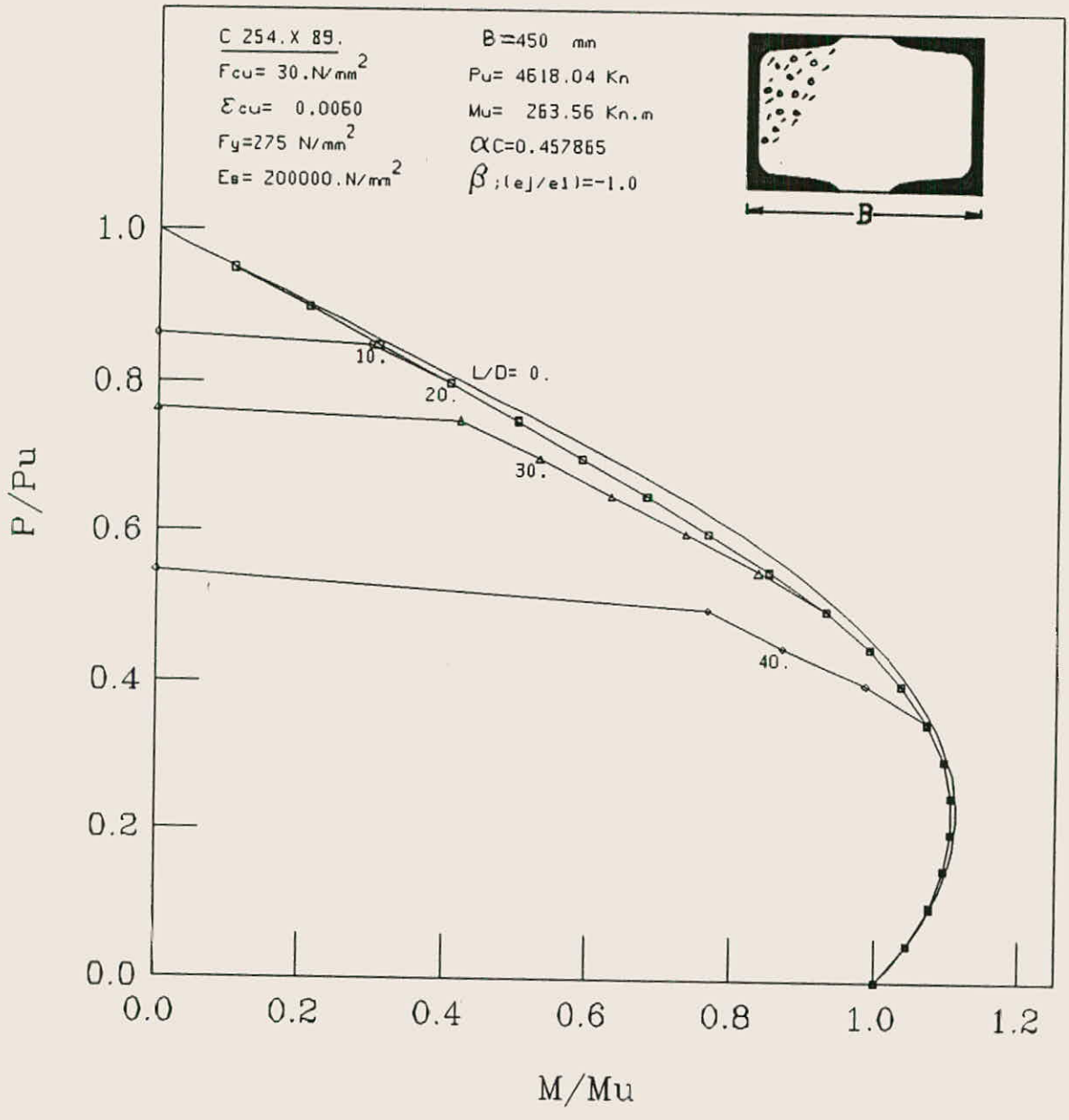

FIG.(49):ULTIMATE STRENGTH INTERACTION CURVES FOR SLENDER BATTENED COMPOSITE COLUMN UNDER UNIAXIAL BENDING MOMENT ABOUT MINOR AXIS

For short and medium length columns, the maximum failure moment occurs at a non-zero axial load. This can be seen from the Figures for failure moments (M/Mu) greater that unity. This increase in the moment capacity, beyond the ultimate moment (Mu), depends mainly on the area of the concrete in the section and its strength.

The effect of the column length on its strength can clearly be seen from these Figures. Significant loss of strength can be noticed for slender columns, while short ones showed little evidence of instability, even when subjected to large flexural loads.

Analytical results indicate that the column capacity increase as the eccentricity ratio (β) decreases from 1.0 to 0.0 for the case of single curvature bending. Comparison of results shows that this increase in the capacity is quite considerable for eccentrically slender columns.

Tables 4.2 and 4.3 show the effect of reducing β from 1.0 to 0.0 on the capacity of column sections number 1 and 3 for L/D ratio of 30 and 40*. As can be seen , the maximum increase in the column strength is about 0.4 Mu and this increase depends on the axial load level, as well as, on the concrete contribution factor (αc).

For the case of double curvature bending (i.e $\beta < 0.$), the column will be able to sustain a higher load compared to that under single curvature bending ($\beta \geq 0.$).

---

* These values are taken as examples for the purpose of

P/Pu	Section no. 1 Pu = 2003 Kn. Mu = 79.8 Kn.m			Section no. 3 Pu = 4618 Kn. Mu = 263.6 Kn.m		
	β=0.	β=1.	incr.*	β=0.	β=1.	incr.*
0.1	1.055	0.855	0.200	1.075	0.840	0.235
0.2	1.055	0.735	0.320	1.08	0.725	0.355
0.3	0.930	0.555	0.375	0.95	0.555	0.395
0.4	0.70	0.405	0.295	0.71	0.40	0.310
0.5	0.510	0.285	0.225	0.51	0.28	0.230
0.6	0.325	0.175	0.15	0.31	0.16	0.150

* Increase in column strength as a fraction of Mu.

Table (4.2) Increase in column strength (M/Mu) due to reduction of β from 1.0 to 0. , L/d = 30

P/Pu	Section no. 1 Pu = 2003 Kn. Mu = 79.8 Kn.m			Section no. 3 Pu = 4618 Kn. Mu = 263.6 Kn.m		
	β=0.	β=1.	incr.*	β=0.	β=1.	incr.*
0.1	1.050	0.755	0.295	1.055	0.725	0.330
0.2	0.925	0.55	0.375	0.905	0.520	0.385
0.3	0.62	0.335	0.285	0.570	0.305	0.265
0.4	0.36	0.185	0.175	0.285	0.145	0.140
0.5	0.125	0.065	0.06	0.025	0.015	0.010
0.6	-	-	-	-	-	-

* Increase in column strength as a fraction of Mu.

Table (4.3) Increase in column strength (M/Mu) due to reduction of β from 1.0 to 0. , L/d = 40

Tables 4.4 and 4.5 show the increase in the column strength as a fraction of the ultimate moment (Mu) due to reduction of β from 0.0 to -1.0 for L/D ratio of 30 and 40 of column sections number 1 and 3.

As can be seen from the table, the maximum increase in strength is 0.43 Mu for L/d ratio of 30 and 0.74 Mu for L/D ratio of 40. It can also be noticed that the reduction of β from 0.0 to -1.0 is more effective at higher loads levels.

P/Pu	Section no. 1 Pu = 2003 Kn. Mu = 79.8 Kn.m			Section no. 3 Pu = 4618 Kn. Mu = 263.6 Kn.m		
	β=0.	β=-1	incr.*	β=0.	β=-1	incr.*
0.1	1.055	1.055	0.00	1.075	1.075	0.00
0.2	1.055	1.065	0.010	1.08	1.105	0.025
0.3	0.930	1.035	0.105	0.950	1.095	0.145
0.4	0.700	0.965	0.265	0.71	1.035	0.325
0.5	0.510	0.83	0.32	0.51	0.930	0.420
0.6	0.325	0.670	0.345	0.31	0.735	0.425

* Increase in column strength as a fraction of Mu.

Table (4.4) Increase in column strength (M/Mu) due to reduction of β from 0. to -1. , L/d = 30

P/Pu	Section no. 1 Pu = 2003 Kn. Mu = 79.8 Kn.m			Section no. 3 Pu = 4618 Kn. Mu = 263.6 Kn.m		
	β=0.	β=-1	incr.*	β=0.	β=-1	incr.*
0.1	1.050	1.055	0.005	1.055	1.075	0.020
0.2	0.925	1.065	0.140	0.905	1.105	0.200
0.3	0.620	1.035	0.415	0.570	1.095	0.525
0.4	0.360	0.940	0.58	0.285	0.985	0.700
0.5	0.125	0.740	0.615	0.025	0.765	0.74
0.6	-	-	-	-	-	-

* Increase in column strength as a fraction of Mu.

Table (4.5) Increase in column strength (M/Mu) due to reduction of β from 0. to -1 , L/d = 40

4.5 PARAMETRIC STUDY:

Analytical study, evaluating the effect of several parameters on the strength of the battened composite column, is undertaken in this section. Results obtained from such study, can provide a clear picture about which parameters are most effective for design rules, and how the future research can be directed for more understanding of the behaviour of the battened composite columns.

4.5.1 EFFECT OF THE ULTIMATE CONCRETE STRAIN (∈cu) ON THE COLUMN CAPACITY:

Among other parameters, the effect of varying the ultimate concrete strain on the column strength, was of a particular interest. In order to study the effect of this parameter, the column strength has been computed using a lower value of ∈cu=0.004.

The differences in the maximum moments (M/Mu) and concerned curvatures between results obtained for ∈cu = 0.006 and ∈cu = 0.004 are given in Table (4.6). It can be seen from this table, that the effect of this parameter is less pronounced when moments are concerned. The maximum difference between the two values of the maximum moment was found to be less than 5%.

It can also be seen from this table, that the effect of the parameter, in question, is more pronounced when the maximum curvatures are concerned. Differences in the curvature ranging between 31% and 45% were noticed due to the reduction of ∈cu from 0.006 to 0.004.

P/Pu	εcu = 0.006, Mu = 79.76 KN.m, Pu = 2003.21 KN.m		εcu = 0.004, Mu = 79.76 KN.m, Pu = 2003.21 KN.m		Differences	
	$(M/Mu)_{MAX}$	$\phi_{MAX}\times10^{-6}$	$(M/Mu)_{MAX}$	$\phi_{MAX}\times10^{-6}$	$\%\Delta(M/Mu)_{MAX}$	$\%\Delta\phi_{MAX}\times10^{-6}$
0.1	1.051	89.	1.045	49.	0.50	45.
0.2	1.063	73.	1.054	47.	0.85	36.
0.3	1.033	59.	1.020	39.	1.26	34.
0.4	0.961	51.	0.926	35.	3.64	31.
0.5	0.830	48.	0.789	32.	4.94	33.
0.6	0.675	44.	0.648	30.	4.00	32.
0.7	0.517	41.	0.500	27.	3.29	34.
0.8	0.352	38.	0.343	24.	2.56	37.

Table (4.6) Effect of the ultimate concrete strain (εcu) on the column capacity.

4.5.2 EFFECT OF CONCRETE STRENGTH (Fcu) ON THE COLUMN CAPACITY:

Maximum moments and curvatures were computed using Fcu = 20 MPa to study the effect of varying the concrete strength on the column capacity.

Differences in the values of maximum moments and corresponding curvatures for Fcu = 30 MPa and Fcu = 20 MPa, are given in Table (4.7). It can be seen from this table that the differences between the two values varied between 2.1% and 9.94% for moments between 0.0% and 7.9% for curvatures.

P/Pu	Fcu = 30 MPa, Mu = 79.76 KN.m, Pu = 2003.21 KN.m		Fcu = 20 MPa, Mu = 78 KN.m, Pu = 2003.21 KN.m		Differences	
	$(M/Mu)_{MAX}$	$\phi_{MAX} \times 10^{-6}$	$(M/Mu)_{MAX}$	$\phi_{MAX} \times 10^{-6}$	$\%\Delta (M/Mu)_{MAX}$	$\%\Delta \phi_{MAX} \times 10^{-6}$
0.1	1.051	89.	1.029	82.	2.1	7.9
0.2	1.063	73.	1.023	68.	3.76	6.85
0.3	1.033	59.	0.978	56.	5.32	5.85
0.4	0.961	51.	0.890	49.	7.39	3.92
0.5	0.830	48.	0.756	47.	8.92	2.08
0.6	0.675	44.	0.613	44.	9.19	0.00
0.7	0.517	41.	0.468	41.	9.48	0.00
0.8	0.352	38.	0.317	38.	9.94	0.00

Table (4.7) Effect of the concrete strength (Fcu) on the column capacity.

4.5.3 EFFECT OF STEEL STRENGTH ON THE COLUMN CAPACITY:

In order to study the effect of the yield strength of steel on the column capacity, the column strength has been computed for Fy= 347 MPa. The differences between the maximum moments and curvatures for Fy = 275 MPa and Fy = 345 MPa are given in Table (4.8). The differences between the two values varied between 1.52% and 7.23% for moments and between 0.0% and 4.11% for curvatures.

4.5.4 EFFECT OF THE CONCRETE CONTRIBUTION FACTOR ON THE COLUMN CAPACITY:

The area of concrete in a composite section, significantly contributes to its strength. In order to demonstrate this contribution, two different values of concrete contibution factor, for two different concrete area, are used in this analytical study. Differences between the

two values of the maximum moment and curvature are presented in Table (4.9). It can be seen from the table that the strength of the column increases as the concrete area increases. Differences between the two values varied between 1.87% and 8.33% for moments and between 0.0% 10.1% for curvatures.

P/Pu	Fy = 345 MPa, Mu = 98.80 KN.M, Pu = 2321.99 KN.M		Fy = 275 MPa, Mu = 79.76 KN.M, Pu = 2003.21 KN.M		Differences	
	$(M/Mu)_{MAX}$	$\phi_{MAX}\times10^{-6}$	$(M/Mu)_{MAX}$	$\phi_{MAX}\times10^{-6}$	$\%\Delta (M/Mu)_{MAX}$	$\%\Delta \phi_{MAX}\times10^{-6}$
0.1	1.035	86.	1.051	89.	1.52	3.37
0.2	1.035	70.	1.063	73.	2.63	4.11
0.3	0.995	58.	1.033	59.	3.68	1.69
0.4	0.904	51.	0.961	51	5.93	0.00
0.5	0.770	48.	0.830	48.	7.23	0.00
0.6	0.628	44.	0.675	44.	6.96	0.00
0.7	0.482	41.	0.517	41.	6.77	0.00
0.8	0.328	37.	0.352	38.	6.82	2.63

Table (4.8) Effect of the steel strength on the column capacity.

P/Pu	α_c = 0.4391, Mu = 81.188 KN.m, Pu = 2232.948 KN.m		α_c = 0.3748, Mu = 79.757 KN.m, Pu = 2003.206 KN.m		Differences	
	$(M/Mu)_{MAX}$	$\Phi_{MAX} \times 10^{-6}$	$(M/Mu)_{MAX}$	$\Phi_{MAX} \times 10^{-6}$	$\%\Delta (M/Mu)_{MAX}$	$\%\Delta \Phi_{MAX} \times 10^{-6}$
0.1	1.071	99.	1.051	89.	1.87	10.10
0.2	1.099	79.	1.063	73.	3.28	7.59
0.3	1.080	63.	1.033	59.	4.35	6.34
0.4	1.018	54.	0.961	51	5.60	5.56
0.5	0.896	48.	0.830	48.	7.37	0.00
0.6	0.733	45.	0.675	44.	7.91	2.22
0.7	0.562	42.	0.517	41.	8.01	2.38
0.8	0.384	39.	0.352	38.	8.33	2.63

Table (4.9) Effect of the concrete contribution factor (α_c) on the column capacity.

4.6 DUCTILITY OF THE BATTENED COMPOSITE COLUMN SECTION.

Usually, the ductility of a member is expressed as the ratio of the ultimate deformation to the deformation at first yield, which can be represented by what so called the curvature ductility.

The ratio $\Phi m/\Phi y$ gives a measure of the curvature ductility of the section, where Φm can be defined as the maximum curvature when the maximum moment for a given axial load is reached. While Φy can be defined as the curvature at first yield of the tension steel, which can be given by the following equation, (see Figure 4.10).

$$\Phi y = \frac{Fy/Es}{D - Dn} \qquad (4.1)$$

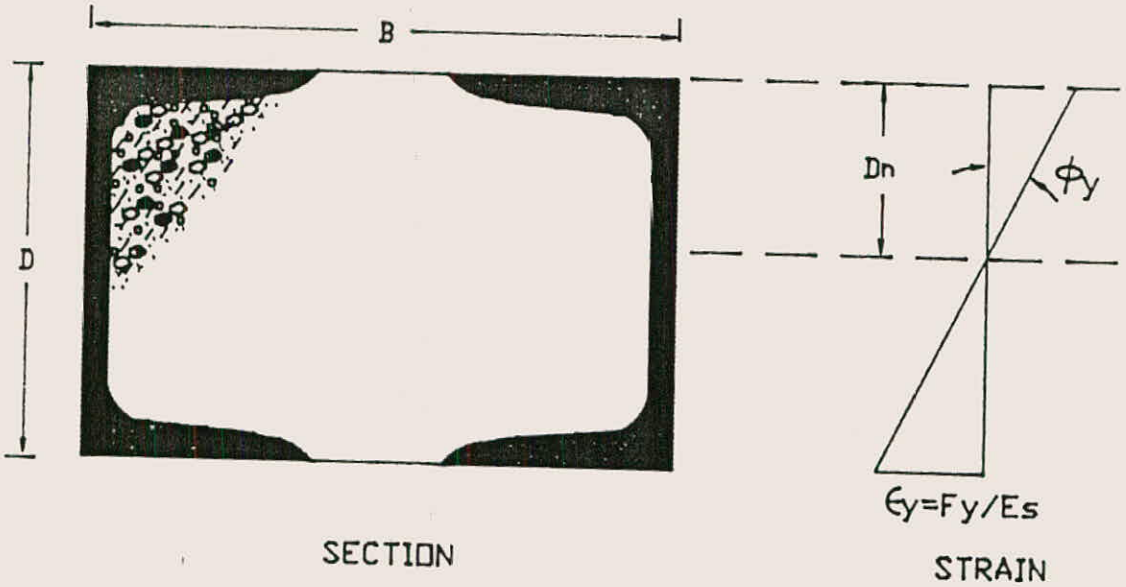

FIG.(4.10) Battened Composite column section at first yield

The effect of the axial load level and the section properties, such as the ultimate concrete strain (∈cu),concrete strength (Fcu), and the steel yield strength (Fy), on the Φm/Φy ratio appear clearly in Figures 4.11,4.12 and 4.13. Reference to these Figures (with other variables held constant) shows that:

1. An increase in the concrete strength, increases the ductility because Dn is decreased, therefore Φy is decreased and Φm is increased.
2. An increase in the ultimate concrete strain, increases the ductility because Φm is increased.
3. An increase in the steel yield strength decreases the ductility because both Fy/Es and Dn are increased, therefore, Φy is increased and Φm is decreased.

The effect of the axial load level on Φm/Φy can also be seen from these Figures. Hence the ductility decreased when the axial load level increased; because Φm is decreased.

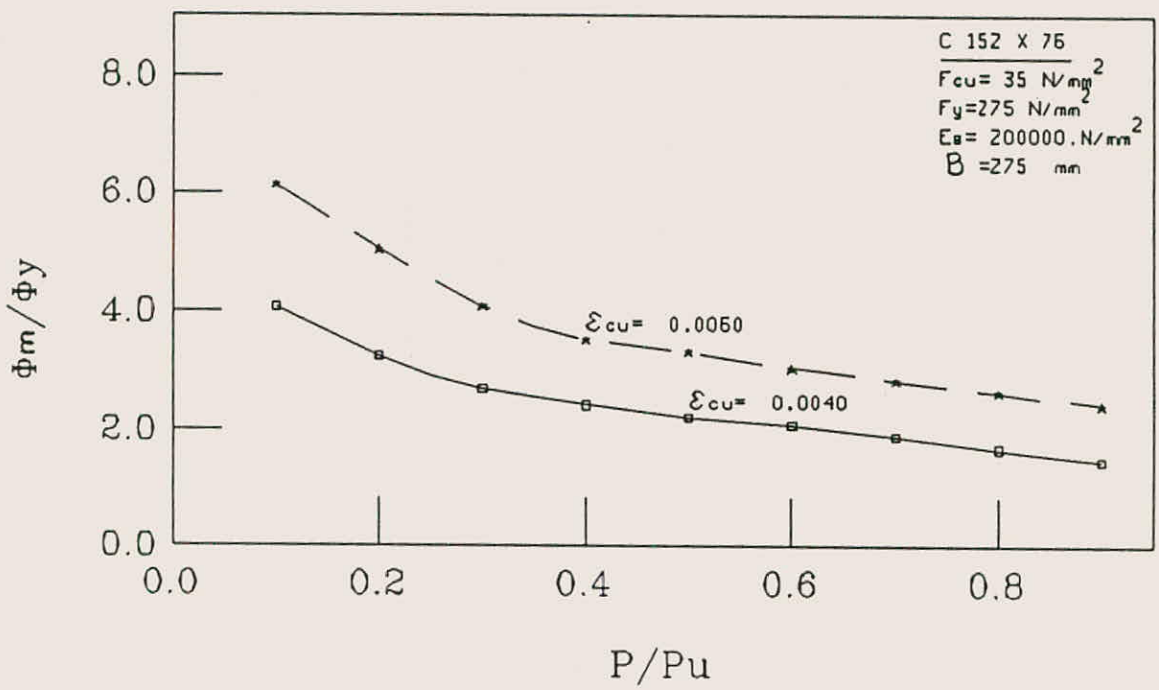

FIG. (4-10): EFFECT OF THE AXIAL LOAD LEVEL AND CRUSHING CONCRETE STRAIN ON THE CURVATURE DUCTILITY .

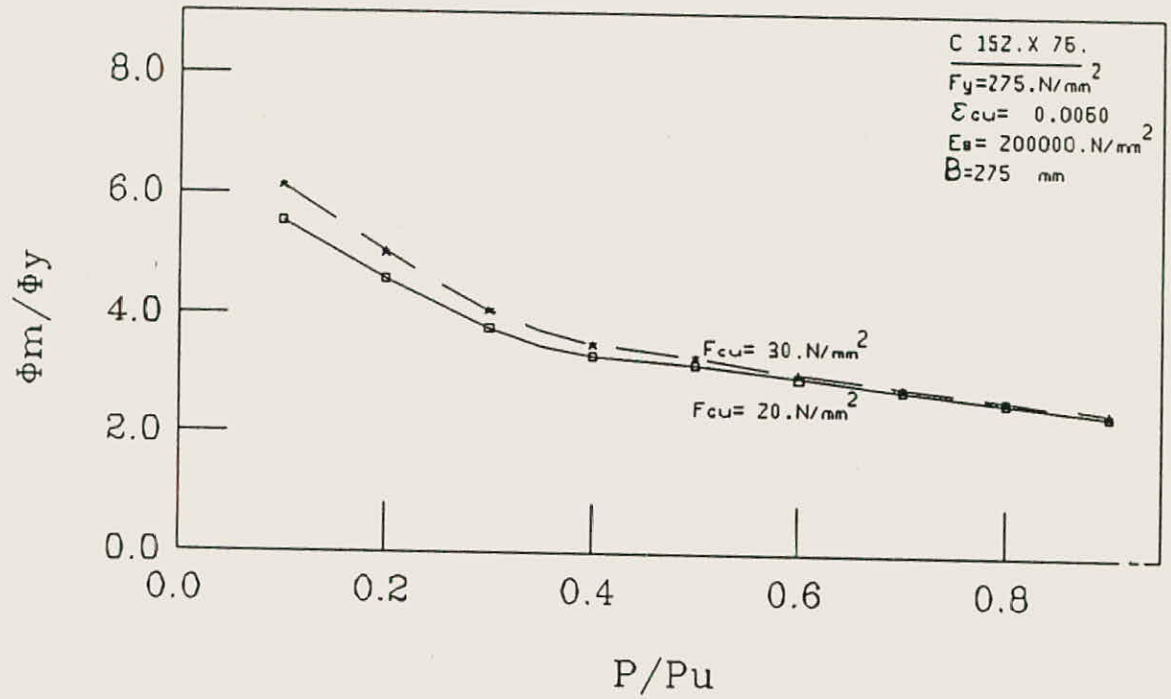

FIG. (4-12) : EFFECT OF THE AXIAL LOAD LEVEL AND THE CONCRETE STRENTH ON THE CURVATURE DUCTILITY .

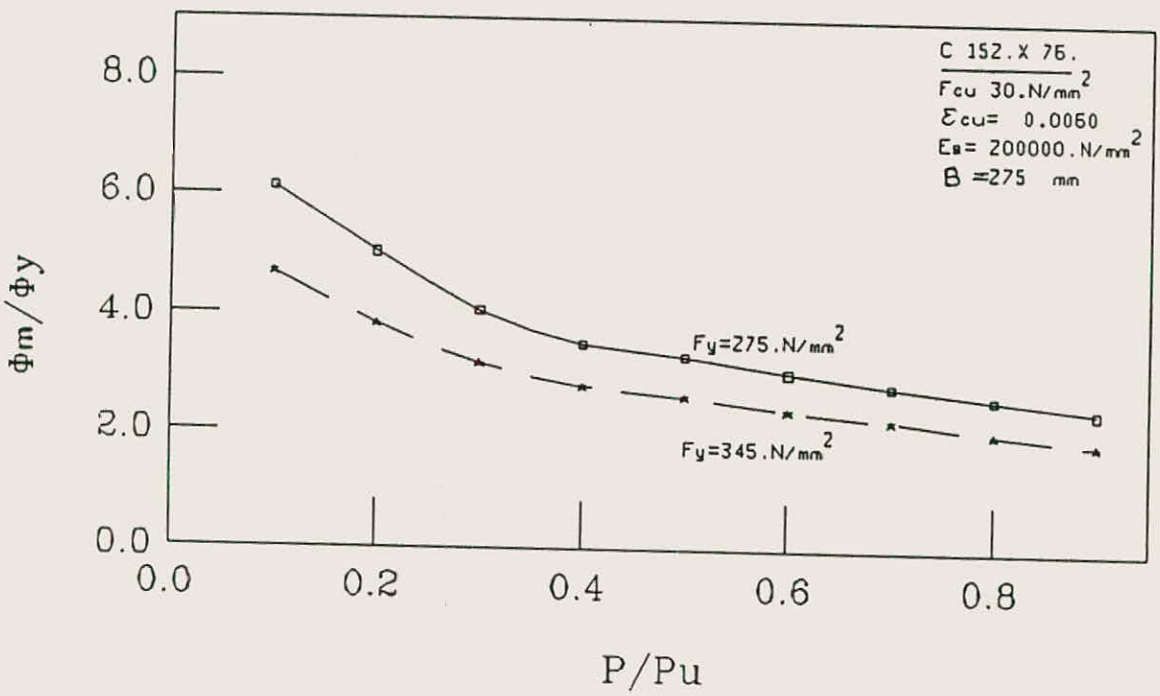

FIG. (4-13) : EFFECT OF THE AXIAL LOAD LEVEL AND THE STEEL YIELD STRENTH ON THE CURVATURE DUCTILITY .

4.7 ACCURACY OF THE PRESENTED COMPUTATIONAL METHOD:

The most significant sources of inaccuracy in the deflected shape of the column, obtained from the presented computer program, was found out to be affected by the following factors:

1. Number of the length intervals.
2. Linear interpolation of the curvature values from the M-Φ-P curves.
3. Size of the strip elements.

For the present investigation, this inaccuracy has been practically eliminated as follows:

1. Using twenty equal length intervals.
2. Using a curvature increments of 10^{-6} 1/mm.
3. Using an optimum number of small size strip elements. This number does not have a fixed value; because it depends on the block depth and the material composed in it*.

It was found that further increase in the number of intervals as well as the number of the strip elements, or using small curvature increment more than 10^{-6}, did not produce a change in the final deflections. Thus, these values were considered to be satisfactory to justify the accuracy and the extra computational time required.

---

* As mentioned previously in chapter II, the column cross section has been divided in to ten blocks of steel and seven blocks of concrete.

4.8 COMPARISON WITH AVAILABLE TEST RESULTS:

The validity of the presented method is demonstrated by comparison with the available test results for the battened composite columns tested at the University of Manchester by Hunaiti [7].

Details of the test column are shown in Table (4.10). The theoritical failure loads, computed by the analytical method presented in Chapter II, are given together with the experimental failure loads of these columns in Table (4.11).

The discrepancy between the theoritical and experimental results was found to lie within the range of 1.9% to 4.5%.

It should be mentioned that in calculating the failure loads, the following effects were not included in the analytical model:

1. Creep and shrinkage effect which would tend to reduce the failure loads and;
2. Strain hardening effect of steel and tensile strength effect of concrete, whch would tend to increase the failure loads.

Thus the calculated failure loads clearly demonstrated that the method, adopted in this study, is sufficiently accurate for practical purposes.

col. No.	Size of channel mmxmm	th of column mm	Steel channels			concrete core			Effect Length Le mm
			Area As/2 mm^2	Yield strength Fy N/mm^2	Elastic modulus Es Kn/mm^2	Area Ac mm^2	Cube strength Fcu N/mm^2	Elastic modulus Ec N/mm^2	
1	152x76	350	2277	312	207.0	48786	38.3	34.04	2910
2	152x76	350	2277	267	211.7	48786	42.4	35.81	2910
3	152x76	350	2277	274	221.3	48786	41.6	35.47	2910
4	152x76	350	2277	278	221.6	48786	38.8	34.26	2910
5	152x76	350	2277	277	225.5	48786	34.3	32.21	2910

Table (4.10) Properties of column sections tested by Hunaiti

col. No.	Eccentr-city e mm	Squash load Pu Kn	Experment failure load Pe	Calculat. failure load Pc	$\frac{(Pc-Pe)}{Pe}$ x100%
1	40	2972	1357	1397	2.94
2	100	2933	0777	0762	1.90
3	120	2932	0643	0668	3.89
4	140	2837	0553	0578	4.52
5	160	2650	0491	0501	2.04

Table (4.11) Comparison of theoretical results with experimental done by Hunaiti.

CHAPTER V

SUMMARY AND CONCLUSION

A computer method for calculating the failure loads of pin-ended battened composite column, under minor axis bending, is adopted in this study. The calculations include five slenderness ratios of L/D = 0,10,20,30 and 40 , and five eccentricities ratios of β = -1,-0.5,0.,0.5 and 1. .

The method of calculation is based upon inelastic column theory, through which **Newmark's** integration procedure is used for computing the true equilibrium shape of the deflected column.

The adopted method can also be used, with minor modifications, to calculate the failure loads for other types of composite columns for different stress-strain relationships.

There is a good agreement between the experimental and theoretical results. And the conclusions of this study are briefly mentioned below:

1. The battened composite column proved to be a reliable type of composite columns and can be safely used in practice, since the difference btween the experimental and theoretical loads is less than 5%.

2. Comparison of the theoretical loads with the experimental ones proved the validity of the presented method. Therefore, the method

can be considered sufficiently accurate for practical purposes.

3. Analytical results indicate that the capacity of the battened composite column decreases as the eccentricity ratio, β, increases.

4. Significant loss of strength was observed for slender columns. Also it has been demonstrated that there is a range of slender columns for which instability will occur prior to developing the full flexural strength.

5. Reduction of the ultimate concrete strain $\in cu$ from 0.006 to 0.004 produces about 3.7% loss of strength.

6. Reduction of Fcu from 30 MPa to 20 MPa gives about 9% loss of strength.

7. Increasing the steel yield strength from 275 MPa to 345 MPa gives an enhancement in the capacity ranging between 1.5% to 7.2%.

8. Analytical results show that the battened composite column can provide excellent ductility and load retention even after extensive concrete damage. Therefore, this column can be considered a viable type of composite columns.

9. Theoretical results demonstrated that the ductility of the column, under

consideration, is much affected by the ultimate concrete strain ($\in cu$). Difference between the ductilities, obtained by using $\in cu$ of 0.006 and 0.004, is about 33%.

10. Increasing the concrete strength from Fcu = 20 MPa to Fcu = 30 MPa gives an increase in the ductility about 10%.

11. Reduction of the steel yield strength from 345 MPa to 275 MPa gives an increase in the ductility about 25%.

12. Most of the computer time is used for establishing the moment-curvature-thrust relationships. Therefore if the M-Φ-P data was available as basic input in the program, the presented method would be fast and inexpensive (see Appendix [B]).

More experimental research to study the behavior of the battened composite columns under minor axis bending seems to be desirable; in order to confirm the analytical findings and validity of the present solution. Research on other aspects, such as details of beam-column connections, effect of residual stresses, and behavior of the battened composite columns under biaxial bending seems to be necessary.

APPENDIX A

IDEALIZATION OF THE CHANNEL SECTIONS

APPENDIX A

IDEALIZATION OF THE CHANNEL SECTIONS

The channel sections have been idealized as shown in Figure A1.b. The area of the idealized channel is the same as the area of the standard channel given in the Table (7).

The dimensions, T_1 and T_2. (as shown in Figure A1.b) are given as follows :

$$T_1 = T - \frac{b}{2} \tan 5^o \qquad \ldots\ldots A.1$$

$$T_2 = (A_{ss} - D_{ch}t - 2bT_1)/b \qquad \ldots\ldots A.2$$

where

A_{ss} = the area of the channel section and all the dimensions are as shown in Figure A.1

The idealized value of the centroid of the channel is given by :

$$C_{yi} = t + \frac{b^2 T_1 + b^2 T_2/3 - D_{ch}t^2/2}{D_{ch}t + 2b T_1 + b T_2} \qquad \ldots\ldots A.3$$

The second moment of area about the major axis is given by :

$$I_{xxi} = \{3t D_{ch}^3 + 6b T_1^3 + 18b T_1 (D_{ch}-T_1)^2 + 2b T_2^3 + b T_2 (3 D_{ch} - 6 T_1 - 2 T_2)^2\}/36$$

$\ldots\ldots A.4$

The second moment of area about the minor axis is given by :

$$I_{yyi} = \{3\ D_{ch}t^3 + 9\ D_{ch}t\ (2\ C_{yi}-t)^2 + 6\ T_1\ b^3 + 18\ T_1 b(b+2t-C_{yi})^2 + 2\ T_2 b^3 + 4\ T_2 b\ (b + 3t - 3C_{yi})^2\}/36$$

.... A.5

The results of the idealization of the channels are given in Table A.1, together with the percentage error when compared to the nominal values given in the Table

Table A.1 : Idealised properties of channel sections

Channel size	Depth of Section	Width of Section	Thickness				Area of Section	Centroid			Moment of Inertia					
	D_{ch}	B_{ch}	t	T	T_1	T_2	A_{ss}	C_y	C_{y1}	%	I_{xx}	I_{xx1}	%	I_{yy}	I_{yy1}	%
mm	mm	mm	mm	mm	mm	mm	cm^2	cm	cm	error	cm^4	cm^4	error	cm^4	cm^4	error
432x102	431.8	101.8	12.2	16.8	12.9	8.7	83.49	2.32	2.35	1.12	21399	21409	0.05	628.6	637.7	1.45
381x102	381.0	101.8	10.4	16.3	12.3	8.9	70.19	2.52	2.56	1.45	14894	14918	0.16	579.7	587.8	1.40
305x102	304.8	101.8	10.2	14.8	10.8	8.7	58.83	2.66	2.70	1.43	8214	8214	0.00	499.6	506.2	1.32
305x 89	304.8	88.9	10.2	13.7	10.3	7.5	53.11	2.18	2.21	1.28	7061	7056	0.10	325.4	329.8	1.35
254x 89	254.0	88.9	9.1	13.6	10.1	7.9	45.52	2.42	2.46	1.65	4448	4463	0.34	302.4	306.1	1.22
254x 76	254.0	76.2	8.1	10.9	7.9	6.9	36.03	1.86	1.89	1.61	3367	3367	0.30	162.6	165.1	1.54
229x 89	228.6	88.9	8.6	13.3	10.2	7.1	41.73	2.53	2.60	2.69	3387	3400	0.38	285.0	291.8	2.39
229x 76	228.6	76.2	7.6	11.2	8.2	6.7	33.20	2.00	2.04	1.93	2610	2617	0.27	158.7	161.4	1.70
203x 89	203.2	88.9	8.1	12.9	9.4	7.9	37.94	2.65	2.70	1.74	2491	2499	0.32	264.4	267.0	0.98
203x 76	203.2	76.2	7.1	11.2	8.2	6.7	30.34	2.13	2.18	2.25	1950	1955	0.25	151.3	153.6	1.52
178x 89	177.8	88.9	7.6	12.3	8.7	7.9	34.15	2.76	2.81	1.81	1753	1759	0.34	241.0	242.8	0.75
178x 76	177.8	76.2	6.6	10.3	7.3	6.8	26.54	2.20	2.25	2.26	1337	1341	0.30	134.0	135.7	1.27
152x 89	152.4	88.9	7.1	11.6	8.0	7.8	30.36	2.86	2.93	2.37	1166	1170	0.34	215.1	216.8	0.79
152x 76	152.4	76.2	6.4	9.0	6.0	6.8	22.77	2.21	2.26	2.13	852.5	852.3	0.09	113.8	114.9	0.97

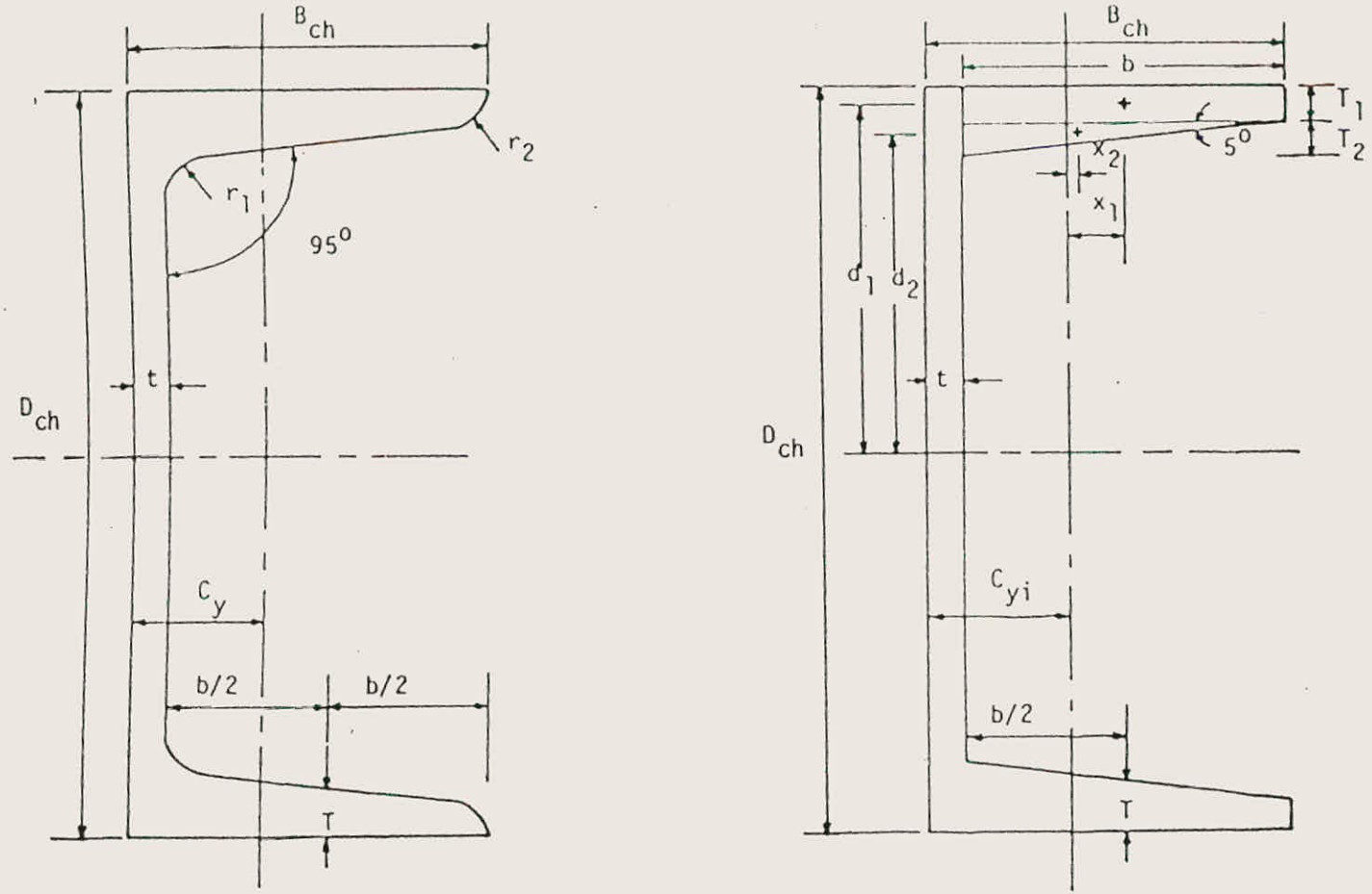

a) standard section

b) idealised section

Figure A.1 : Idealisation of the channel sections

APPENDIX B

SAMPLES FROM THE COMPUTER PROGRAM OUTPUT

B.1 : Load carrying capacity results for the section due to uniaxial bending about minor axis.

B.2 : Number of cycles for computing the eqlibrium deflected shape.

B.3 : Run time required for computing the M-Φ relations and the failure loads.

APP. B.1 : Load carrying capacity results for the section due to uniaxial bending about minor axis.

```
**************************************
* BATTENED COMPOSITE COLUMN SECTION *
**************************************

LOAD CARRYING CAPACITY RESULTS OF THE
SECTION DUE TO UNIAXIAL BENDING ABOUT
            MINOR AXIS

FAILURE LOADS WILL BE COMPUTED USING
   THE MOMENT -ROTATION CRETERIA

              DIMENSIONS
              **********

        i   _  LENGTH :  mm
        ii  _  FORCE  :  N

          CROSS SECTION DIMENSIONS
          ************************

  SECTION  WIDTH     B =    275.0000
  SECTION  DEPTH     D =    152.4000
  FLANGE THICKNESS   T =    9.40000
  CHANNEL AREA     Ass =    2277.000

            MATERIAL PROPERTIES
            *******************

28-DAY CUBE CONCRETE STENGTH Fcu =    30.00000
ULTIMATE CONCRETE STRAIN   =  6.0000001E-03
YIELD STRENGTH OF STEEL  Fy =    275.0000
MODULUS OF ELASTICITY FOR STEEL  Es =    200000.0

          SHORT COLUMN PROPERTIES
          ***********************

   SQUACH LOAD ( Pu ) =     2003206.
   ULTIMATE MOMENT ( Mu )=  7.9757128E+07

NO. OF NODES WHICH WILL BE USED IN THE ANALYSIS =20

   ECCENTRICITY RATIO ( ej/ei)= 1.0
```

L/D=10.00

P/Pu= 0.200

M/Mu= 1.000

CRITICAL DEFLECTION	======>	0.14135E+02
CRITICAL ROTATION AT END i	======>	0.22366E-01
CRITICAL ROTATION AT END j	======>	0.22366E-01

L/D=20.00

P/Pu= 0.200

M/Mu= 0.885

CRITICAL DEFLECTION	======>	0.36785E+02
CRITICAL ROTATION AT END i	======>	0.32568E-01
CRITICAL ROTATION AT END j	======>	0.32568E-01

L/D=30.00

P/Pu= 0.200

M/Mu= 0.735

CRITICAL DEFLECTION	======>	0.67307E+02
CRITICAL ROTATION AT END i	======>	0.43107E-01
CRITICAL ROTATION AT END j	======>	0.43107E-01

L/D=40.00

P/Pu= 0.200

M/Mu= 0.550

CRITICAL DEFLECTION	======>	0.12868E+03
CRITICAL ROTATION AT END i	======>	0.50157E-01
CRITICAL ROTATION AT END j	======>	0.50157E-01

L/D=10.00

P/Pu= 0.400

M/Mu= 0.845

CRITICAL DEFLECTION	======>	0.11896E+02
CRITICAL ROTATION AT END i	======>	0.24667E-01
CRITICAL ROTATION AT END j	======>	0.24667E-01

L/D=20.00

P/Pu= 0.400

M/Mu= 0.620

CRITICAL DEFLECTION	======>	0.38069E+02
CRITICAL ROTATION AT END i	======>	0.25636E-01
CRITICAL ROTATION AT END j	======>	0.25636E-01

L/D=30.00

P/Pu= 0.400

M/Mu= 0.405

CRITICAL DEFLECTION	======>	0.66926E+02
CRITICAL ROTATION AT END i	======>	0.26049E-01
CRITICAL ROTATION AT END j	======>	0.26050E-01

L/D=40.00

P/Pu= 0.400

M/Mu= 0.185

CRITICAL DEFLECTION	======>	0.49397E+02
CRITICAL ROTATION AT END i	======>	0.26106E-01
CRITICAL ROTATION AT END j	======>	0.26106E-01

L/D=10.00

P/Pu= 0.600

M/Mu= 0.545

CRITICAL DEFLECTION	======>	0.88315E+01
CRITICAL ROTATION AT END i	======>	0.14734E-01
CRITICAL ROTATION AT END j	======>	0.14734E-01

L/D=20.00

P/Pu= 0.600

M/Mu= 0.360

CRITICAL DEFLECTION	======>	0.12985E+02
CRITICAL ROTATION AT END i	======>	0.14033E-01
CRITICAL ROTATION AT END j	======>	0.14033E-01

L/D=30.00

P/Pu= 0.600

M/Mu= 0.175

CRITICAL DEFLECTION	======>	0.35251E+02
CRITICAL ROTATION AT END i	======>	0.16108E-01
CRITICAL ROTATION AT END j	======>	0.16108E-01

L/D=10.00

P/Pu= 0.800

M/Mu= 0.260

CRITICAL DEFLECTION	======>	0.46146E+01
CRITICAL ROTATION AT END i	======>	0.66048E-02
CRITICAL ROTATION AT END j	======>	0.66048E-02

L/D=20.00

P/Pu= 0.800

M/Mu= 0.125

CRITICAL DEFLECTION	======>	0.11886E+02
CRITICAL ROTATION AT END i	======>	0.95096E-02
CRITICAL ROTATION AT END j	======>	0.95097E-02

```
**************************************
* BATTENED COMPOSITE COLUMN SECTION *
**************************************

LOAD CARRYING CAPACITY RESULTS OF THE
SECTION DUE TO UNIAXIAL BENDING ABOUT
            MINOR AXIS

FAILURE LOADS WILL BE COMPUTED USING
   THE MOMENT -ROTATION CRETERIA

                DIMENSIONS
                **********

          i   _  LENGTH :  mm
          ii  _  FORCE  :  N

          CROSS SECTION DIMENSIONS
          ************************

 SECTION  WIDTH     B =    275.0000
 SECTION  DEPTH     D =    152.4000
 FLANGE THICKNESS   T =    9.40000
 CHANNEL AREA     Ass =    2277.000

              MATERIAL PROPERTIES
              *******************

28-DAY CUBE CONCRETE STENGTH Fcu =    30.00000
ULTIMATE CONCRETE STRAIN  =  6.0000001E-03
YIELD STRENGTH OF STEEL  Fy =    275.0000
MODULUS OF ELASTICITY FOR STEEL  Es =    200000.0

            SHORT COLUMN PROPERTIES
            ***********************

  SQUACH LOAD ( Pu ) =     2003206.
  ULTIMATE MOMENT ( Mu )=  7.9757128E+07

NO. OF NODES WHICH WILL BE USED IN THE ANALYSIS =30

  ECCENTRICITY RATIO ( ej/ei)= 1.0
```

L/D=10.00

P/Pu= 0.200

M/Mu= 1.000

CRITICAL DEFLECTION	======>	0.14033E+02
CRITICAL ROTATION AT END i	======>	0.22342E-01
CRITICAL ROTATION AT END j	======>	0.22343E-01

L/D=20.00

P/Pu= 0.200

M/Mu= 0.885

CRITICAL DEFLECTION	======>	0.35846E+02
CRITICAL ROTATION AT END i	======>	0.32542E-01
CRITICAL ROTATION AT END j	======>	0.32542E-01

L/D=30.00

P/Pu= 0.200

M/Mu= 0.735

CRITICAL DEFLECTION	======>	0.65499E+02
CRITICAL ROTATION AT END i	======>	0.43044E-01
CRITICAL ROTATION AT END j	======>	0.43045E-01

L/D=40.00

P/Pu= 0.200

M/Mu= 0.550

CRITICAL DEFLECTION	======>	0.10473E+03
CRITICAL ROTATION AT END i	======>	0.49965E-01
CRITICAL ROTATION AT END j	======>	0.49966E-01

L/D=10.00

P/Pu= 0.400

M/Mu= 0.845

CRITICAL DEFLECTION	======>	0.11852E+02
CRITICAL ROTATION AT END i	======>	0.24614E-01
CRITICAL ROTATION AT END j	======>	0.24614E-01

L/D=20.00

P/Pu= 0.400

M/Mu= 0.620

CRITICAL DEFLECTION	======>	0.31456E+02
CRITICAL ROTATION AT END i	======>	0.25584E-01
CRITICAL ROTATION AT END j	======>	0.25585E-01

L/D=30.00

P/Pu= 0.400

M/Mu= 0.405

CRITICAL DEFLECTION	======>	0.64673E+02
CRITICAL ROTATION AT END i	======>	0.25979E-01
CRITICAL ROTATION AT END j	======>	0.25979E-01

L/D=40.00

P/Pu= 0.400

M/Mu= 0.185

CRITICAL DEFLECTION	======>	0.49150E+02
CRITICAL ROTATION AT END i	======>	0.25956E-01
CRITICAL ROTATION AT END j	======>	0.25956E-01

```
**************************************
* BATTENED COMPOSITE COLUMN SECTION *
**************************************

LOAD CARRYING CAPACITY RESULTS OF THE
SECTION DUE TO UNIAXIAL BENDING ABOUT
            MINOR AXIS

FAILURE LOADS WILL BE COMPUTED USING
   THE MOMENT -ROTATION CRETERIA

                DIMENSIONS
                **********

          i   _  LENGTH :  mm
          ii  _  FORCE  :  N

          CROSS SECTION DIMENSIONS
          ************************

  SECTION  WIDTH     B =    275.0000
  SECTION  DEPTH     D =    152.4000
  FLANGE THICKNESS   T =    9.40000
  CHANNEL AREA     Ass =    2277.000

            MATERIAL PROPERTIES
            *******************

28-DAY CUBE CONCRETE STENGTH Fcu =    30.00000
ULTIMATE CONCRETE STRAIN  =  6.0000001E-03
YIELD STRENGTH OF STEEL  Fy =    275.0000
MODULUS OF ELASTICITY FOR STEEL  Es =    200000.0

          SHORT COLUMN PROPERTIES
          ***********************

    SQUACH LOAD ( Pu ) =     2003206.
    ULTIMATE MOMENT ( Mu )=  7.9757128E+07

NO. OF NODES WHICH WILL BE USED IN THE ANALYSIS =20

    ECCENTRICITY RATIO ( ej/ei)= -1.0
```

L/D=10.00

P/Pu= 0.200

M/Mu= 1.065

CRITICAL DEFLECTION		======>	0.62996E+00
CRITICAL ROTATION AT END	i	======>	0.52384E-02
CRITICAL ROTATION AT END	j	======>	-0.52384E-02

L/D=20.00

P/Pu= 0.200

M/Mu= 1.065

CRITICAL DEFLECTION		======>	0.25550E+01
CRITICAL ROTATION AT END	i	======>	0.10647E-01
CRITICAL ROTATION AT END	j	======>	-0.10647E-01

L/D=30.00

P/Pu= 0.200

M/Mu= 1.065

CRITICAL DEFLECTION		======>	0.58855E+01
CRITICAL ROTATION AT END	i	======>	0.16421E-01
CRITICAL ROTATION AT END	j	======>	-0.16421E-01

L/D=40.00

P/Pu= 0.200

M/Mu= 1.065

CRITICAL DEFLECTION		======>	0.10824E+02
CRITICAL ROTATION AT END	i	======>	0.22909E-01
CRITICAL ROTATION AT END	j	======>	-0.22909E-01

L/D=10.00

P/Pu= 0.400

M/Mu= 0.965

CRITICAL DEFLECTION		======>	0.61494E+00
CRITICAL ROTATION AT END	i	======>	0.55780E-02
CRITICAL ROTATION AT END	j	======>	-0.55779E-02

L/D=20.00

P/Pu= 0.400

M/Mu= 0.965

CRITICAL DEFLECTION		======>	0.25349E+01
CRITICAL ROTATION AT END	i	======>	0.11804E-01
CRITICAL ROTATION AT END	j	======>	-0.11803E-01

L/D=30.00

P/Pu= 0.400

M/Mu= 0.965

CRITICAL DEFLECTION		======>	0.60097E+01
CRITICAL ROTATION AT END	i	======>	0.20054E-01
CRITICAL ROTATION AT END	j	======>	-0.20054E-01

L/D=40.00

P/Pu= 0.400

M/Mu= 0.940

CRITICAL DEFLECTION		======>	0.16198E+02
CRITICAL ROTATION AT END	i	======>	0.31321E-01
CRITICAL ROTATION AT END	j	======>	-0.31320E-01

L/D=10.00

P/Pu= 0.600

M/Mu= 0.680

CRITICAL DEFLECTION		======>	0.47493E+00
CRITICAL ROTATION AT END	i	======>	0.42434E-02
CRITICAL ROTATION AT END	j	======>	-0.42434E-02

L/D=20.00

P/Pu= 0.600

M/Mu= 0.680

CRITICAL DEFLECTION		======>	0.19971E+01
CRITICAL ROTATION AT END	i	======>	0.95549E-02
CRITICAL ROTATION AT END	j	======>	-0.95549E-02

L/D=30.00

P/Pu= 0.600

M/Mu= 0.670

CRITICAL DEFLECTION		======>	0.75157E+01
CRITICAL ROTATION AT END	i	======>	0.19388E-01
CRITICAL ROTATION AT END	j	======>	-0.19388E-01

L/D=10.00

P/Pu= 0.800

M/Mu= 0.355

CRITICAL DEFLECTION		======>	0.37404E+00
CRITICAL ROTATION AT END	i	======>	0.28648E-02
CRITICAL ROTATION AT END	j	======>	-0.28647E-02

L/D=20.00

P/Pu= 0.800

M/Mu= 0.355

CRITICAL DEFLECTION		======>	0.16591E+01
CRITICAL ROTATION AT END	i	======>	0.74792E-02
CRITICAL ROTATION AT END	j	======>	-0.74791E-02

APP. B.2 : Number of cycles for computing the eqlibrium deflected shape.

```
**************************************
* BATTENED COMPOSITE COLUMN SECTION *
**************************************

LOAD CARRYING CAPACITY RESULTS OF THE
SECTION DUE TO UNIAXIAL BENDING ABOUT
            MINOR AXIS

FAILURE LOADS WILL BE COMPUTED USING
   THE MOMENT -ROTATION CRETERIA

                DIMENSIONS
                **********

          i   _  LENGTH :  mm
          ii  _  FORCE  :  N

            CROSS SECTION DIMENSIONS
            ************************

  SECTION  WIDTH     B =    275.0000
  SECTION  DEPTH     D =    152.4000
  FLANGE THICKNESS   T =    9.40000
  CHANNEL AREA     Ass =    2277.000

              MATERIAL PROPERTIES
              *******************

28-DAY CUBE CONCRETE STENGTH Fcu =    30.00000
ULTIMATE CONCRETE STRAIN   =  6.0000001E-03
YIELD STRENGTH OF STEEL  Fy =    275.0000
MODULUS OF ELASTICITY FOR STEEL  Es =    200000.0

            SHORT COLUMN PROPERTIES
            ***********************

    SQUACH LOAD ( Pu ) =     2003206.
    ULTIMATE MOMENT ( Mu )=  7.9757128E+07

NO. OF NODES WHICH WILL BE USED IN THE ANALYSIS =20

      ECCENTRICITY RATIO ( ej/ei)= 1.0
```

L/D=30 P/Pu=0.2

M/Mu	THETA	# OF CYCLES
0.50000E-02	0.61577E-04	1
0.10000E-01	0.12315E-03	1
0.15000E-01	0.18473E-03	1
0.20000E-01	0.24631E-03	1
0.25000E-01	0.30788E-03	1
0.30000E-01	0.36946E-03	1
0.35000E-01	0.43104E-03	1
0.40000E-01	0.49261E-03	1
0.45000E-01	0.55419E-03	1
0.50000E-01	0.61577E-03	1
0.55000E-01	0.67758E-03	2
0.60000E-01	0.73917E-03	2
0.65000E-01	0.80077E-03	2
0.70000E-01	0.86237E-03	2
0.75000E-01	0.92397E-03	2
0.80000E-01	0.98557E-03	2
0.85000E-01	0.10472E-02	2
0.90000E-01	0.11088E-02	2
0.95000E-01	0.11704E-02	2
0.10000E+00	0.12320E-02	2
0.10500E+00	0.12936E-02	2
0.11000E+00	0.13552E-02	2
0.11500E+00	0.14168E-02	2
0.12000E+00	0.14783E-02	2
0.12500E+00	0.15399E-02	2
0.13000E+00	0.16015E-02	2
0.13500E+00	0.16631E-02	2
0.14000E+00	0.17247E-02	2
0.14500E+00	0.17864E-02	2
0.15000E+00	0.18480E-02	2
0.15500E+00	0.19096E-02	2
0.16000E+00	0.19712E-02	2
0.16500E+00	0.20329E-02	2
0.17000E+00	0.20945E-02	2
0.17500E+00	0.21561E-02	2
0.18000E+00	0.22178E-02	2
0.18500E+00	0.22794E-02	2
0.19000E+00	0.23411E-02	2
0.19500E+00	0.24027E-02	2
0.20000E+00	0.24643E-02	2
0.20500E+00	0.25260E-02	2
0.21000E+00	0.25886E-02	2
0.21500E+00	0.26521E-02	2
0.22000E+00	0.27155E-02	2
0.22500E+00	0.27790E-02	2
0.23000E+00	0.28425E-02	2
0.23500E+00	0.29068E-02	2
0.24000E+00	0.29715E-02	3
0.24500E+00	0.30360E-02	3

L/D=30 P/Pu=0.2

M/Mu	THETA	# OF CYCLES
0.75500E+00	0.10715E-01	4
0.76000E+00	0.10796E-01	4
0.76500E+00	0.10877E-01	4
0.77000E+00	0.10959E-01	4
0.77500E+00	0.11041E-01	4
0.78000E+00	0.11122E-01	4
0.78500E+00	0.11204E-01	4
0.79000E+00	0.11286E-01	4
0.79500E+00	0.11368E-01	4
0.80000E+00	0.11450E-01	4
0.80500E+00	0.11532E-01	4
0.81000E+00	0.11614E-01	4
0.81500E+00	0.11696E-01	4
0.82000E+00	0.11778E-01	4
0.83500E+00	0.12025E-01	4
0.84000E+00	0.12108E-01	4
0.84500E+00	0.12190E-01	4
0.85000E+00	0.12273E-01	4
0.85500E+00	0.12355E-01	4
0.86000E+00	0.12438E-01	4
0.86500E+00	0.12521E-01	4
0.87000E+00	0.12604E-01	5
0.87500E+00	0.12687E-01	5
0.88000E+00	0.12770E-01	5
0.88500E+00	0.12853E-01	5
0.89000E+00	0.12937E-01	5
0.91000E+00	0.13271E-01	5
0.91500E+00	0.13357E-01	5
0.92000E+00	0.13443E-01	5
0.92500E+00	0.13529E-01	5
0.93000E+00	0.13615E-01	5
0.93500E+00	0.13701E-01	5
0.94000E+00	0.13788E-01	5
0.94500E+00	0.13874E-01	5
0.95000E+00	0.13961E-01	5
0.95500E+00	0.14048E-01	5
0.96000E+00	0.14145E-01	5
0.96500E+00	0.14242E-01	5
0.97000E+00	0.14338E-01	5
0.97500E+00	0.14435E-01	5
0.99000E+00	0.14725E-01	5
0.99500E+00	0.14836E-01	5
0.10100E+01	0.15172E-01	5
0.10300E+01	0.15650E-01	5
0.10350E+01	0.15772E-01	5
0.10400E+01	0.15895E-01	5
0.10450E+01	0.16026E-01	5
0.10500E+01	0.16157E-01	5
0.10550E+01	0.16288E-01	5
0.10600E+01	0.16421E-01	5

L/D=30 P/Pu=0.6

M/Mu	THETA	# OF CYCLES
0.50000E-02	0.78018E-04	1
0.10000E-01	0.15604E-03	1
0.15000E-01	0.23434E-03	2
0.20000E-01	0.31245E-03	2
0.25000E-01	0.39056E-03	2
0.30000E-01	0.46867E-03	2
0.35000E-01	0.54679E-03	2
0.40000E-01	0.62490E-03	2
0.50000E-01	0.78112E-03	2
0.55000E-01	0.85924E-03	2
0.60000E-01	0.93735E-03	2
0.65000E-01	0.10155E-02	2
0.70000E-01	0.10936E-02	2
0.75000E-01	0.11717E-02	2
0.80000E-01	0.12500E-02	3
0.85000E-01	0.13281E-02	3
0.90000E-01	0.14062E-02	3
0.10000E+00	0.15624E-02	3
0.10500E+00	0.16406E-02	3
0.11000E+00	0.17187E-02	3
0.11500E+00	0.17968E-02	3
0.12000E+00	0.18749E-02	3
0.12500E+00	0.19531E-02	3
0.13000E+00	0.20312E-02	3
0.13500E+00	0.21093E-02	3
0.14000E+00	0.21874E-02	3
0.14500E+00	0.22656E-02	3
0.15000E+00	0.23437E-02	3
0.15500E+00	0.24218E-02	3
0.16000E+00	0.24999E-02	3
0.16500E+00	0.25780E-02	3
0.17000E+00	0.26562E-02	3
0.17500E+00	0.27343E-02	3
0.18000E+00	0.28124E-02	3
0.18500E+00	0.28905E-02	3
0.19000E+00	0.29687E-02	3
0.19500E+00	0.30468E-02	3
0.20000E+00	0.31249E-02	3
0.20500E+00	0.32030E-02	3
0.21000E+00	0.32811E-02	3
0.21500E+00	0.33593E-02	3
0.22000E+00	0.34374E-02	3
0.22500E+00	0.35155E-02	3
0.23000E+00	0.35936E-02	3
0.23500E+00	0.36718E-02	3
0.24000E+00	0.37499E-02	3
0.24500E+00	0.38280E-02	3
0.25000E+00	0.39061E-02	3
0.25500E+00	0.39842E-02	3

L/D=30 P/Pu=0.6

M/Mu	THEATA	# OF CYCLES
0.50500E+00	0.79486E-02	4
0.51000E+00	0.80488E-02	4
0.51500E+00	0.81584E-02	4
0.52000E+00	0.82680E-02	4
0.52500E+00	0.83778E-02	5
0.53000E+00	0.84875E-02	5
0.53500E+00	0.85977E-02	5
0.54000E+00	0.87349E-02	5
0.54500E+00	0.88745E-02	5
0.55000E+00	0.90287E-02	5
0.55500E+00	0.91861E-02	5
0.56000E+00	0.93580E-02	5
0.56500E+00	0.95301E-02	6
0.57000E+00	0.97025E-02	6
0.57500E+00	0.98996E-02	6
0.58000E+00	0.10108E-01	6
0.58500E+00	0.10326E-01	6
0.59000E+00	0.10557E-01	6
0.59500E+00	0.10799E-01	7
0.60000E+00	0.11084E-01	7
0.60500E+00	0.11377E-01	7
0.61000E+00	0.11695E-01	7
0.61500E+00	0.12039E-01	8
0.62000E+00	0.12400E-01	8
0.62500E+00	0.12818E-01	8
0.63000E+00	0.13278E-01	9
0.63500E+00	0.13787E-01	9
0.64000E+00	0.14345E-01	10
0.64500E+00	0.15007E-01	10
0.65000E+00	0.15762E-01	11
0.65500E+00	0.16686E-01	13
0.66000E+00	0.17835E-01	15
0.66500E+00	0.19388E-01	18

```
**************************************
* BATTENED COMPOSITE COLUMN SECTION *
**************************************

LOAD CARRYING CAPACITY RESULTS OF THE
SECTION DUE TO UNIAXIAL BENDING ABOUT
            MINOR AXIS

FAILURE LOADS WILL BE COMPUTED USING
   THE MOMENT -ROTATION CRETERIA

                DIMENSIONS
                **********

          i   _  LENGTH :  mm
          ii  _  FORCE  :  N

          CROSS SECTION DIMENSIONS
          ************************

  SECTION  WIDTH     B =    275.0000
  SECTION  DEPTH     D =    152.4000
  FLANGE THICKNESS   T =    9.40000
  CHANNEL AREA     Ass =    2277.000

              MATERIAL PROPERTIES
              *******************

28-DAY CUBE CONCRETE STENGTH Fcu =    30.00000
ULTIMATE CONCRETE STRAIN    =  6.0000001E-03
YIELD STRENGTH OF STEEL  Fy =    275.0000
MODULUS OF ELASTICITY FOR STEEL  Es =    200000.0

          SHORT COLUMN PROPERTIES
          ***********************

   SQUACH LOAD ( Pu ) =     2003206.
   ULTIMATE MOMENT ( Mu )=  7.9757128E+07

NO. OF NODES WHICH WILL BE USED IN THE ANALYSIS =20

  ECCENTRICITY RATIO ( ej/ei)= -1.0
```

L/D=30 P/Pu=0.2

M/Mu	THETA	# OF CYCLES
0.50000E-02	0.21136E-03	1
0.10000E-01	0.42273E-03	1
0.15000E-01	0.63419E-03	2
0.20000E-01	0.84559E-03	2
0.25000E-01	0.10570E-02	2
0.30000E-01	0.12684E-02	2
0.35000E-01	0.14798E-02	2
0.40000E-01	0.16912E-02	2
0.45000E-01	0.19026E-02	2
0.50000E-01	0.21140E-02	2
0.55000E-01	0.23254E-02	2
0.60000E-01	0.25368E-02	2
0.65000E-01	0.27482E-02	2
0.70000E-01	0.29596E-02	2
0.75000E-01	0.31710E-02	2
0.80000E-01	0.33824E-02	3
0.85000E-01	0.35938E-02	3
0.90000E-01	0.38052E-02	3
0.95000E-01	0.40166E-02	3
0.10000E+00	0.42280E-02	3
0.10500E+00	0.44395E-02	3
0.11000E+00	0.46510E-02	3
0.11500E+00	0.48626E-02	3
0.12000E+00	0.50742E-02	3
0.12500E+00	0.52859E-02	3
0.13000E+00	0.54975E-02	3
0.13500E+00	0.57091E-02	3
0.14000E+00	0.59208E-02	3
0.14500E+00	0.61324E-02	3
0.15000E+00	0.63440E-02	3
0.15500E+00	0.65596E-02	4
0.16000E+00	0.67810E-02	5
0.16500E+00	0.70054E-02	5
0.17000E+00	0.72318E-02	5
0.17500E+00	0.74599E-02	5
0.18000E+00	0.76894E-02	6
0.18500E+00	0.79200E-02	6
0.19000E+00	0.81517E-02	6
0.19500E+00	0.83834E-02	6
0.20000E+00	0.86177E-02	6
0.20500E+00	0.88588E-02	6
0.21000E+00	0.91032E-02	6
0.21500E+00	0.93501E-02	6
0.22000E+00	0.95988E-02	6
0.22500E+00	0.98492E-02	7
0.23000E+00	0.10101E-01	7
0.23500E+00	0.10353E-01	7
0.24000E+00	0.10607E-01	7
0.24500E+00	0.10866E-01	7

L/D=30 P/Pu=0.2

M/Mu	THETA	# OF CYCLES
0.50500E+00	0.25597E-01	9
0.51000E+00	0.25896E-01	9
0.51500E+00	0.26195E-01	9
0.52000E+00	0.26494E-01	9
0.52500E+00	0.26794E-01	9
0.53000E+00	0.27093E-01	9
0.53500E+00	0.27394E-01	9
0.54000E+00	0.27695E-01	9
0.54500E+00	0.27997E-01	9
0.55000E+00	0.28299E-01	9
0.55500E+00	0.28602E-01	9
0.56000E+00	0.28905E-01	9
0.56500E+00	0.29208E-01	9
0.57000E+00	0.29512E-01	9
0.57500E+00	0.29816E-01	9
0.58000E+00	0.30121E-01	9
0.58500E+00	0.30426E-01	9
0.59000E+00	0.30732E-01	9
0.59500E+00	0.31037E-01	9
0.60000E+00	0.31343E-01	9
0.60500E+00	0.31650E-01	9
0.61000E+00	0.31958E-01	9
0.61500E+00	0.32265E-01	9
0.62000E+00	0.32573E-01	9
0.62500E+00	0.32882E-01	9
0.63000E+00	0.33191E-01	9
0.63500E+00	0.33504E-01	9
0.64000E+00	0.33821E-01	9
0.64500E+00	0.34142E-01	9
0.65000E+00	0.34466E-01	9
0.65500E+00	0.34791E-01	9
0.66000E+00	0.35118E-01	9
0.66500E+00	0.35460E-01	10
0.67000E+00	0.35822E-01	10
0.67500E+00	0.36196E-01	10
0.68000E+00	0.36580E-01	11
0.68500E+00	0.36979E-01	11
0.69000E+00	0.37426E-01	12
0.69500E+00	0.37902E-01	12
0.70000E+00	0.38412E-01	13
0.70500E+00	0.38975E-01	14
0.71000E+00	0.39582E-01	15
0.71500E+00	0.40245E-01	16
0.72000E+00	0.40975E-01	17
0.72500E+00	0.41852E-01	19
0.73000E+00	0.43044E-01	25
0.73500E+00	0.43107E-01	25

L/D=30 P/Pu=0.6

M/Mu	THETA	# OF CYCLES
0.50000E-02	0.46126E-03	4
0.10000E-01	0.92261E-03	5
0.15000E-01	0.13840E-02	6
0.20000E-01	0.18453E-02	6
0.25000E-01	0.23067E-02	7
0.30000E-01	0.27681E-02	7
0.35000E-01	0.32294E-02	7
0.40000E-01	0.36909E-02	8
0.45000E-01	0.41522E-02	8
0.50000E-01	0.46136E-02	8
0.55000E-01	0.50749E-02	8
0.60000E-01	0.55363E-02	8
0.65000E-01	0.59977E-02	9
0.70000E-01	0.64591E-02	9
0.75000E-01	0.69205E-02	9
0.80000E-01	0.73818E-02	9
0.85000E-01	0.78432E-02	9
0.90000E-01	0.83046E-02	9
0.95000E-01	0.87659E-02	9
0.10000E+00	0.92282E-02	10
0.10500E+00	0.96917E-02	10
0.11000E+00	0.10156E-01	10
0.11500E+00	0.10620E-01	11
0.12000E+00	0.11087E-01	11
0.12500E+00	0.11555E-01	12
0.13000E+00	0.12023E-01	12
0.13500E+00	0.12493E-01	13
0.14000E+00	0.12966E-01	13
0.14500E+00	0.13440E-01	13
0.15000E+00	0.13915E-01	14
0.15500E+00	0.14399E-01	15
0.16000E+00	0.14905E-01	16
0.16500E+00	0.15425E-01	17
0.17000E+00	0.16013E-01	25
0.17500E+00	0.16108E-01	25

APP. B.3 : Run time required for computing the M-Φ relations and the failure loads.

P/PU	M-ϕ	L/D = 10	L/D = 20	L/D = 30	L/D = 40
0.1	12.72	0.91	1.13	1.26	1.43
0.2	13.45	1.00	1.14	1.28	1.31
0.3	13.92	0.84	1.05	1.05	0.99
0.4	14.24	0.76	0.82	0.67	0.71
0.5	15.12	0.61	0.52	0.54	0.48
0.6	15.52	0.40	0.38	0.37	0.04
0.7	15.88	0.26	0.27	0.26	-
0.8	16.12	0.16	0.18	-	-

Table (B.1). CPU time (in seconds) for computing M-ϕ values failure loads (β = 1.0).
(section 1, Table 4.1)

APPENDIX C

MOMENT-CURVATURE CURVES

&

INTERACTION DIAGRAMS

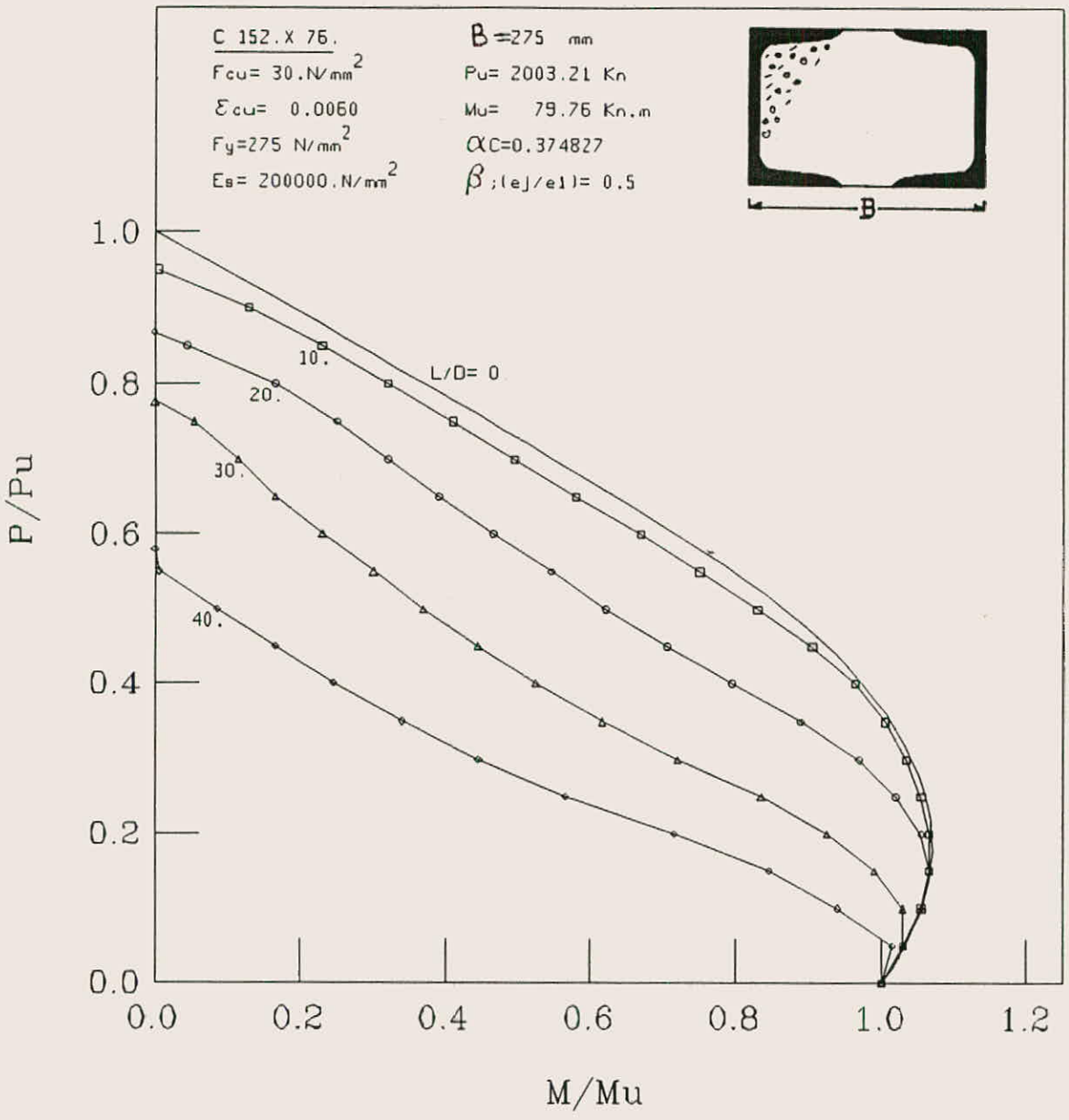

FIG.(C.1):ULTIMATE STRENGTH INTERACTION CURVES FOR SLENDER BATTENED COMPOSITE COLUMN UNDER UNIAXIAL BENDING MOMENT ABOUT MINOR AXIS

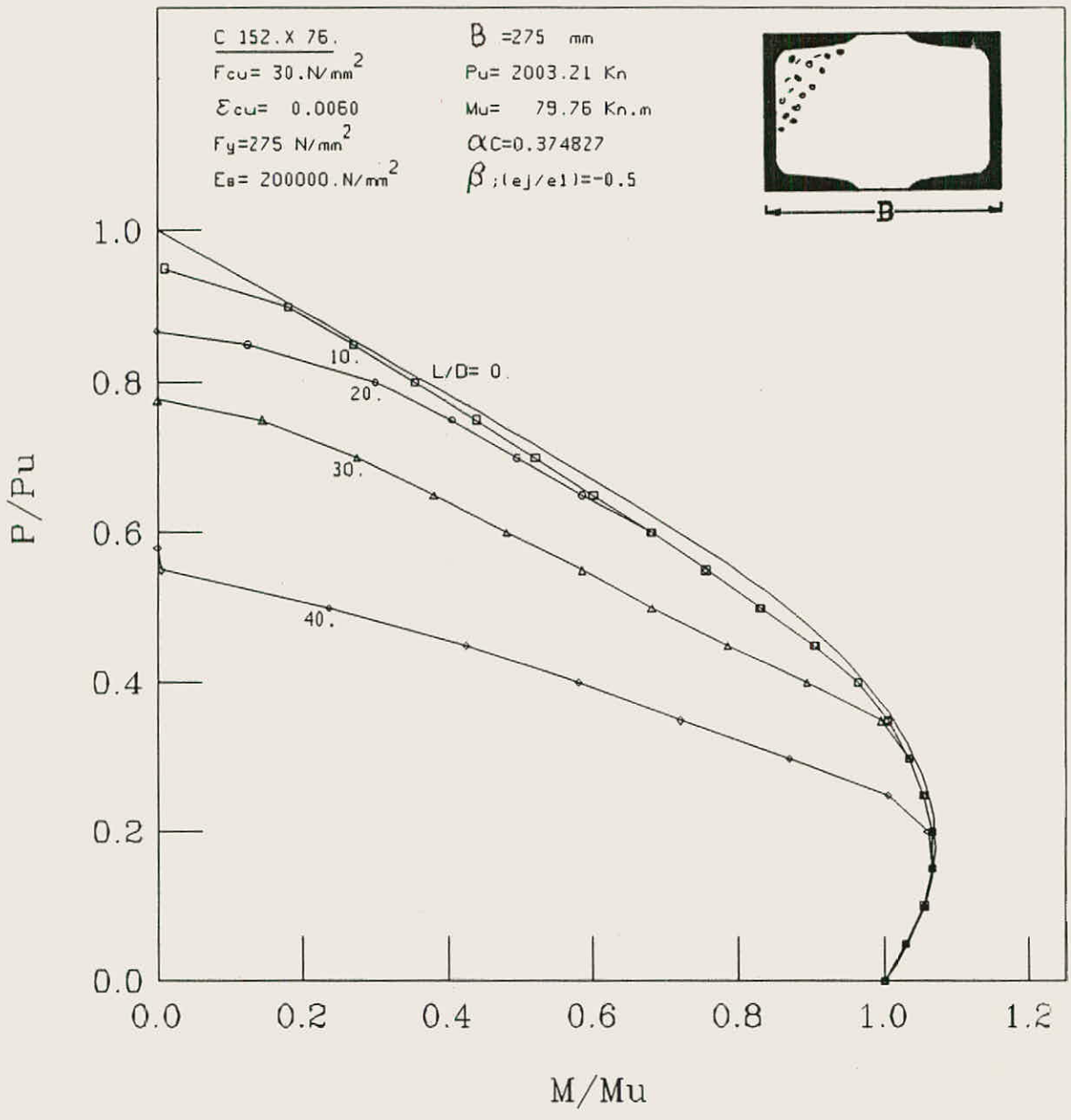

FIG.(C-2):ULTIMATE STRENGTH INTERACTION CURVES FOR SLENDER BATTENED COMPOSITE COLUMN UNDER UNIAXIAL BENDING MOMENT ABOUT MINOR AXIS

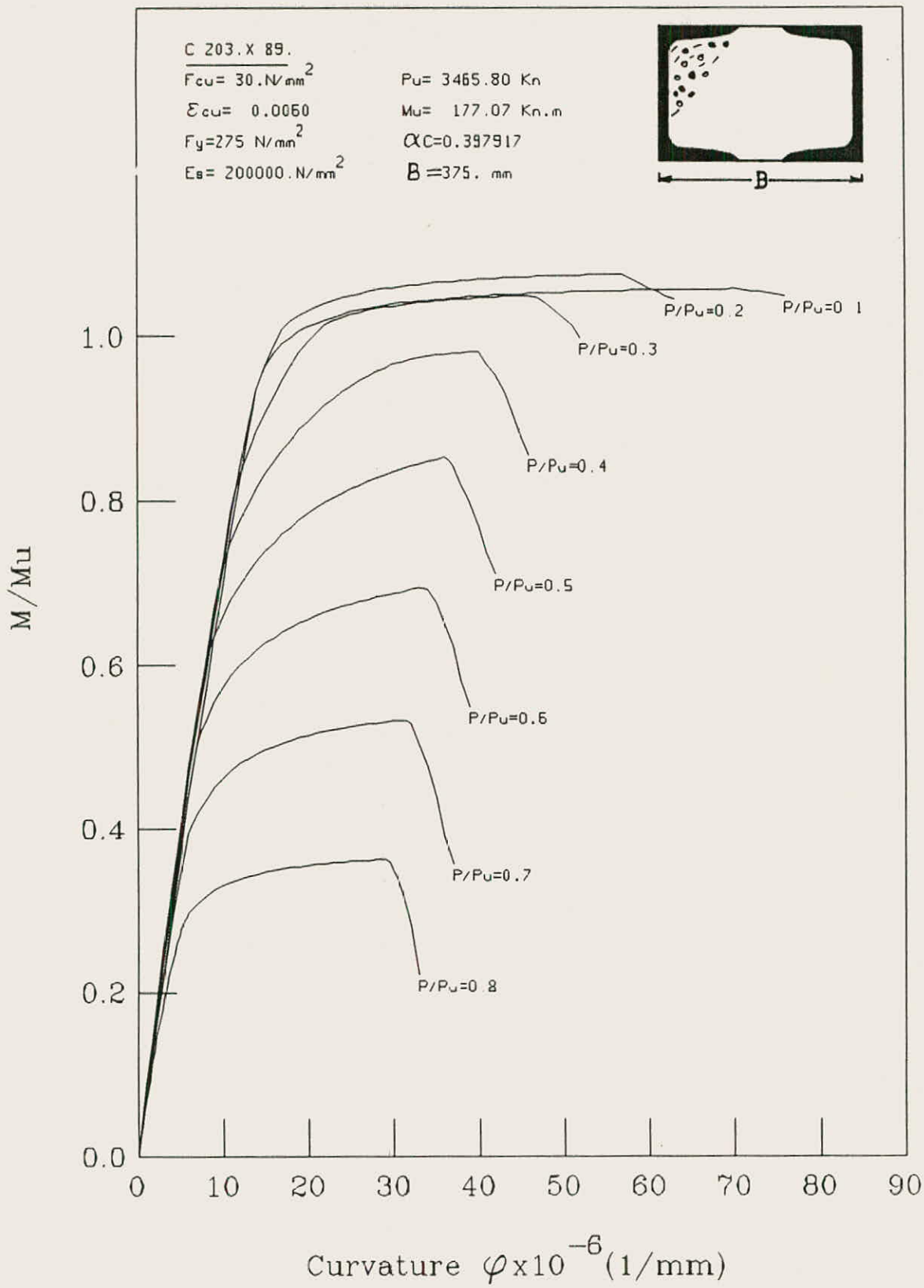

FIG.(C-3):MOMENT-CURVATURE-THRUST CURVES FOR BATTENED COMPOSITE COLUMN UNDER UNIAXIAL BENDING MOMENT ABOUT MINOR AXIS .

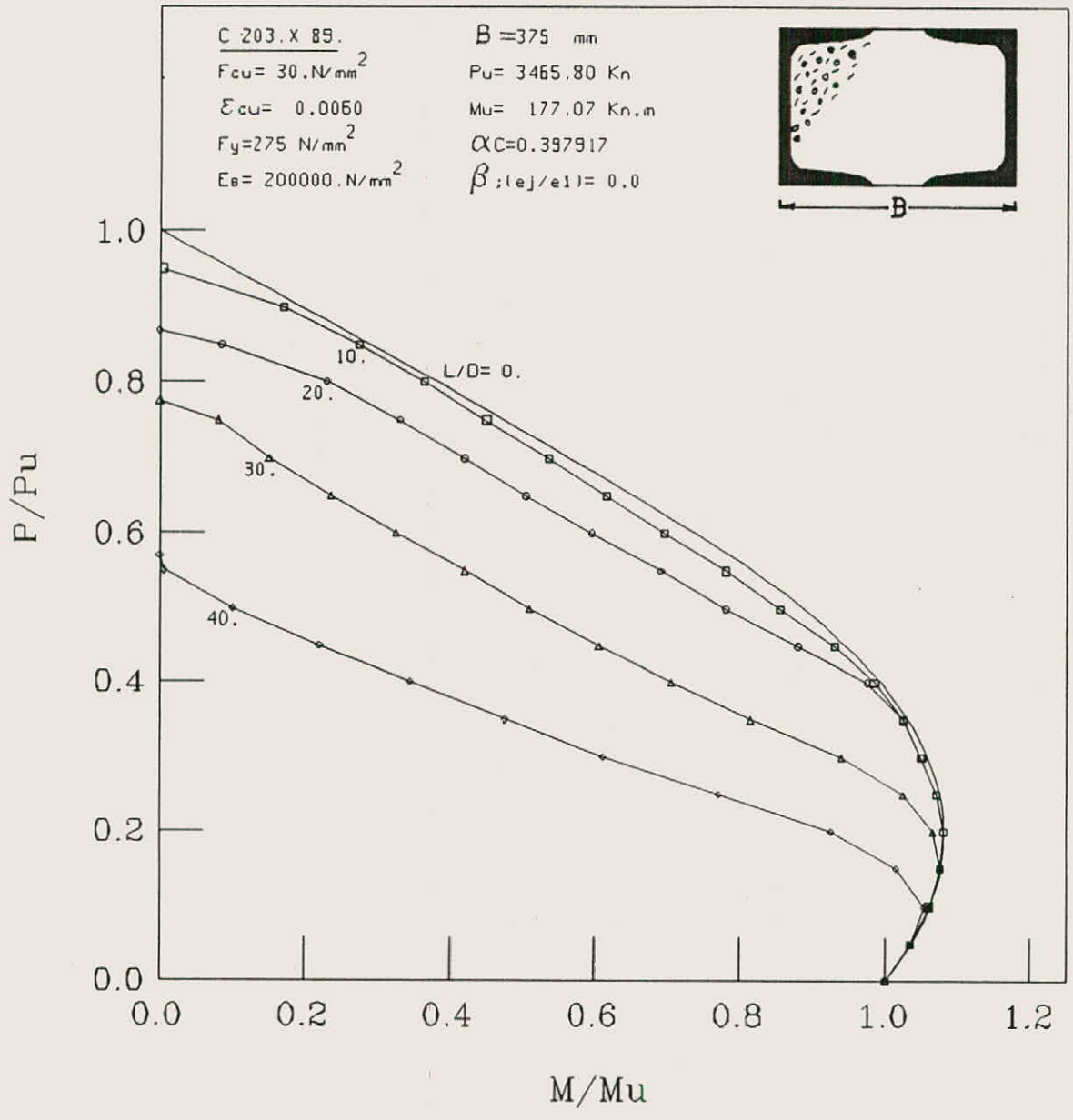

FIG.(C·4):ULTIMATE STRENGTH INTERACTION CURVES FOR SLENDER BATTENED COMPOSITE COLUMN UNDER UNIAXIAL BENDING MOMENT ABOUT MINOR AXIS

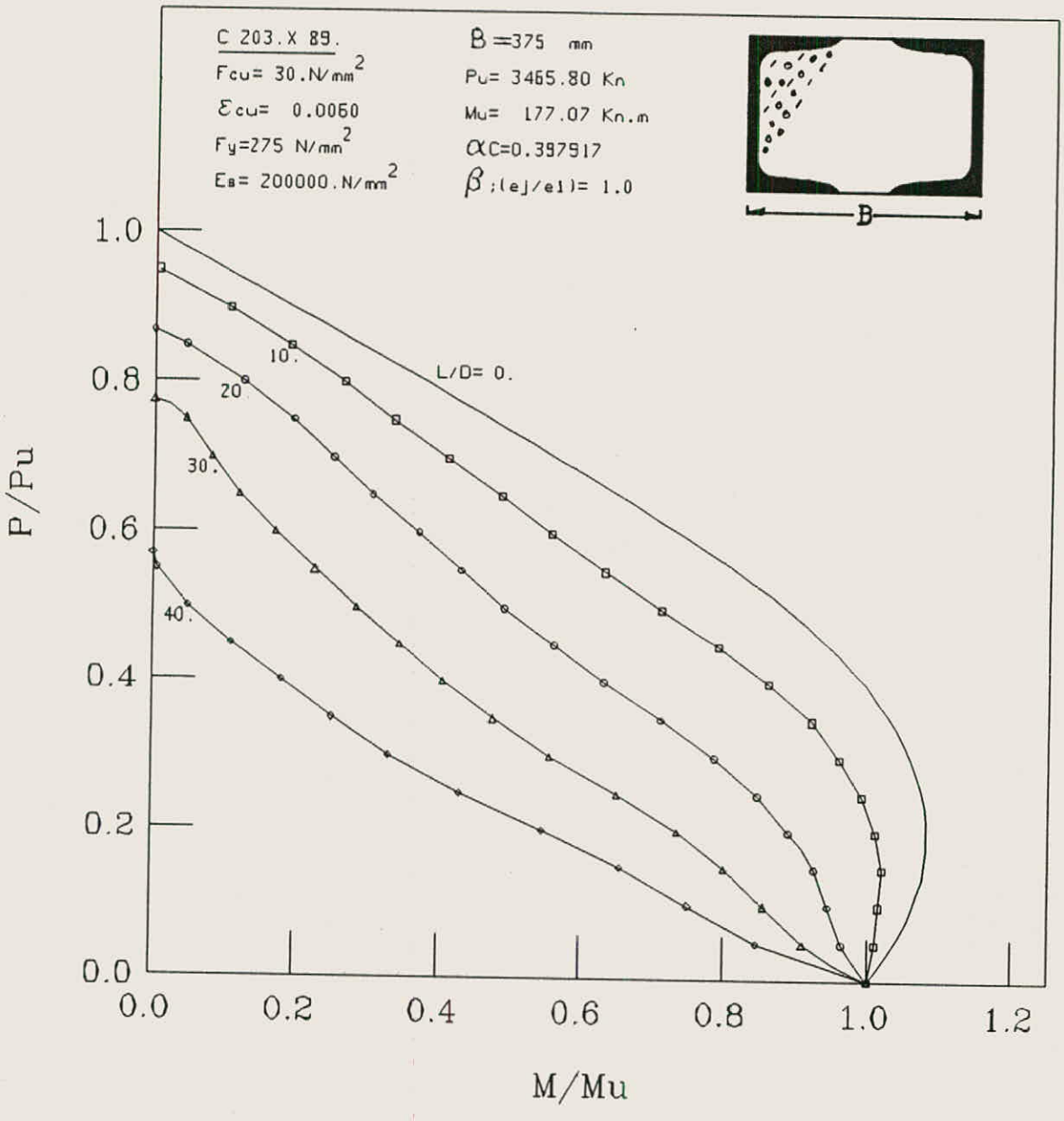

FIG. (C-5): ULTIMATE STRENGTH INTERACTION CURVES FOR SLENDER BATTENED COMPOSITE COLUMN UNDER UNIAXIAL BENDING MOMENT ABOUT MINOR AXIS

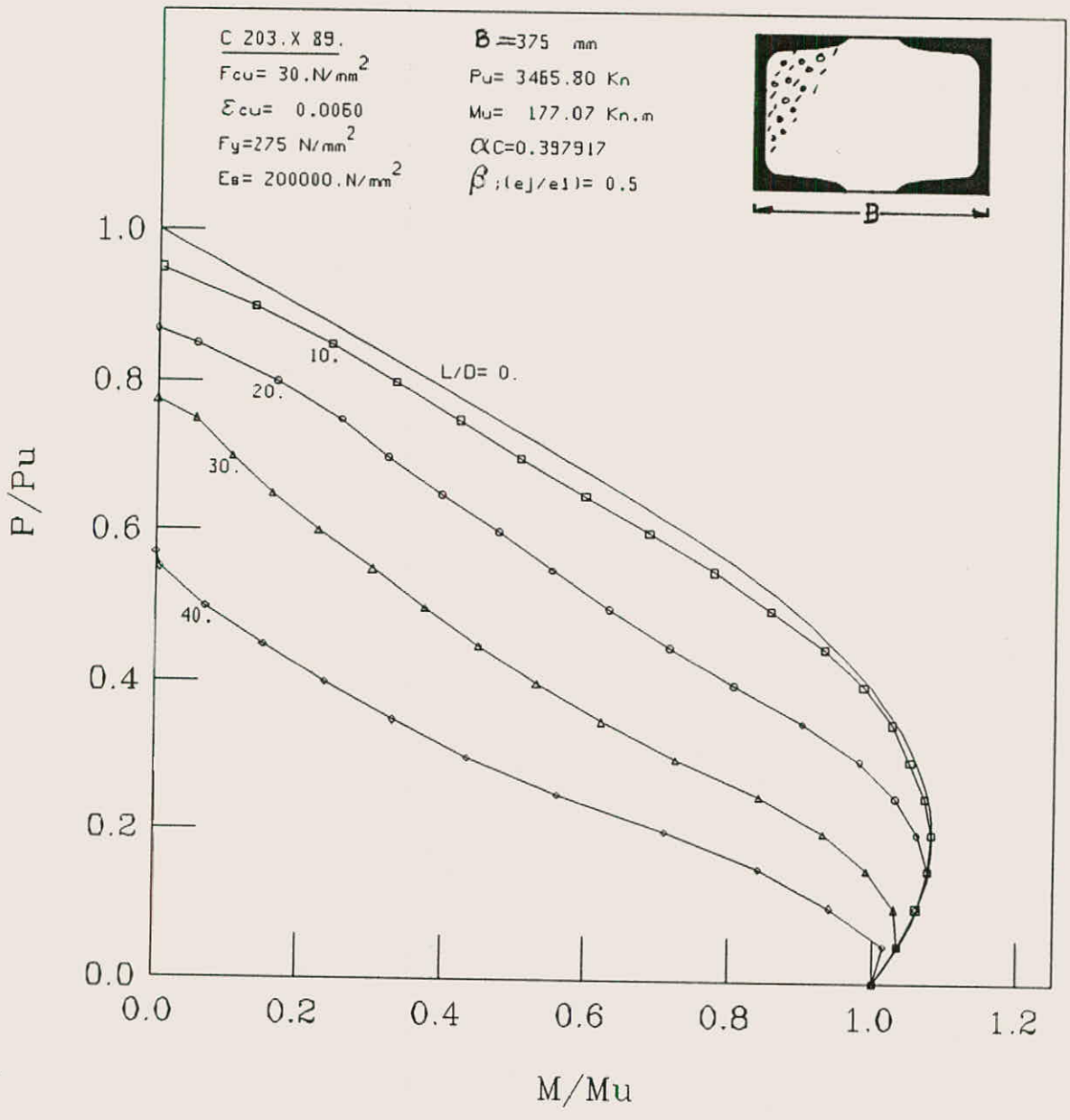

FIG. (C.6): ULTIMATE STRENGTH INTERACTION CURVES FOR SLENDER BATTENED COMPOSITE COLUMN UNDER UNIAXIAL BENDING MOMENT ABOUT MINOR AXIS

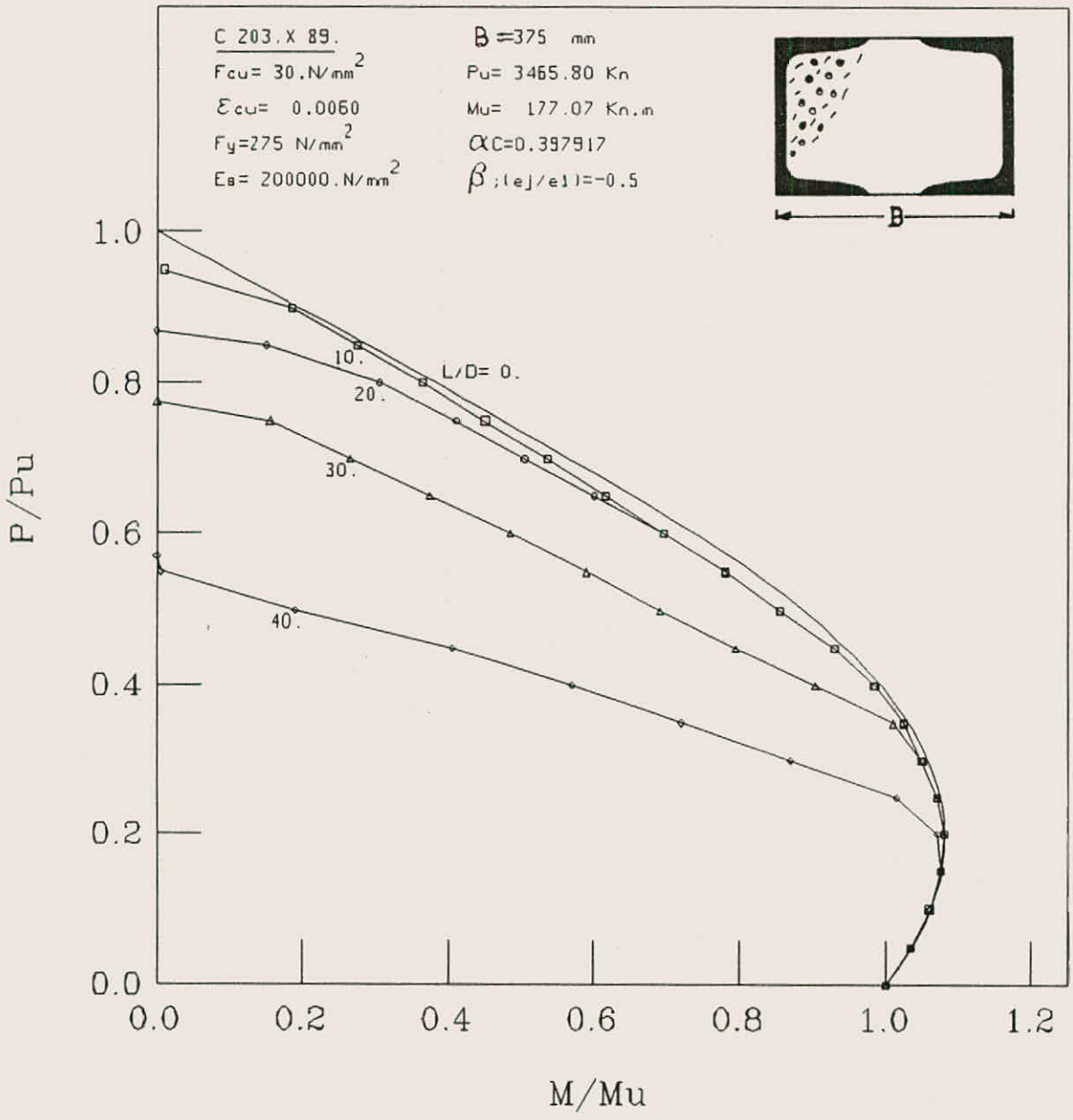

FIG.(C-7):ULTIMATE STRENGTH INTERACTION CURVES FOR SLENDER BATTENED COMPOSITE COLUMN UNDER UNIAXIAL BENDING MOMENT ABOUT MINOR AXIS

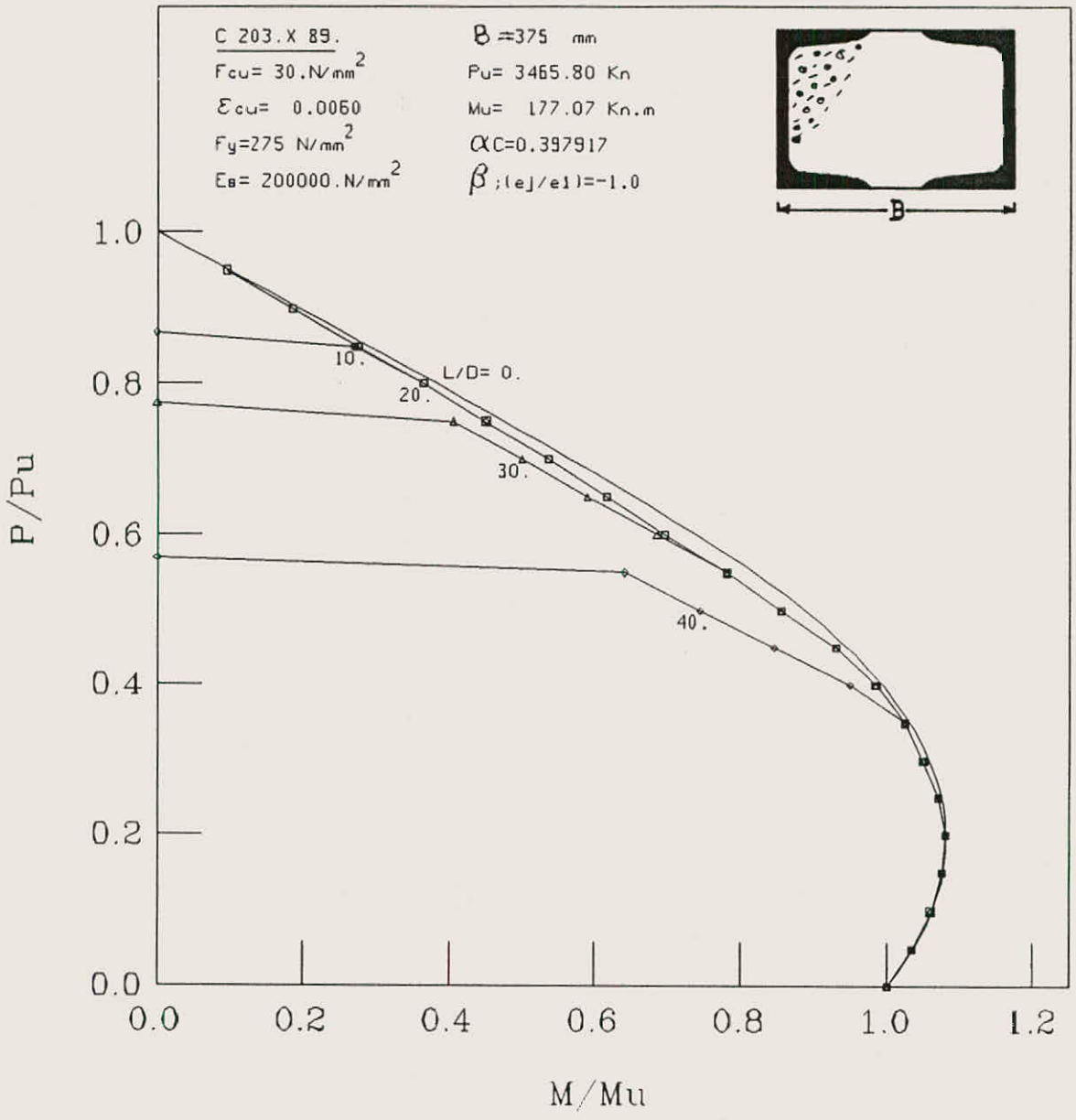

FIG. (C-8): ULTIMATE STRENGTH INTERACTION CURVES FOR SLENDER BATTENED COMPOSITE COLUMN UNDER UNIAXIAL BENDING MOMENT ABOUT MINOR AXIS

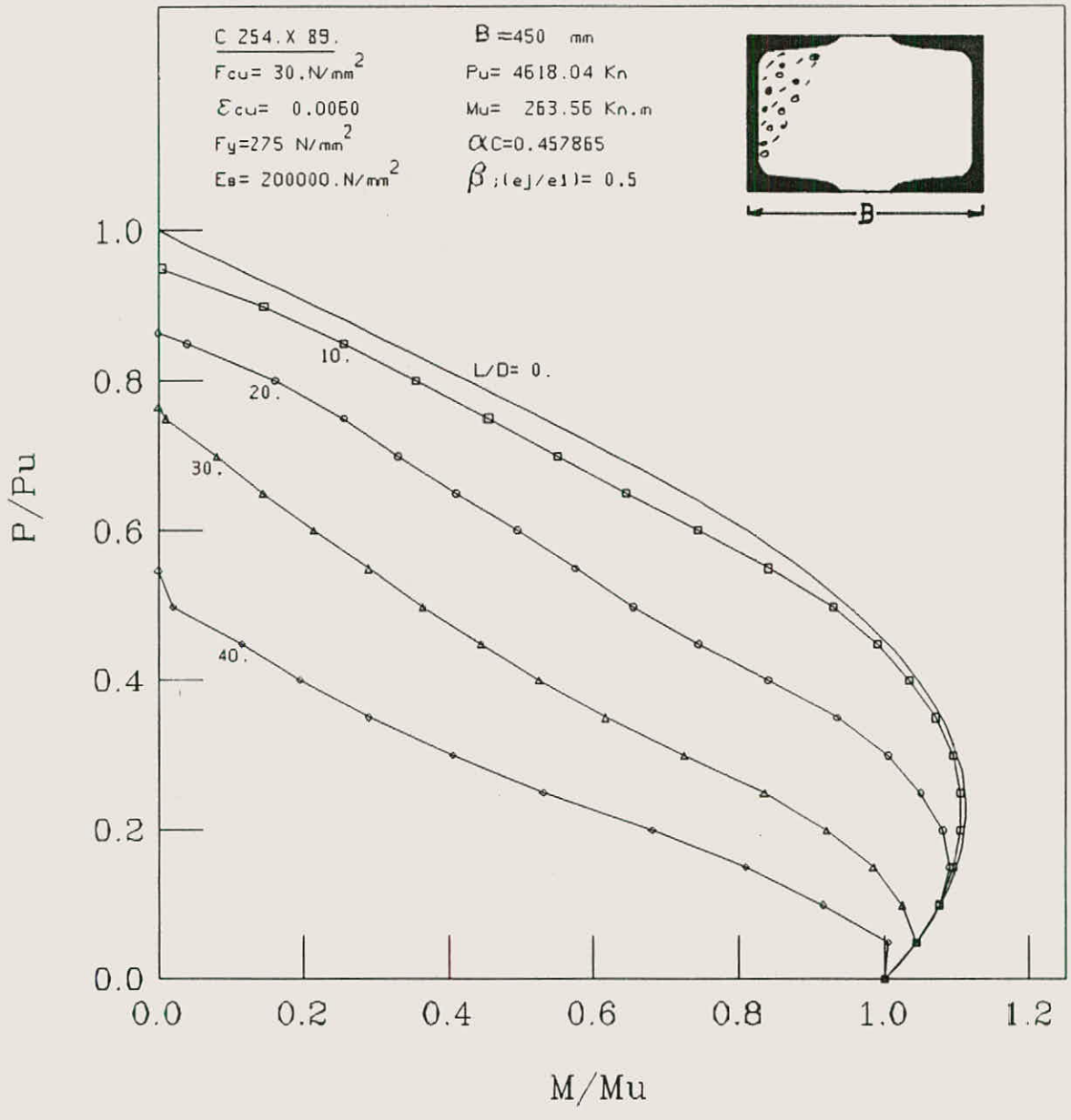

FIG. (C-9): ULTIMATE STRENGTH INTERACTION CURVES FOR SLENDER BATTENED COMPOSITE COLUMN UNDER UNIAXIAL BENDING MOMENT ABOUT MINOR AXIS

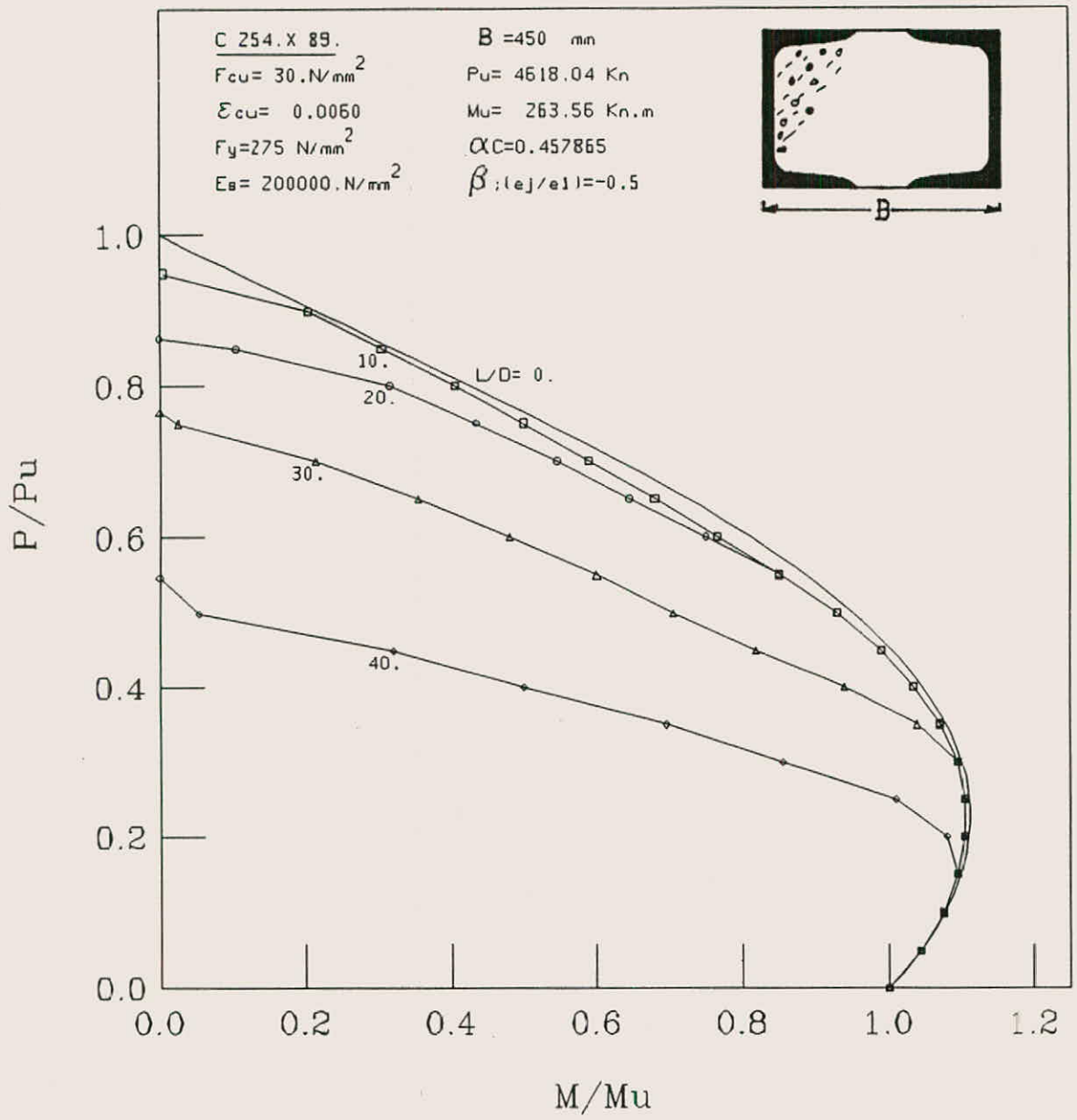

FIG. (C-10) : ULTIMATE STRENGTH INTERACTION CURVES FOR SLENDER BATTENED COMPOSITE COLUMN UNDER UNIAXIAL BENDING MOMENT ABOUT MINOR AXIS

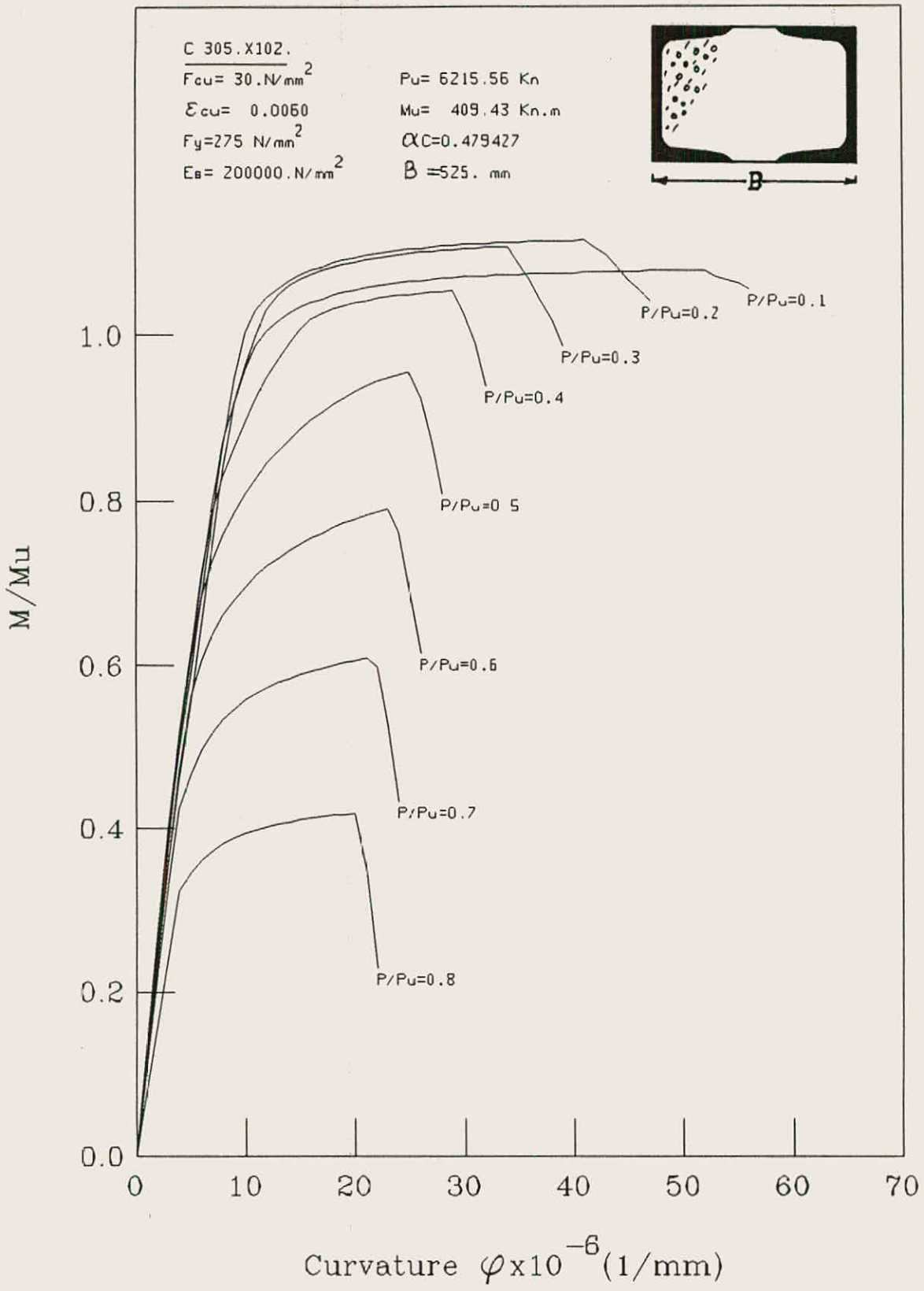

FIG. (C.11): MOMENT-CURVATURE-THRUST CURVES FOR BATTENED COMPOSITE COLUMN UNDER UNIAXIAL BENDING MOMENT ABOUT MINOR AXIS .

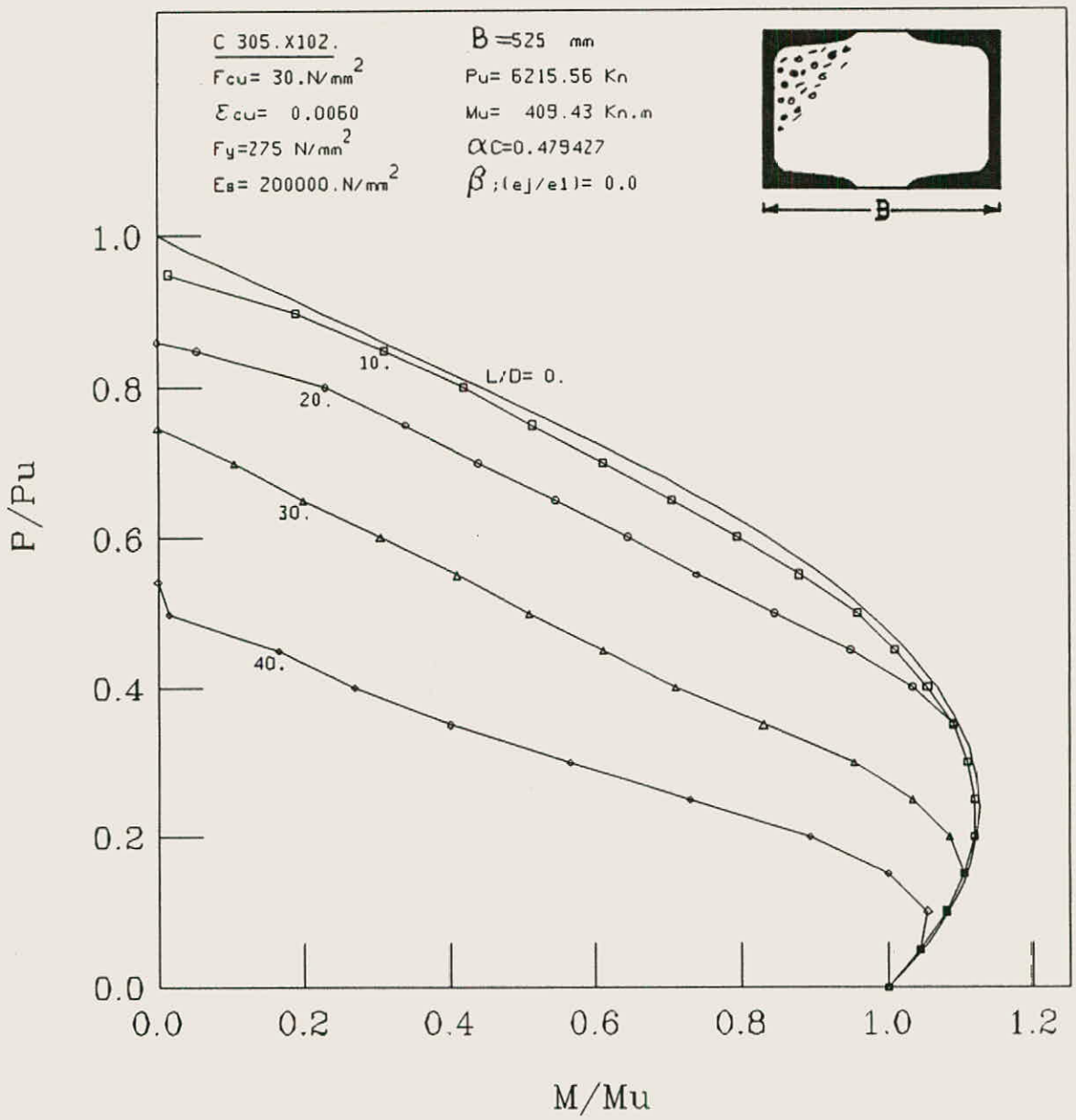

FIG. (C-12): ULTIMATE STRENGTH INTERACTION CURVES FOR SLENDER BATTENED COMPOSITE COLUMN UNDER UNIAXIAL BENDING MOMENT ABOUT MINOR AXIS

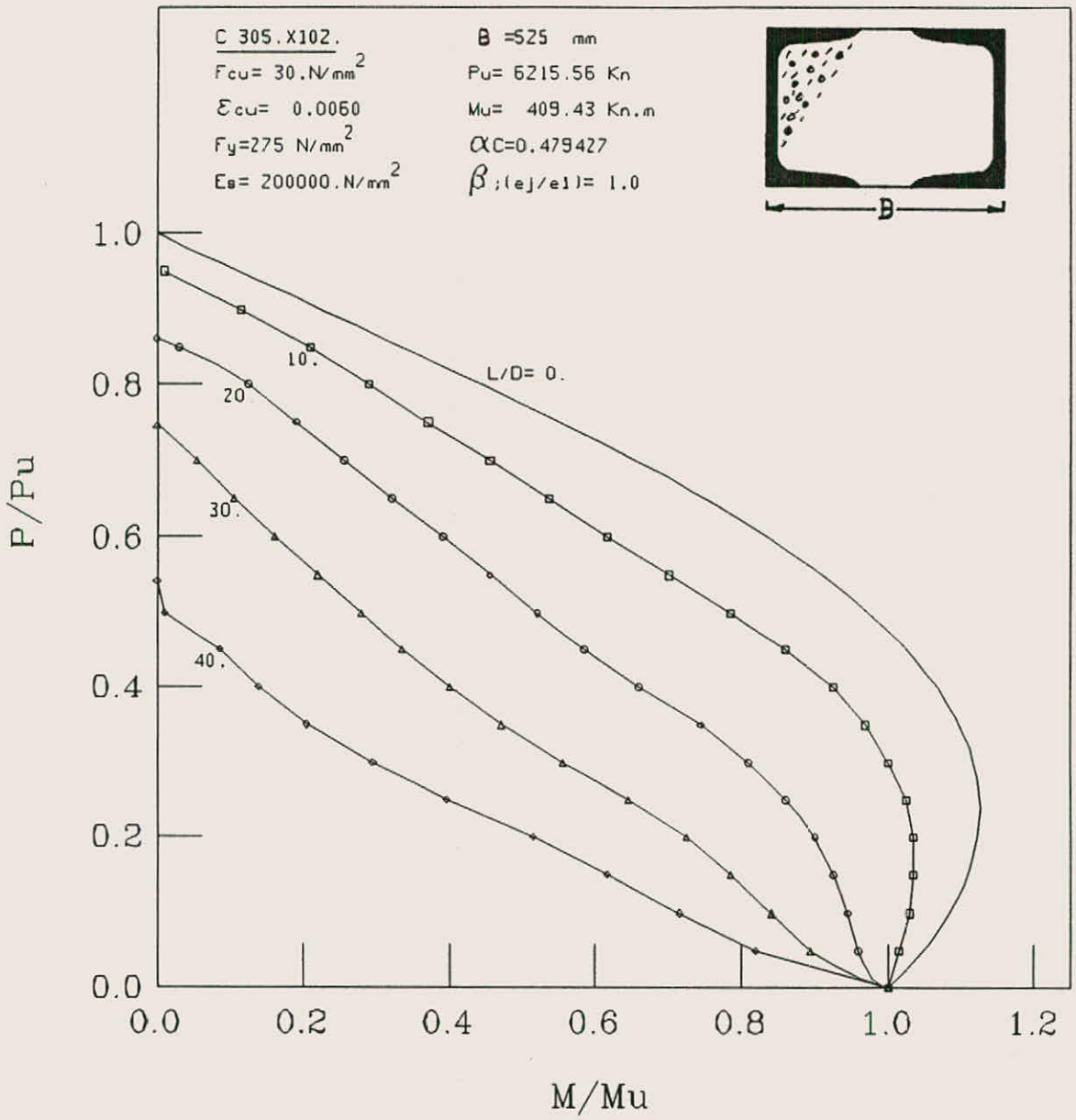

FIG. (C·13): ULTIMATE STRENGTH INTERACTION CURVES FOR SLENDER BATTENED COMPOSITE COLUMN UNDER UNIAXIAL BENDING MOMENT ABOUT MINOR AXIS

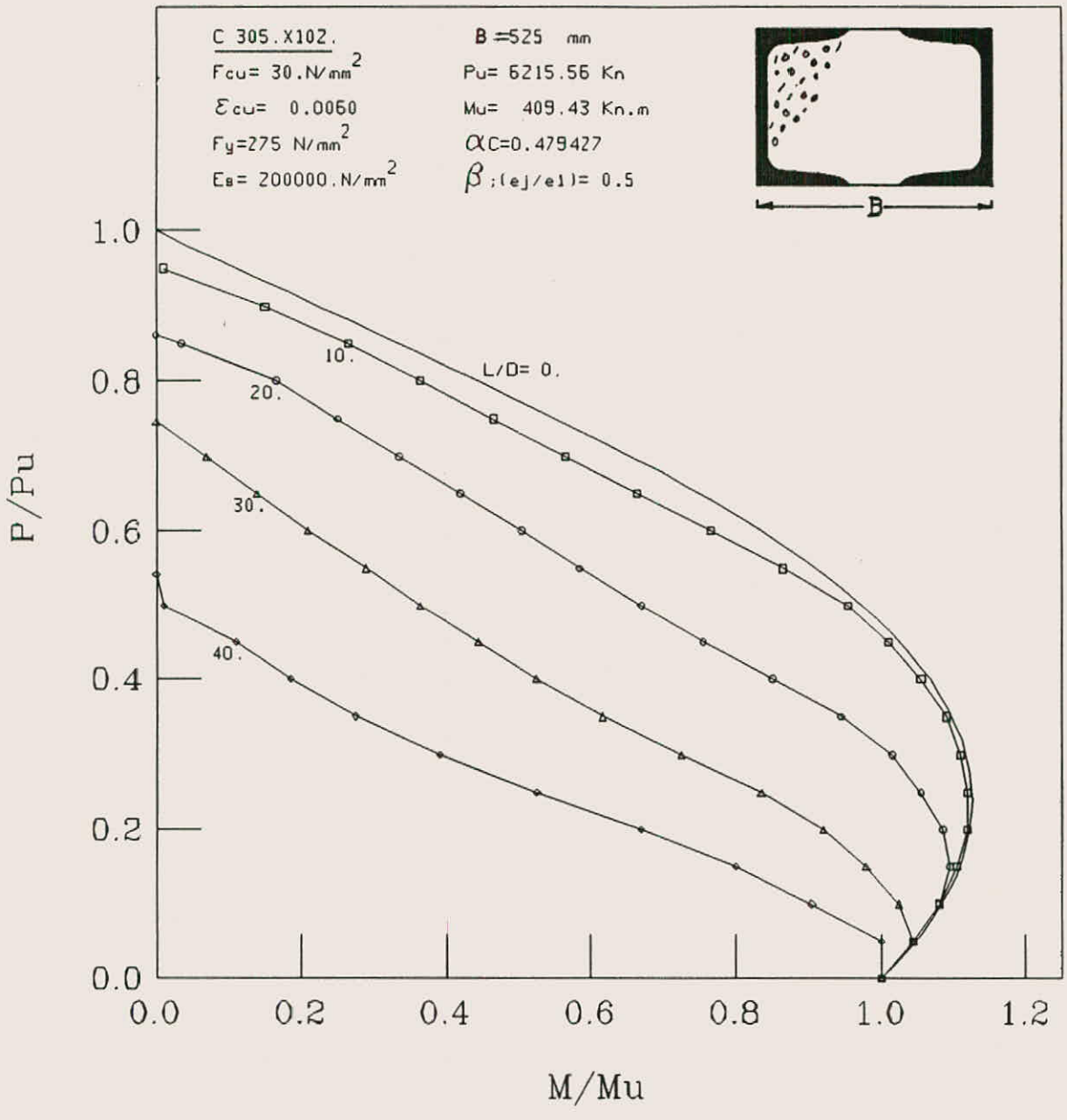

FIG. (C-14): ULTIMATE STRENGTH INTERACTION CURVES FOR SLENDER BATTENED COMPOSITE COLUMN UNDER UNIAXIAL BENDING MOMENT ABOUT MINOR AXIS

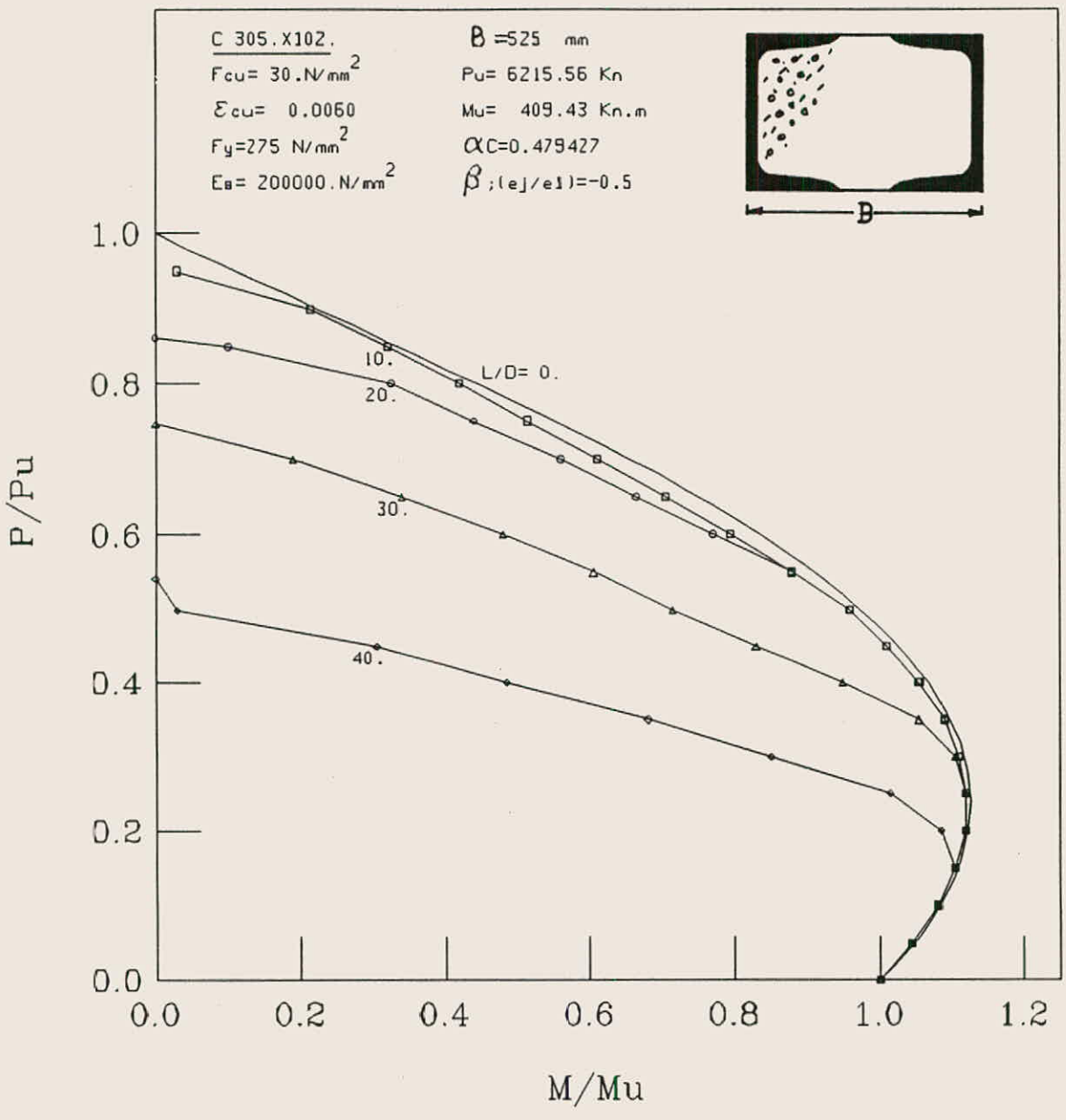

FIG. (C-15): ULTIMATE STRENGTH INTERACTION CURVES FOR SLENDER BATTENED COMPOSITE COLUMN UNDER UNIAXIAL BENDING MOMENT ABOUT MINOR AXIS

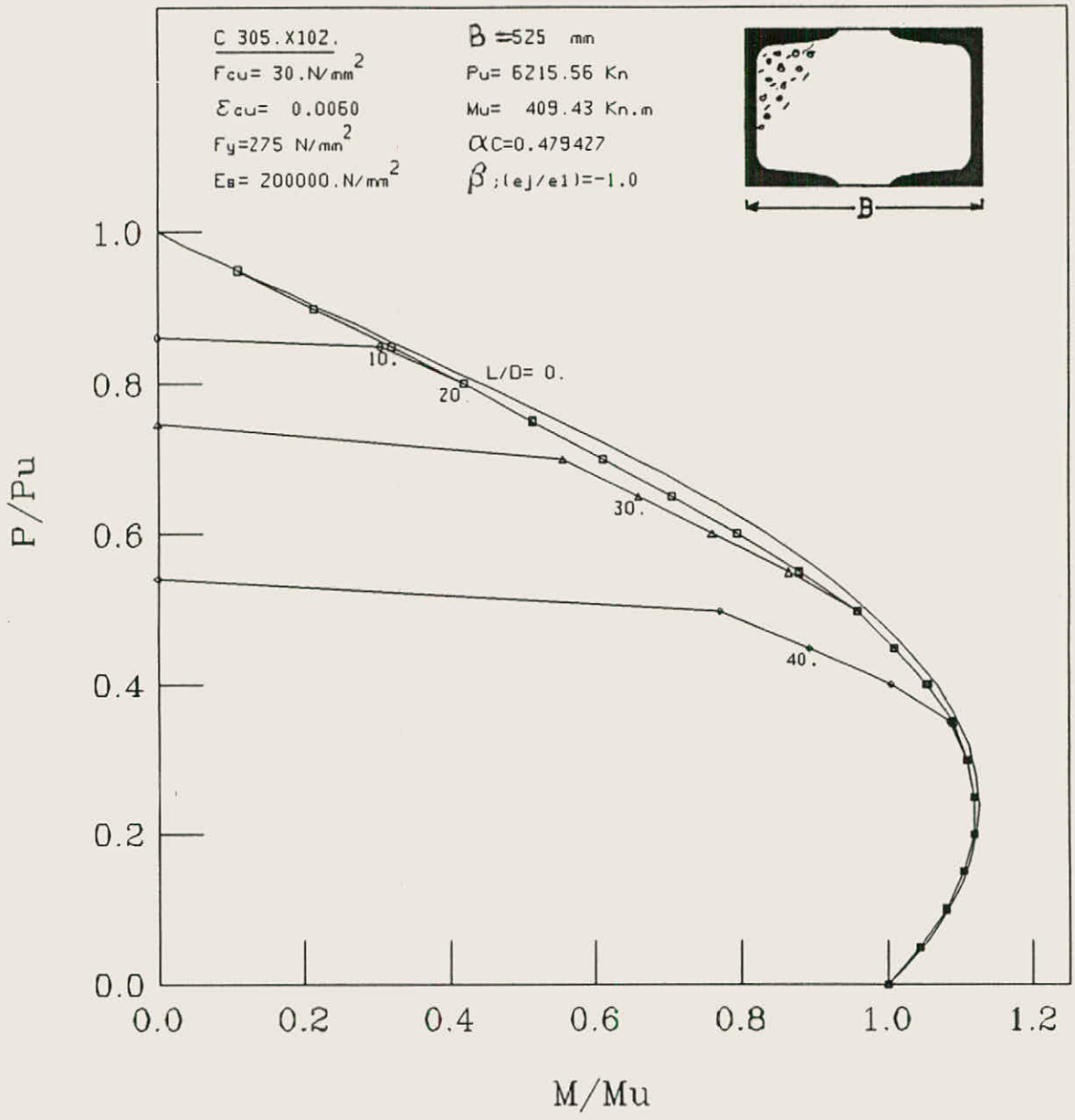

FIG. (C-16): ULTIMATE STRENGTH INTERACTION CURVES FOR SLENDER BATTENED COMPOSITE COLUMN UNDER UNIAXIAL BENDING MOMENT ABOUT MINOR AXIS

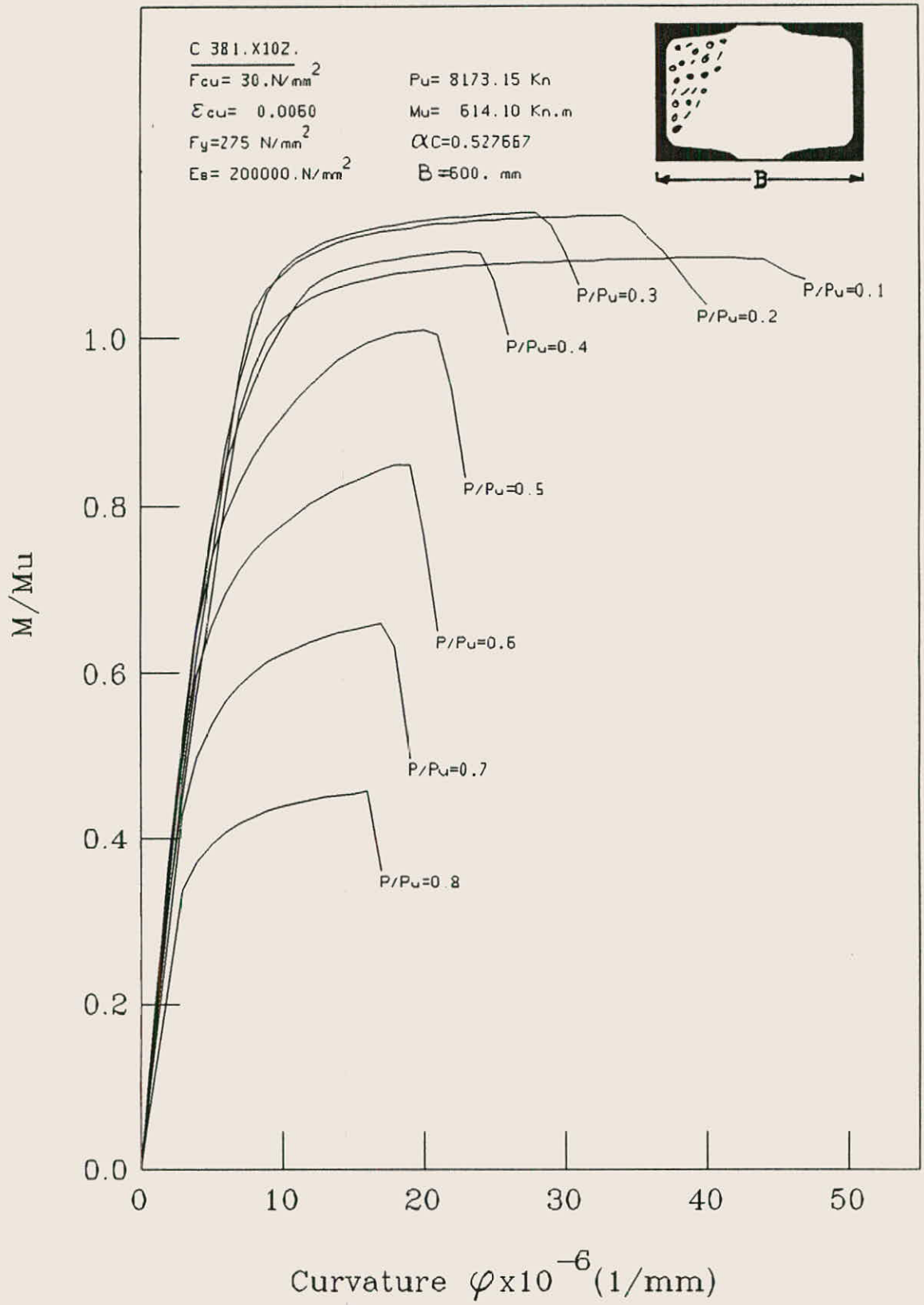

FIG. (C/7): MOMENT-CURVATURE-THRUST CURVES FOR BATTENED COMPOSITE COLUMN UNDER UNIAXIAL BENDING MOMENT ABOUT MINOR AXIS .

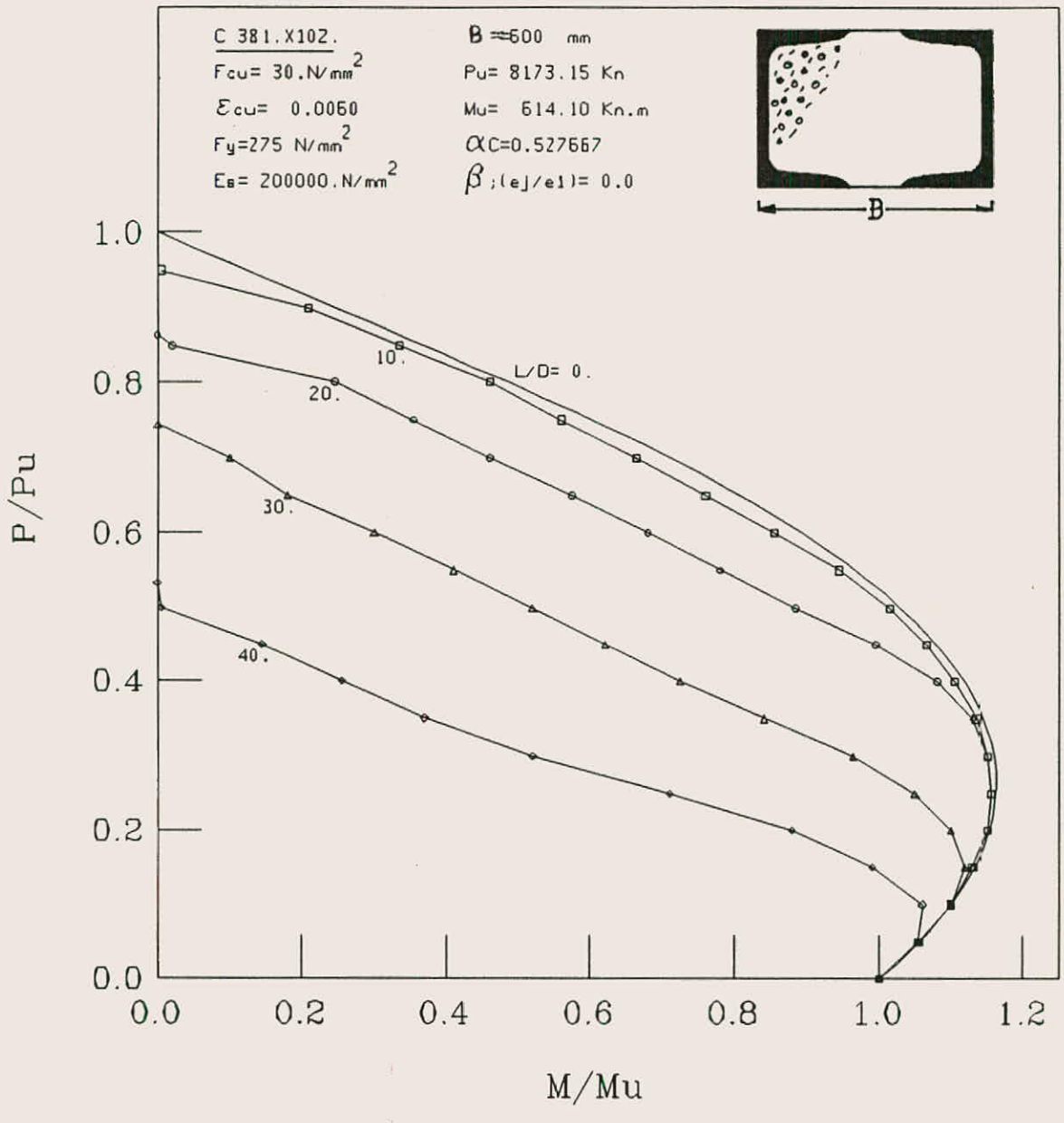

FIG. (C-18): ULTIMATE STRENGTH INTERACTION CURVES FOR SLENDER BATTENED COMPOSITE COLUMN UNDER UNIAXIAL BENDING MOMENT ABOUT MINOR AXIS

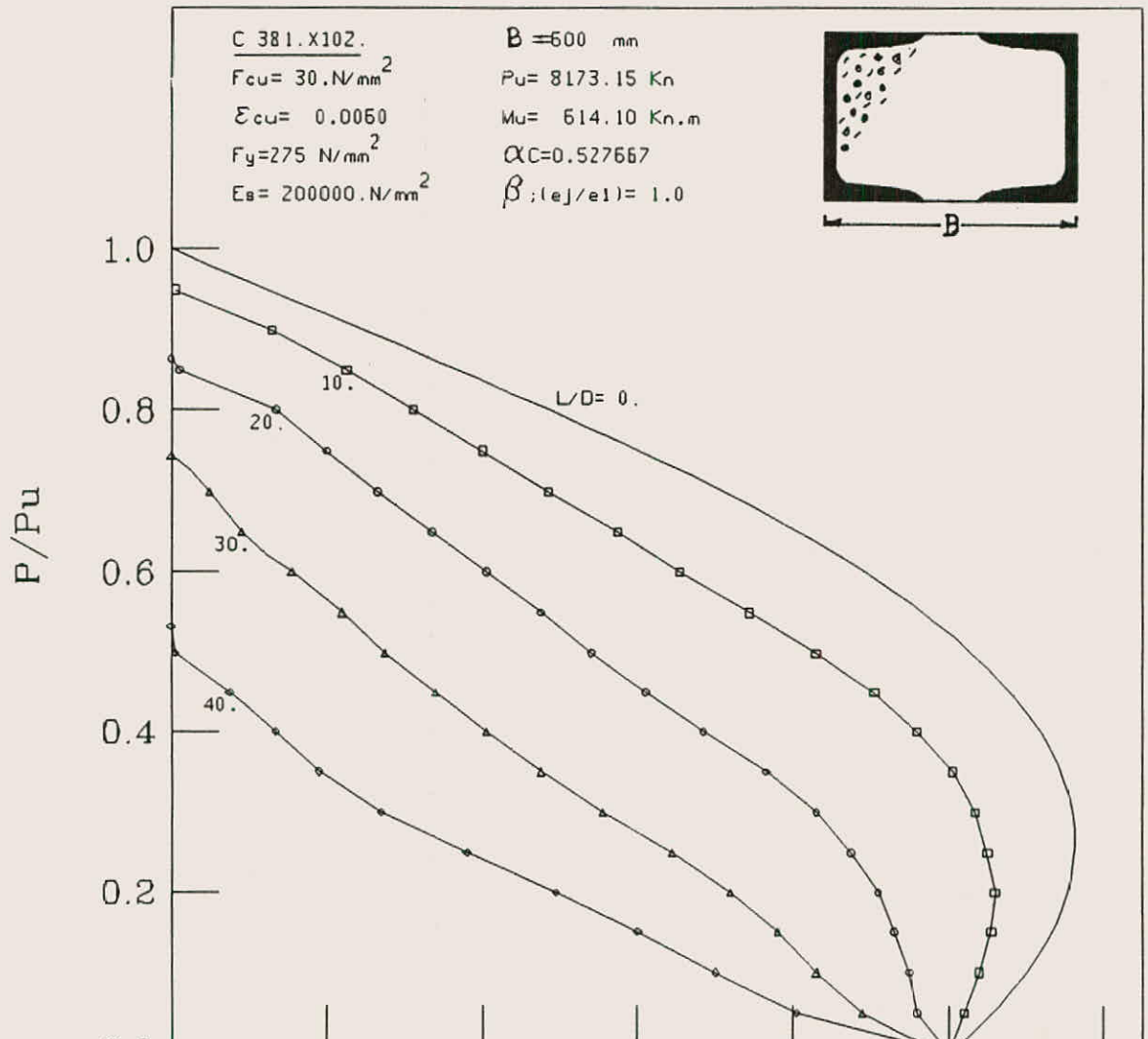

FIG. (C-19): ULTIMATE STRENGTH INTERACTION CURVES FOR SLENDER BATTENED COMPOSITE COLUMN UNDER UNIAXIAL BENDING MOMENT ABOUT MINOR AXIS

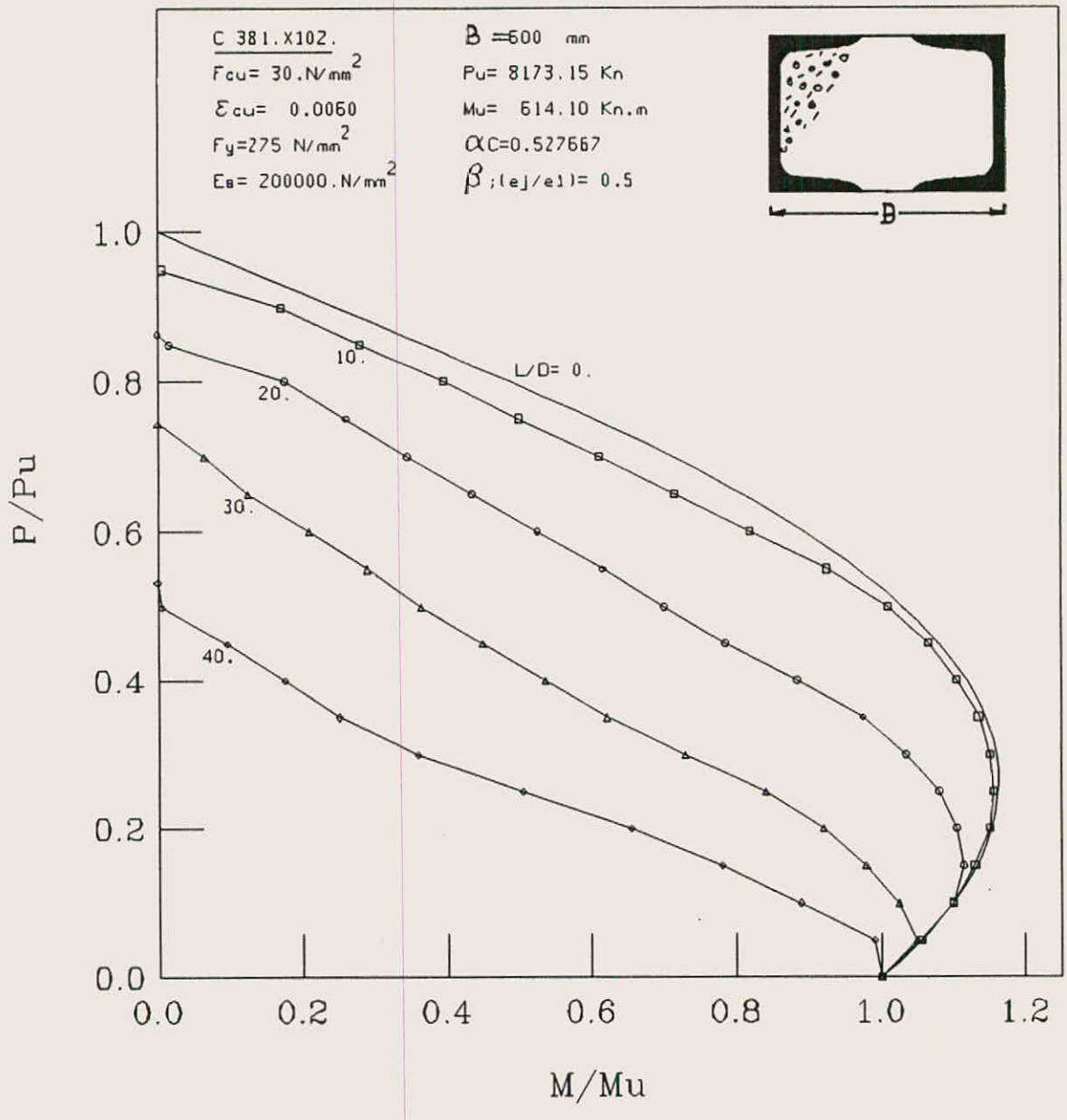

FIG.(C-20):ULTIMATE STRENGTH INTERACTION CURVES FOR SLENDER BATTENED COMPOSITE COLUMN UNDER UNIAXIAL BENDING MOMENT ABOUT MINOR AXIS

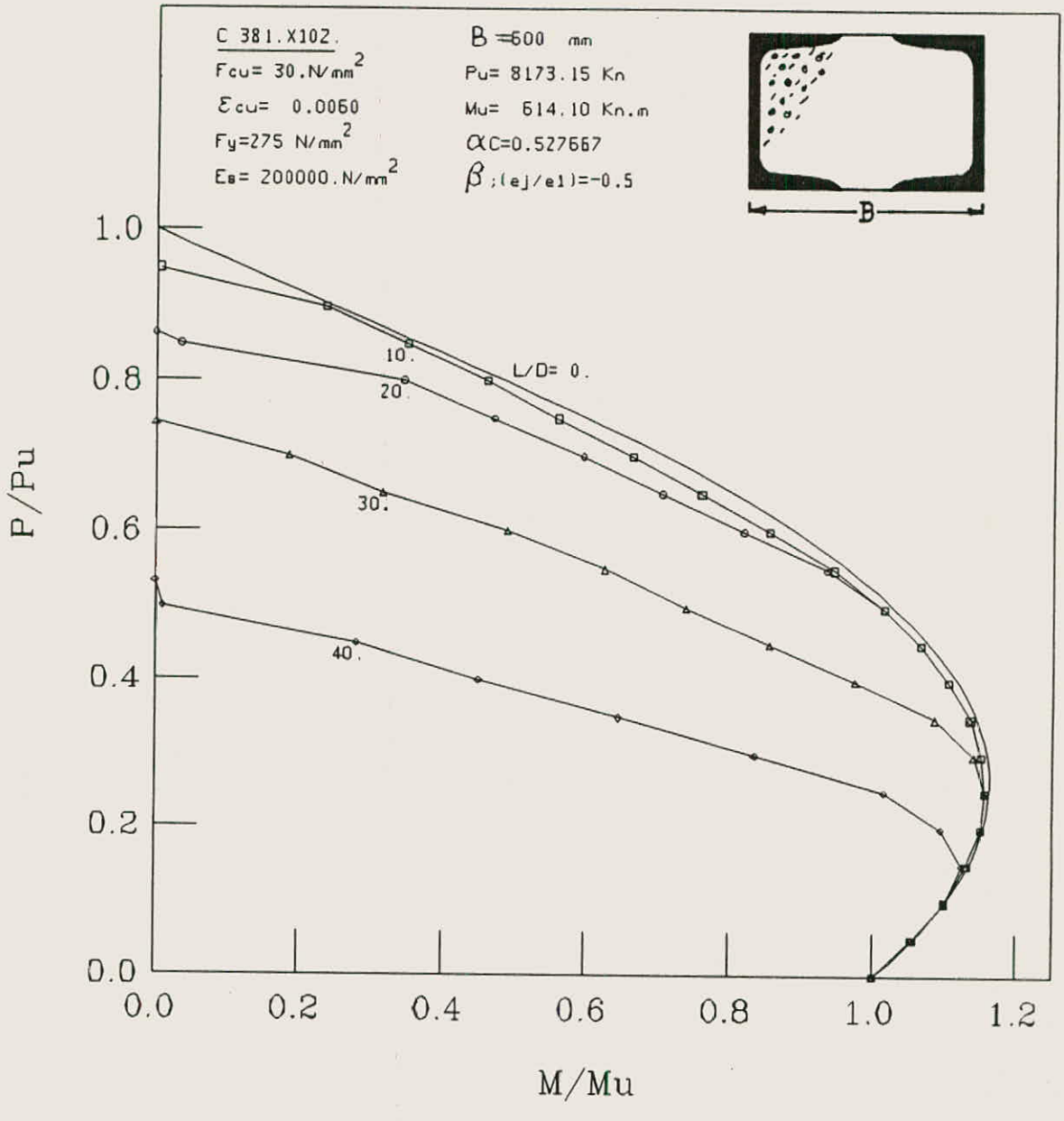

FIG. (C-21): ULTIMATE STRENGTH INTERACTION CURVES FOR SLENDER BATTENED COMPOSITE COLUMN UNDER UNIAXIAL BENDING MOMENT ABOUT MINOR AXIS

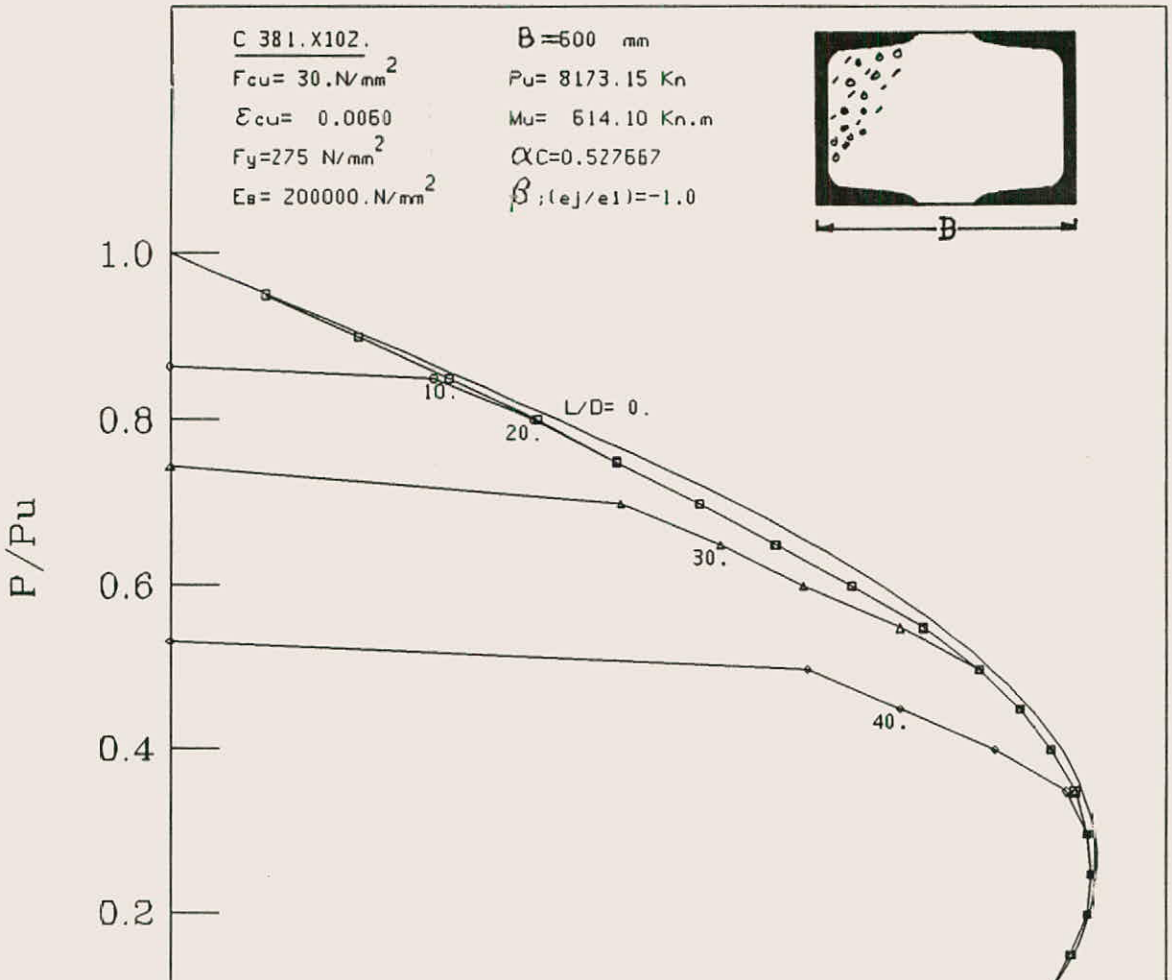

FIG. (C.22): ULTIMATE STRENGTH INTERACTION CURVES FOR SLENDER BATTENED COMPOSITE COLUMN UNDER UNIAXIAL BENDING MOMENT ABOUT MINOR AXIS

REFERENCES

1-ABO-HAMD,M: 'Slender composite beam-columns',Journal of Structural division, ASCE, Vol. 114, No 10, October 1988.

2-BASU,A.K. : 'Computation of failure loads of composite columns' Proc. Instin. Civil Engineers,Vol. 36, March 1967, PP557-578.

3-BASU, A.K and HILL,W.F. : 'A more exact computation of failure loads of composite columns': Proc. Inst. Civil Engineers, Vol 40, May,1968, PP 37-60.

4-BASU,A.K. and SOMMERVILLE,W : 'Derivation of formulae for the design of rectangular composite columns' : Proc. Instin. Civil Engineers, Supp. Vol., 1969, PP 233-280.

5-BRIDGE, R.Q. and RODERIC, J.W. : 'Behavior of built-up composite columns' : Journal of the Structural Division, ASCE, Vol 104, ST7,July 1978, PP 1141-1155.

6-FABER, O.:'More rational design of cased stanchions':The Structural Engineer, Vol. 34, March 1956, PP 88-109.

7-HUNAITI, Y. : 'Behavior of battened composite columns';Ph.D Thesis, University of Manchester, England, 1985.

8-JONES, R. and RIZK,A.A. : ' An investigation on the behaviour of encased steel columns under load' : The Structural Engineer, Vol. 41, January 1962, PP 21-33.

9-JOHNSON, R. P. :' Composite structures of steel and concrete'; Vol. 1, Geranada, london, 1975.

10-RYALAT, S.S. : 'Load carrying capacity of battened composite column under major axis bending' , M.Sc. thesis, Univercity of Jordan Amman , 1990.

11-STEVENS, R.F. :'Encased steel stanchions and BS449' : Engineering, Vol. 188, October 1959, PP 376-377.

12-STEVENS, R.F. :'Encased stanchions' : The Structural Engineer, Vol. 43, February 1965, PP 59-66.

13-TAYLOR, R. SHAKIR-KHALIL, H., YEE, K.M. :'Some tests on a new type of composite column'; Proc. Instn. Civil Engineers, Vol. 75, June 1983, PP 283-296.

14-TIMSHENKO, S.P. : 'Theory of elastic stability' : Second Edition, McGRAW-HILL BOOK Company, 1963, PP 1-14.

15-VIRDI, K.S. and DOWLING, P.J. :'A unified design method for composite columns axial bending' : Publications, IABSE Vol. 36 II,1976, PP 165-184.

16-YEE, K.M., SHAKIR-KHALIL, H., TAYLOR,R. : 'Design expressions for a new type of composite column' : Journal Const. Steel Research, Vol. 2, June 1982, PP 26-32.